Western Graduate&PostdoctoralStudies

Western University
Scholarship@Western

Electronic Thesis and Dissertation Repository

10-2-2020 3:20 PM

Development of a Route to Functional Polymers via Click Chemistry

Kyle Classen, *The University of Western Ontario*

Supervisor: Workentin, Mark S., *The University of Western Ontario*

A thesis submitted in partial fulfillment of the requirements for the Master of Science degree in Chemistry

© Kyle Classen 2020

Follow this and additional works at: https://ir.lib.uwo.ca/etd

 Part of the Polymer Chemistry Commons

Recommended Citation

Classen, Kyle, "Development of a Route to Functional Polymers via Click Chemistry" (2020). *Electronic Thesis and Dissertation Repository*. 7421.
https://ir.lib.uwo.ca/etd/7421

This Dissertation/Thesis is brought to you for free and open access by Scholarship@Western. It has been accepted for inclusion in Electronic Thesis and Dissertation Repository by an authorized administrator of Scholarship@Western. For more information, please contact wlswadmin@uwo.ca.

Abstract

Functional polymers are desirable due to their use in applications such as drug delivery and bioimaging. This work describes the development of a functional polymer template, expanding upon current routes to creating functional polymer libraries. The methodology utilizes a masking-unmasking strategy to protect and then reveal a strained alkyne for the introduction of functional entities via post-polymerization modification.

The synthesis and characterization by high-resolution mass spectrometry as well as ^{1}H NMR, UV-Vis, and FT-IR spectroscopy of a masked strained alkyne monomer is presented. First, the strained alkyne, masked as a cyclopropenone moiety, was synthesized. Next, a norbornene derivative was covalently attached to the masked strained alkyne to make a monomer capable of ring-opening polymerization and post-polymerization functionalization. The polymerization of masked monomer was then performed and characterized by ^{1}H NMR, UV-Vis, and FT-IR spectroscopy which confirmed the retention of the cyclopropenone moiety. The unmasking of strained alkyne polymer via UV light irradiation and modification via strain-promoted azide-alkyne cycloaddition is also presented. The azides introduced included benzyl azide and a Au_{25} azide nanocluster. The benzyl functionalized polymer was characterized by ^{1}H NMR, UV-Vis, and FT-IR spectroscopy. The Au_{25} functionalized polymer was characterized by UV-Vis, FT-IR, and X-ray photoelectron spectroscopy.

The amenability of this strategy to both small molecule and more complex azides is displayed. This provides an exciting new route towards post-polymerization modification to yield a library of functional polymers. This strategy also has the potential for applications in photopatterning as the unmasking method has spatiotemporal control.

Keywords

Functional polymers, click chemistry, strained alkyne, strain-promoted azide-alkyne cycloaddition, post-polymerization modification, functional polymer template

Summary for Lay Audience

Polymers are materials made of long chains consisting of repeated subunits called monomers. Polymers are made by a process which links monomers together to from these long chains, referred to as polymerization. Polymers in everyday life include plastics such as those used in grocery bags or rubbers such as those used in the making of tires. Functional polymers, a subset of polymer, are desirable because they are capable of function beyond that of the bulk polymer. Their synthesis is often difficult via traditional methods as the desired functionalities that must be incorporated into monomer are often sensitive and do not survive polymerization. Two ways to circumvent this problem include masking the functional group on the monomer during polymerization or introducing the functional group to polymer after polymerization. This work presents a method of producing functional polymers using both beforementioned methods. The monomer masking-unmasking method used involves shining UV light on the polymer to remove the masking group, which leaves as carbon monoxide gas — meaning no purification is required. After unmasking, the method used to introduce functionality to the polymer post-polymerization is both fast and efficient, requiring little purification. Reported herein is a novel monomer, its unique masking/unmasking method, polymerization, and post-polymerization modification to introduce functionality. This novel monomer and subsequent functionalized polymers were characterized using standard techniques such as nuclear magnetic resonance, UV-Visible, and infrared spectroscopy.

Co-Authorship Statement

The work discussed in this thesis contains contributions from the author and my supervisor Prof. Mark S. Workentin, Prof. Joe B. Gilroy, and colleague Michael Anghel. The contributions of each are described below.

Chapter 1 was written by the author and edited by Prof. Mark S. Workentin.

Chapter 2 describes the synthesis of monomer and subsequent polymer that were completed by the author, assisted by Michael Anghel. The chapter was written by the author and edited by Prof. Mark. S. Workentin.

Chapter 3 describes the post-polymerization functionalization of the monomer and polymer that were completed by the author. The chapter was written by the author and edited by Prof. Mark S. Workentin.

Chapter 4 was written by the author and edited by Prof. Mark S. Workentin.

Acknowledgments

Firstly, I would like to extend sincere appreciation to Prof. Mark S. Workentin. Your mentorship was invaluable to me, from both a technical and soft-skill perspective. This project taught me the art of chemistry far beyond where I thought it could go. Your friendship was also invaluable to me, from the personal advice to Briscola at lunch to holiday gift exchanges. You put up with my eccentricity and odd sense of humor better than most could have. Never would I have imagined that a chemistry group could have looked the way ours did and I'm proud to have been a part of molding that. You truly are a model father figure and your family are lucky to have you.

I would like to thank all the people that make the UWO Chemistry Department run as smoothly as it does. This includes Mat Willans for his management of the NMR Facility, Aneta Borecki for running all my SEC experiments, Doug Hairsine for running all my mass spectrometry experiments, and all administrative and ChemBioStores staff. I would also like to thank Dr. Mark Biesinger at Surface Science Western who assisted in consultation about and running of X-ray photoelectron spectroscopy samples.

I would like to thank my various lab mates over my time here. The social dynamic of this group is simply unparalleled. From the late-night lab antics, the lunch dates, the weekend get-togethers, and the card games to the modelling of how we would handle theoretical situations like a zombie apocalypse. They all cumulated to an amazing experience I wouldn't trade for anything. This includes but is not limited to (in no particular order) Wilson Luo, Praveen Gunawardene, Tommaso Ramagnoli, Alex Van Belois, Rajeshwar Vasdev, Justin Park, Andy Lim, Christian Petrozza, Komal Patel, Grace Lee, Johanna de Jong, and Julia Martin. A separate shout-out to Jake Rosati, who I had the pleasure of mentoring during his 4th year thesis project. You were a great student and better friend — you'll make a great teacher. To those acquaintances in the department that may be reading this, I thank you for helping shape my experience as well.

I would like to thank my friends and family for all their support throughout my time here. I couldn't have made it through undergrad let alone grad school without my parents. This includes thanking my father, Tom, the most technically/spatially intelligent person that I know for all the support, no matter the hour, with any fixing, troubleshooting, or important decision-making. This includes my mother, Lee, the most loving person that I know for all the support with any advice or anything really, even if I don't want it (stop trying to give me food). This includes my roommates, both past and present, for putting up with my beforementioned eccentricity, especially my screaming at an inanimate screen for hours on end. I truly hold on to every night out, every night in, and every bad decision we ever made and hope they continue for as long as we do. A very special mention goes to Justin Park, my roommate and friend throughout the entirety of my MSc and undergrad. Thank you for putting up with me all those years and good luck in your PhD, you'll make a great professor.

Finally, I'd like to thank my best friend Twitch. I *could not* have survived without your countless hours of entertainment. I came to you at my best times and my worst times and you were always a dependable source of mindless recharging after a long day. PeepoHappy.

Table of Contents

List of Tables

List of Figures

List of Schemes

List of Appendices

List of Abbreviations

°C	Degree Celsius
^{13}C	Carbon-13
^{1}H	Hydrogen-1 (proton)
ATR	Attenuated total reflectance
BnN_3	Benzyl azide
Bu	Butyl
$CDCl_3$	Deuterated chloroform
cm^{-1}	Wavenumber
CuAAC	Copper (I)-assisted alkyne-azide cycloaddtion
DP_n	Degree of polymerization
DIBO	Dibenzocyclooctyne
DCM	Dichloromethane
DMSO-d6	Deuterated dimethylsulfoxide
EVE	Ethyl vinyl ether
Eq.	Equivalence
FT	Fourier-transform
GPC	Gel permeation chromatography
G-III	Grubbs' 3rd generation catalyst
h	Hours

HRMS	High-resolution mass spectrometry
$h\nu$	Light Energy
Hz	Hertz
IR	Infrared
IUPAC	International Union of Pure and Applied Chemistry
kcal	kilocalorie
kg	kilogram
L	Liter
M	Molar
MeCN	Acetonitrile
min	Minutes
mL	Milliliter
mm	Millimeter
mmol	Millimole
mol	Mole
nm	Nanometer
NMR	Nuclear magnetic resonance
$\bar{M}_n$	Number-average molecular weight
$\bar{M}_w$	Weight-average molecular weight
Ph	Phenyl

PDI	Polydispersity Index
PPM	Post-polymerization modification
ROMP	Ring-opening metathesis polymerization
SEC	Size exclusion chromatography
SPAAC	Strain-promoted azide-alkyne cycloaddition
UV	Ultraviolet
UV-Vis	Ultraviolet-Visible
λ_{max}	Wavelength of maximum absorption
δ	Chemical shift
μmol	Micromole

Chapter 1

1 Introduction

Polymers are an integral part of modern life and make up a variety of important industrial goods such as plastics, fibers, and rubbers. The word “polymer” was introduced in 1833 by Swedish chemist J.J. Berzelius, though the definition is distinct from the modern IUPAC definition.[1] The modern representation of polymers as “macromolecules composed of repeating subunits” emerged in the 1920s amid prolonged controversy by Hermann Staudinger, who later won the Nobel Prize in Chemistry in 1953 for work supporting this hypothesis.[2] The standing definition of polymers outlined in the IUPAC Gold Book is: “a molecule of high relative molecular mass, the structure of which essentially comprises the multiple repetition of units derived, actually or conceptually, from molecules of low relative molecular mass”.[3] A simplified representation of a monomer and polymer is shown in **Scheme 1**.

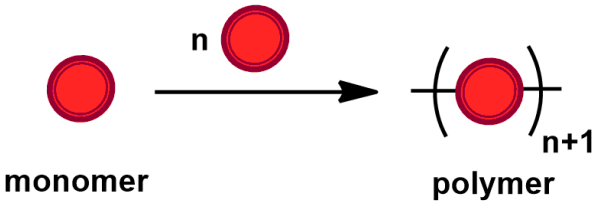

Scheme 1. Simplified representation of a monomer and a polymer.

In general, most commercial polymers feature carbon-carbon and carbon-hydrogen covalent bonds along the backbone as their primary structure. Though, polymers containing heteroatoms such as nitrogen[4], oxygen[5], fluorine[6], and various metals[7,8] have been thoroughly researched as well as polymers containing ionic[9] and metallic bonds.[10]

Polymer structure also relies on secondary interactions between polymer chains including dipole-dipole interactions, London dispersion forces, and hydrogen bonding.[11] These secondary forces are exemplified in proteins, natural macromolecules comprised of chains made up of amino acid monomers, which rely heavily on hydrogen bonds between these amino acid groups in the chains to form highly regular substructures (**Scheme 2**).[12] Proteins are responsible for a variety of functions within organisms such as reaction catalysis and molecule transportation.[12]

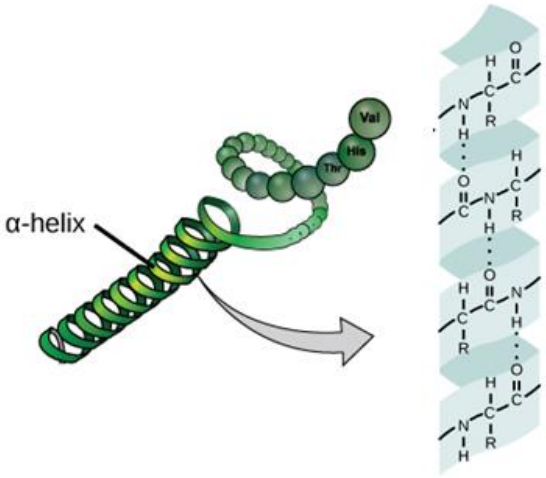

Scheme 2. The secondary structure, α-helix, of a protein that forms as a result of the hydrogen bonding between amino acid groups in the protein backbone. Scheme taken and modified from Clark et. al.[12]

Though primary and secondary structures of polymers govern the majority of their overall structure and function, many of their properties also exhibit a strong dependence upon the size of the polymer chains.[13] These polymer chains vary in their molecular weight and are most accurately described as having a distribution of molecular weights, though are often communicated as an average. The distribution is most often expressed by the following three main parameters[13]:

1. The *number-average molecular weight* $\bar{M}_n$, defined as the sum of the products of the molecular weight of each chain and the number of chains with that molecular weight divided by the sum of the number of chains in a polymer sample.

$$\bar{M}_n = \frac{\sum N_i M_i}{\sum N_i}$$

Where M_i is the molecular weight of a polymer chain and N_i is the number of polymer chains with weight M_i .

2. The *weight-average molecular weight* $\bar{M}_w$, which places a higher mathematical "weight" on the term M_i so as to compensate for the tendency of larger chains to have more contribution to certain polymer properties based on their higher molecular weight.

$$\bar{M}_w = \frac{\sum N_i M_i^2}{\sum N_i M_i}$$

3. *Polydispersity index* (PDI), the measure of the breadth of the molecular weight distribution of a polymer sample. A polymer sample with a PDI of 1.0 is defined as monodisperse and values larger than unity are considered polydisperse.

$$PDI = \frac{\bar{M}_w}{\bar{M}_n}$$

Polymers may be synthesized in a variety of different manners, which are classified into two categories: chain-growth polymerization and step-growth polymerization. Chain-growth polymerization is initiated by the reaction of monomer and initiator, which makes

a number of polymer chains that propagate by reaction with remaining monomer (**Scheme 3A**).[14] This polymerization method generally results in more narrow molecular weight distributions (lower PDI).[14] Commercially made polymers such as polyethylene, polypropylene, and polyvinyl chloride are synthesized by this method.[15] Step-growth polymerization is initiated by the reaction of monomers with each other, which makes a number of polymer chains that propagate by reaction with each other or remaining monomer (**Scheme 3B**).[16] It is generally more difficult to control molecular weight with this method which results in more broad molecular weight distributions (higher PDI).[16] Commercially made polymers such as polyethylene terephthalate and Nylon-6 are synthesized by this method.[17]

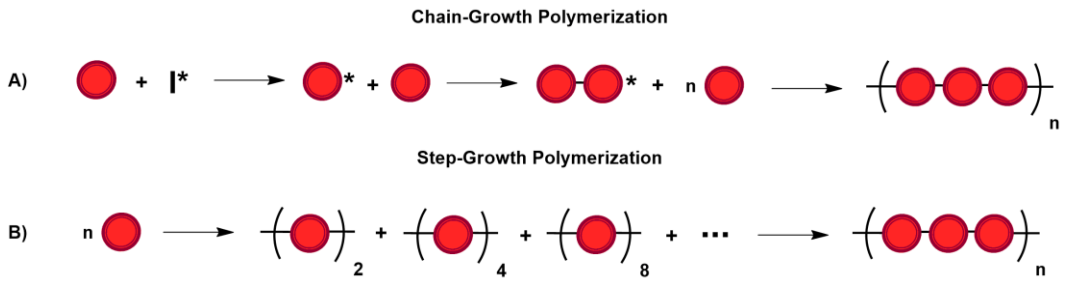

Scheme 3. A simplified representation of a A) chain-growth polymerization and a B) step-growth polymerization.

Many polymerization methods suffer from undesired reactivity during polymerization, causing broader molecular weight distributions and thus less control over PDI and targeted molecular weight. Two of the main mechanisms by which this occurs are chain termination reactions, any reaction that ceases the formation of reactive species in a propagation step, and chain transfer reactions, any reaction that causes the reactive species in a propagation step to be transferred to another molecule or another site on the same molecule.[15] Polymerization methods which eliminate these factors are known as “living”

polymerizations, as defined and demonstrated by Michael Szwarc in 1956.[18] "Living" polymerizations are desirable in applications which require precise molecular weight control, such as materials design.[19] One type of polymerization that may be considered "living" is ring-opening metathesis polymerization (ROMP), if it meets Szwarc's original constraint as well as the following three characteristics[20]: (1) fast and complete initiation of monomer such that the rate at which initiating agent activates monomer occurs much more rapidly than chain propagation, (2) a linear relationship between degree of polymerization (DP; the number of monomer units that comprise each polymer chain) and monomer consumption, and (3) a PDI of <1.5.

ROMP is a chain growth polymerization where cyclic alkenes are converted to a polymeric material (**Scheme 4**). It is known to have exceptional functional group tolerance and molecular weight /PDI control, making it a powerful and broadly applicable method for synthesizing macromolecular materials.[21–23]

Scheme 4. General reaction scheme for the ROMP reaction.

The mechanism of polymerization is based on alkene metathesis, a metal-mediated carbon-carbon double bond exchange process (**Scheme 5**).[24] Initiation involves coordination of a transition metal alkylidene complex to a cyclic alkene and propagation involves subsequent [2+2]-cycloadditions involving a four-membered metallacyclobutane intermediate that effectively forms a growing polymer chain.[25] This intermediate then undergoes cycloreversion to afford a new metal alkylidene and the aforementioned process repeats

until polymerization ceases (all monomer consumed, reaction equilibrium reached, or termination).[25] These reactions are driven by release of ring strain in the cyclic alkene monomers, most of which possess a considerable degree of strain (>5 kcal/mol) such as cyclobutene, cyclopentene, and norbornene.[26]

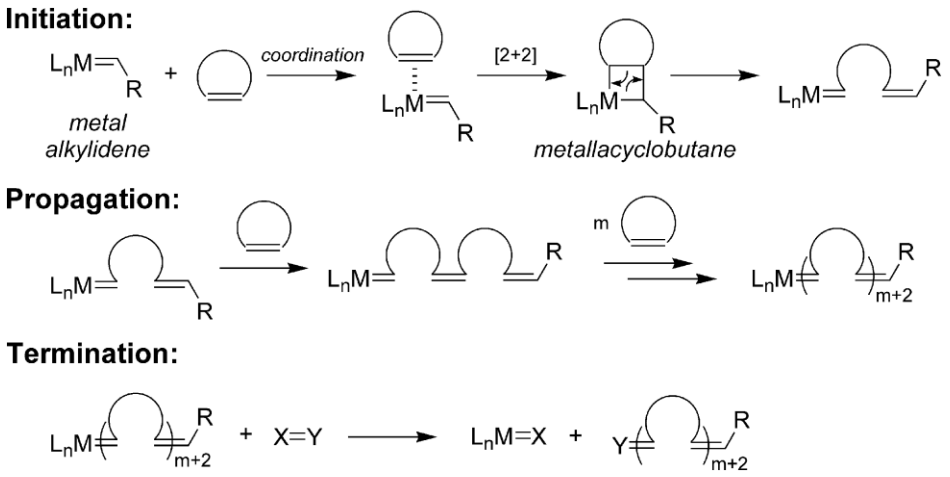

Scheme 5. A generalized reaction mechanism of a typical ROMP reaction.

There are many transition metal catalysts used in ROMP, including a variety of metals such as titanium[27], tantalum[28], tungsten[29], molybdenum[30], and ruthenium.[31] More recently, a set of ruthenium alkylidene catalysts developed by Grubbs and coworkers were shown to be very effective in synthesizing polymers via "living" ROMP. The 1st generation Grubbs' catalyst (**Scheme 6A**) was developed as an alternative to prior work on ruthenium vinylidene complexes that showed poor control over chain transfer reactions[32]. Though chain transfer reactions were mitigated and functional group tolerance increased, it showed slow initiation kinetics.[33,34] To address this problem one of the trialkylphosphine ligands was replaced with a less labile N-heterocyclic carbene, to make the 2nd generation Grubbs' catalyst (**Scheme 6B**).[35,36] The 2nd generation catalyst showed significantly increased activity, though control over molecular weight and PDI showed to

be poor due still to slow initiation kinetics.[37] A further adjustment, replacing the remaining trialkylphoshine ligand and a chloride ligand with a weakly coordinating pyridine derivative, proved to increase reaction kinetics significantly and allowed for high control over molecular weight and very low PDIs, leading to the 3rd generation Grubbs' catalyst (G-III) (**Scheme 6C**).[38,39] As an example, this 3rd generation catalyst has been shown to mediate the ROMP of norbornene and a variety of its derivatives with extremely low PDIs (1.05-1.10) and high molecular weight control.[39]

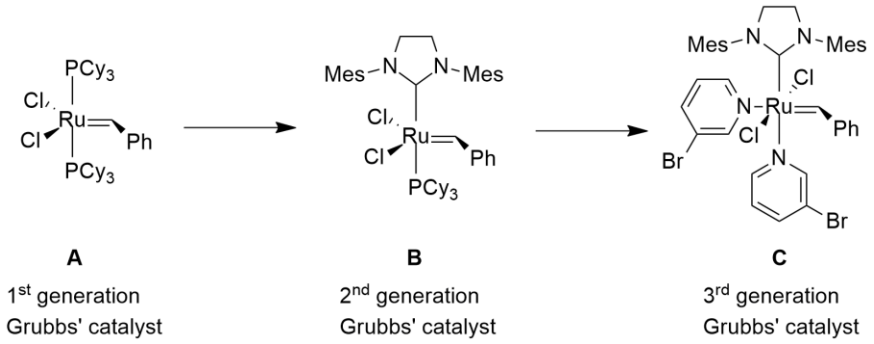

Scheme 6. Ruthenium-based alkylidene catalysts developed by Grubbs and coworkers commonly utilized in ROMP reactions.

Certain polymerization methods, especially those considered "living", allow for the synthesis of polymers with precise control over molecular weight, composition, and architecture. This control has allowed for polymers with a variety of different functions to be synthesized, owing to impactful applications such as drug delivery systems[40], self-healing materials[41], and electronic chemical sensors[42]. However, the design of functional polymers often requires that sensitive functional groups be incorporated into their monomers. These functional groups may be susceptible to side reactivity related to polymerization method, not allowing for direct polymerization of the functional monomer. To work around this, functional polymers may be synthesized by the polymerization of

protected monomers – monomers which have functional groups that have been "protected" in some manner from susceptibility to side reactivity. This requires the resulting protected polymer to be deprotected in order to reveal the desired functionality. An example by Noga *et. al.* exemplifies this strategy, using benzyl protecting groups to protect alcohol groups on a lactide monomer that was polymerized and then deprotected to reveal the alcohol groups (**Scheme 7**).[43] Upon further modification, these functional polymers have numerous potential biomedical applications.[43]

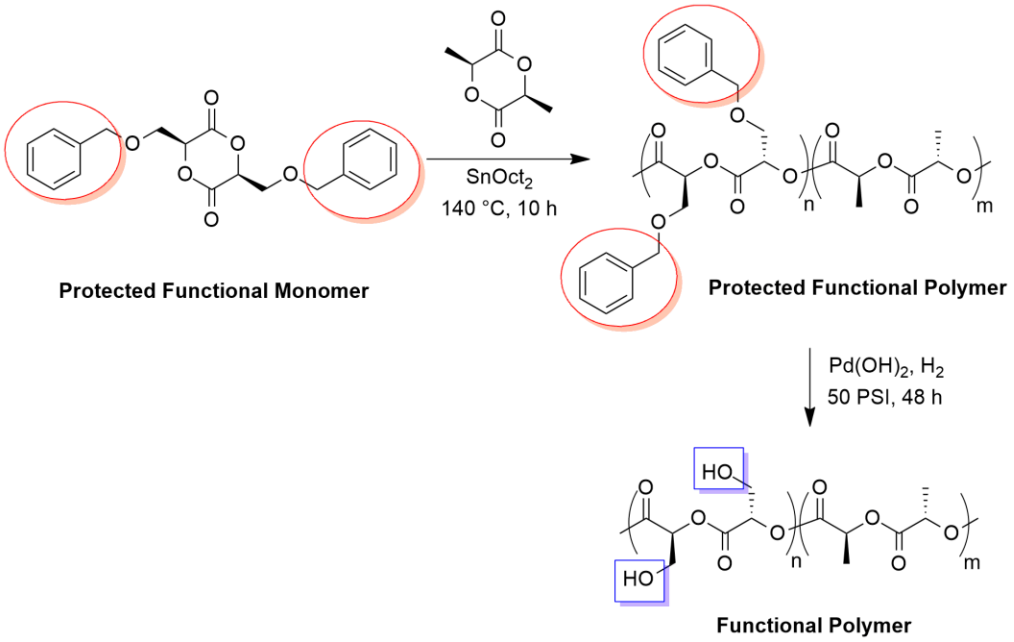

Scheme 7. A route to functional polymers via monomer protection, polymerization, and subsequent polymer deprotection.[43]

Functional polymers may also be synthesized by post-polymerization modification (PPM), a method by which polymers are modified by reaction after polymerization has taken place. This is done by polymerization of monomers with functional groups that are inert to polymerization conditions, but which can be quantitatively converted in a subsequent reaction into a range of other functional groups.[44] An example by Gillies and

coworkers utilized thiol-ene chemistry to functionalize pendant alkene groups on a polymer with various functional thiols (**Scheme 8**).[45] Thiols used included hydrophilic and hydrophobic chains to tune self-assembly and a fluorescent molecule (Rhodamine B derivative) for applications in imaging, self-assemblies, and drug delivery.[45]

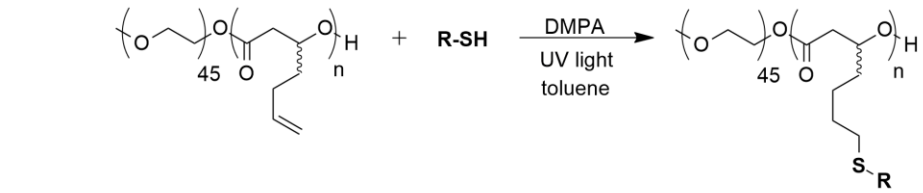

R =

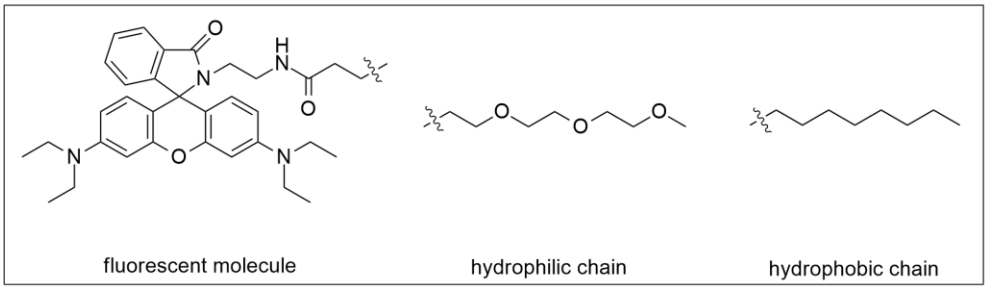

Scheme 8. A route to functional polymers via PPM using thiol-ene chemistry.

Another reaction type capable of synthesizing functional polymers are "click" reactions. Defined as reactions that are highly efficient, require minimal purification, have rapid reaction times, are stereo- and regio-specific, and are highly orthogonal to other reactions.[46] Arguably the most popular of these is the copper(I)-assisted azide-alkyne cycloaddition (CuAAC) which utilizes a copper(I)-catalyst in a Huisgen 1,3-dipolar cycloaddition between an azide an a linear alkyne to afford a 1,2,3-triazole ring (**Scheme 9**).[47] The power of CuAAC came from the ability to construct complex structures that were previously difficult to obtain such as polymer architectures[48] and biomaterials.[49] However, its use in systems relevant to biological applications is limited due to the cytotoxicity of excess copper(I), which aids in the degradation of certain biomolecules.[50]

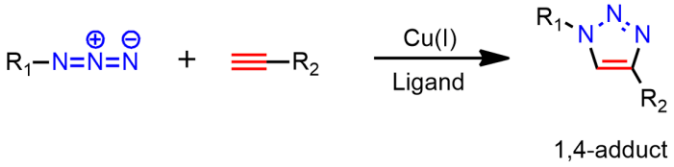

Scheme 9. General reaction scheme for the CuAAC reaction.

A necessity to investigate the activation of the alkyne by other means was realized, and addressed, by Bertozzi and coworkers in their discovery that ring-strain promotes the Huisgen cycloaddition to rates that allow for the omission of a copper(I)-catalyst.[51] This reaction, aptly named the strain-promoted azide-alkyne cycloaddition (SPAAC) (**Scheme 10**), was found to have reaction rates dramatically higher than that of its unstrained counterpart.[52] Despite still having rates multiple orders of magnitude lower than observed for CuAAC[53], they were successfully able to employ the SPAAC for selective modification of biomolecules and living cells with no negative effects on cell viability.

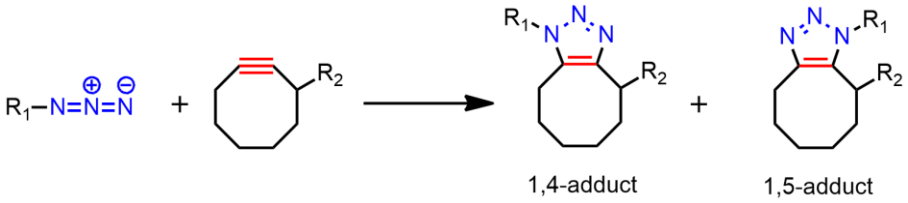

Scheme 10. General reaction scheme for the SPAAC reaction.

There have been many different strained alkynes developed for the SPAAC reaction. The stability of these cyclic alkynes rapidly decreases with decreasing ring size, with the smallest isolable cycloalkyne found to be cyclooctyne.[54] The acetylene C-C bond angle in cyclooctyne is 163°, significantly deviated from the ideal 180° angle of sp-hybridized carbon atoms.[55] The experimentally determined ring strain of cyclooctyne is ~18 kcal/mol[56] as compared to ~12 kcal/mol for a saturated cyclooctane.[57] This has

made the cyclooctyne arguably the most popular of strained alkynes, with many functionalized derivatives having been synthesized so as to further increase their reactivity, to create sites of conjugation for further modification, and to reduce lengthiness/increase yield of synthesis (**Scheme 11**).

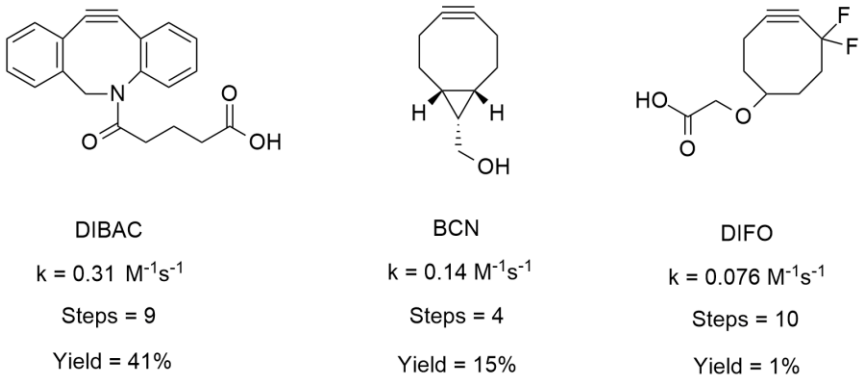

Scheme 11. Examples of modified cyclooctyne reagents for SPAAC.[55]

The SPAAC reaction has been used in the development of a variety of applications including in-vivo imaging[51], topological polymers[58], and step-growth polymer synthesis.[59] Polymer chemistry and SPAAC chemistry tend to coincide due to the simplicity by which polymers may be modified by SPAAC. An example from the Adronov group at McMaster University used SPAAC chemistry post-polymerization to tune the solubility of a fluorescent, strained-alkyne-containing polymer to make hydrogels with potential applications as fluorescent materials (**Scheme 12**).[60] Remarkably, the strained alkyne was able to survive polymerization due to the use of a relatively mild condensation polymerization. This allowed for a strained alkyne to be incorporated into every repeating unit and quantitative functionalization via SPAAC to be achieved. Though, the reported method lacks compatibility with “living” polymerization methods and these polymers suffer from low molecular weight control and high PDIs. Thus, a need to protect the

strained alkyne during polymerization to allow for more harsh “living” polymerization methods still remains.

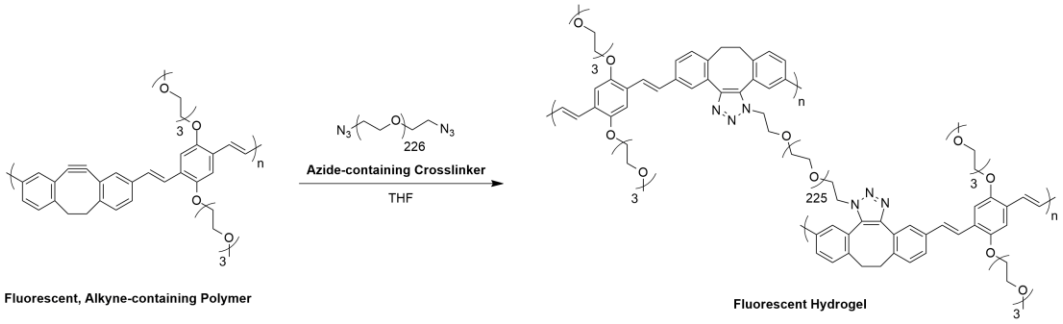

Scheme 12. An example of SPAAC chemistry being used to make polymeric materials.

The increased reactivity of cyclic alkynes that allow for SPAAC to be possible is also the same reason that these reagents are susceptible to side reactivity, such as nucleophilic attack, making applications requiring orthogonality an issue (**Scheme 13a**). A solution to this problem was put forth when the Popik group reported a cyclopropenone-masked dibenzocyclooctyne (hvDIBO) that undergoes decarbonylation in the presence of UV irradiation to yield dibenzocyclooctyne (DIBO) (**Scheme 13b**).[61] This protecting group strategy allows for cyclooctynes to be protected during modification, as often necessary for their inclusion into materials due to their reactive nature in the unprotected state. This strategy is also advantageous in that the only byproduct is carbon monoxide gas, no purification is required, yields are quantitative, and it allows for spatiotemporal control of the SPAAC reaction.[62–64]

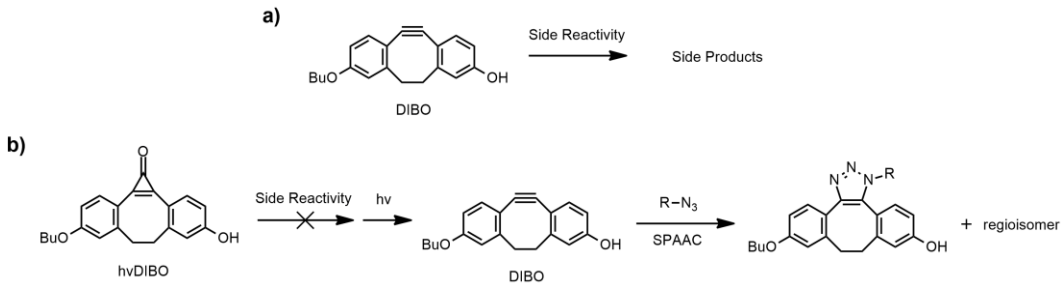

Scheme 13. The cyclopropenone masking strategy of DIBO as reported by Popik and coworkers[61], showing the **a**) susceptibility of unmasked DIBO to side reactivity and **b**) orthogonality of hνDIBO.

This unique spatiotemporal control allows for photopatterning, as shown by Orski *et. al.* in the synthesis of multifunctional polymeric surfaces utilizing SPAAC click chemistry and the cyclopropenone masking strategy of hνDIBO (**Scheme 14**).[65] First, silicon wafers were decorated with a monomer, containing an activated ester group, that was polymerized directly from the surface. A ligand-decorated hνDIBO derivative was then coupled onto the activated ester group on each repeating unit of the polymer. Next, the surface was covered by a square-patterned transmission electron microscope grid and irradiated with UV light to decarbonylate all exposed cyclopropenone. The exposed DIBO molecules were then reacted with Rhodamine-B-azide (550 nm excitation). The grid was then removed, the surface irradiated, and remaining DIBO functionalized with Fluorescein-azide (477 nm excitation). This example shows the power of hνDIBO and the photopatterning technique that the masking strategy allows for, exemplified by the unique ability to create multifunctional materials. Though, SPAAC functionalization was only possible via strained alkynes on the end of each polymer, which does not allow for the same degree of functionalization as if a strained alkyne was included in each repeating unit of the polymer.

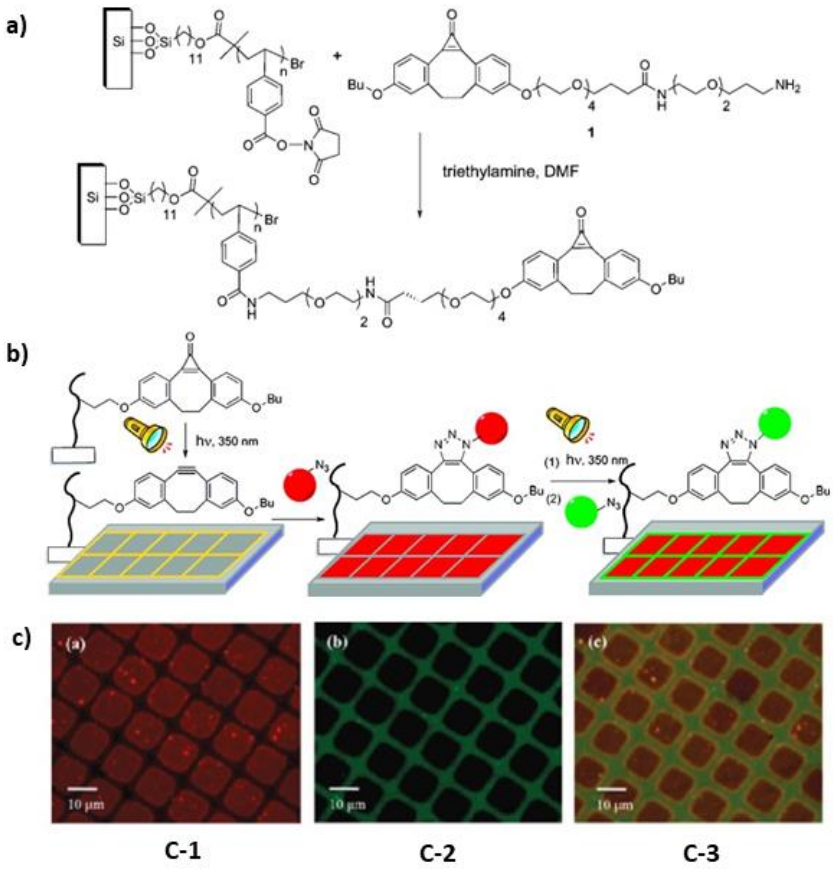

Scheme 14. The synthesis of multifunctional surfaces utilizing surface-bound polymers and the SPAAC click chemistry of DIBO. The synthesis of a a) hνDIBO-decorated, polymer-bound silicon surface that was b) photo-patterned and functionalized via the SPAAC reaction. Fluorescence microscope images of a photo-patterned surface of click-functionalized Rhodamine-B excited at 550 nm (C-1), Fluorescein excited at 477 nm (C-2), and excitation of both dyes under wide-UV excitation at 350 nm (C-3) are shown in c). Schemes taken directly from Orski *et. al.*[65]

The power of click chemistry and the SPAAC reaction has been demonstrated with other types of materials as well. Materials such as polymeric nanoparticles[66], quantum dots[67], polymer-wrapped carbon nanotubes[68], and silicon nanoparticles[69] have all been modified with the use of SPAAC chemistry. Previous work in the Workentin Group showed the ability to decorate small, water-soluble gold nanoparticles with strained alkyne moieties, via the cyclopropenone mask/unmask strategy of hνDIBO, for the surface modification and engineering of functional nanomaterials.[70] This strategy was amenable

to various 1,3-dipoles for the SPAAC reaction including a complex drug model, representing the versatility of potential materials that can be synthesized using this chemistry.

There are many different functionalities that may be introduced to a polymer via SPAAC chemistry. Some of these include nanomaterials such as carbon nanotubes[71], biomolecules such as lactose[72], fluorescent molecules such as Rhodamine-B[73], and other polymers[74]. Another suitable candidate for polymer functionalization using SPAAC chemistry are gold nanoclusters, nanoparticles comprised of a gold core with unique electronic, magnetic, and chemical properties making them prominent nanomaterials with applications in chemical sensing[75], catalysis[76], and optical imaging.[77] Recent work in the Workentin group revealed a novel gold-25 (Au_{25}) nanocluster decorated with 18 azide-appended ligands ($[(CH_3\text{-}(CH_2)_7)_4N][Au_{25}(SCH_2CH_2\text{-}p\text{-}C_5H_4\text{-}N_3)_{18}]$), capable of interfacial surface SPAAC.[78] These novel Au_{25} nanoclusters are ultrasmall (<2 nm), atomically precise, and allow for all surface azide moieties to be functionalized, opening this as a new platform to allow for functional, post-assembly surface modifications.

The ideal functional polymer would generally possess the following characteristics: it may be functionalized with a variety of substrates, functionalized to a high degree, and polymerized with high control over molecular weight and PDI. SPAAC chemistry provides a clean, rapid way to functionalize a polymer with a wide variety of substrates.[51,58,59] A strained alkyne included in every repeating unit of a polymer allows for functionalization of the polymer via SPAAC to a high (quantitative) degree.[60] A way to introduce this strained alkyne such that it is compatible with polymerization conditions, via a unique cyclopropenone masking strategy, is possible.[61–65] Polymers synthesized by “living”

ROMP allow for high molecular weight and low PDIs.[39] The realization that these principles could be combined to design a functional polymer template synthesized by "living" ROMP capable of being functionalized to a high degree with a variety of substrates was realized by Prof. Workentin and Prof. Gilroy at the University of Western Ontario in the design of a monomer containing a ROMP-compatible norbornene group and hνDIBO.[79] This novel monomer, as shown by work contributing to an MSc thesis by Rajeshwar Vasdev, was synthesized in good yield and polymerized via ROMP successfully. The resulting polymer was then unmasked, revealing the strained alkyne in every repeating unit. The polymer was then successfully functionalized to a high degree with three functional substrates (small molecules), showing the ability to functionalize this polymer via SPAAC post-polymerization. The polymerization did not technically meet all criteria to be considered a formally "living" polymerization but was considered a well-behaved process. The polymerization also took longer than desired (optimal time of ~90 mins) and possessed PDIs above 1.6. This was hypothesized to be attributed to the structure of the norbornene portion of the monomer. My work involves the redesign of this novel monomer to a less flexible, more hydrolytically stable, and potentially more reactive version in an attempt to bring this polymerization from "well-behaved" to formally "living" (**Scheme 15**). This choice of monomer was based upon work by Choi and Grubbs in 2003, where they showed the ability to polymerize a similar structure of monomer by ROMP with a high degree of molecular weight control and low PDI (1.08) in just 30 mins.[39] My work also attempts to branch out from the functional small molecules introduced via SPAAC to the polymer by Rajeshwar – to make a polymer-Au_{25} material hybrid via SPAAC post-polymerization using a Au_{25} azide substrate.

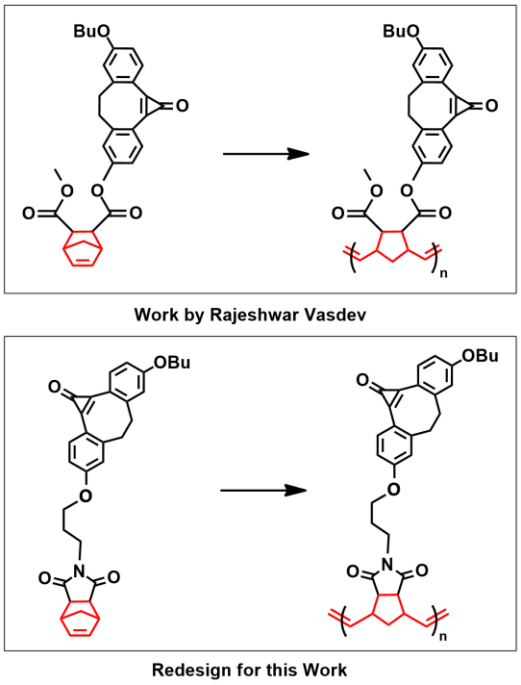

Scheme 15. The redesign of a novel monomer for the synthesis of a functional polymer template

Herein described is a strategy for synthesizing well-defined, high molecular weight functional polymers with high molecular weight control and low PDIs. First, a polymerizable unit, a derivative of norbornene, was covalently linked via a short alkyl chain to hvDIBO. This monomer, which contains a cyclopropenone group masking a strained alkyne, was then polymerized via ROMP of the strained alkene of norbornene using G-III. Next, the cyclopropenone groups in the polymer were decarbonylated by irradiation with UV light, revealing the strained alkyne in every repeating unit of the polymer. Finally, the polymer was functionalized via PPM by SPAAC using a model azide and then a Au_{25} nanocluster decorated with azide groups. This functional polymer, and its subsequent unmasked and functionalized derivatives, were then characterized using standard polymer characterization methods. This strategy is powerful in that it involves

both polymer functionalization strategies described earlier: the protected monomer and PPM strategies (**Scheme 16**). The reactive group on the monomer, the strained alkyne, is protected using the cyclopropenone masking strategy which allows for a well-defined, highly controlled polymerization to occur without side reactivity of the strained alkyne. The PPM strategy, introducing functionality via functional azide to perform SPAAC, is used once the strained alkyne has been unmasked in every repeating unit of the polymer. This strategy is also unique because every single repeating unit of the polymer is decorated with a (masked) strained alkyne. This allows for full functionalization of the polymer post-unmasking, demonstrating the usefulness of the polymer as a functional material template. The demonstration of the power of this type of polymer may also be shown by the ability to modify it with not only functional small molecules but with gold nanoclusters, allowing for the synthesis of more complex multifunctional materials.

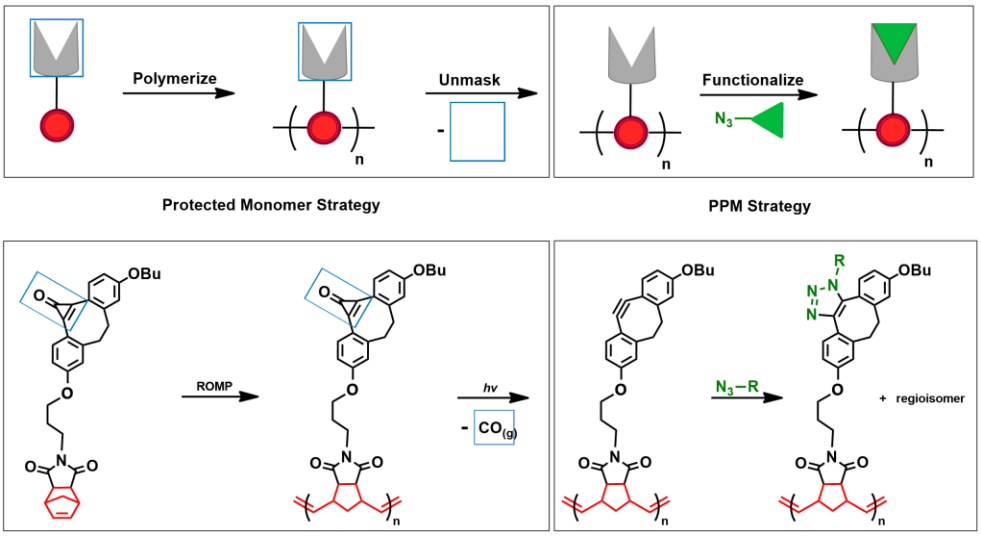

Scheme 16. ROMP and SPAAC functionalization of a novel polymer using a masked alkyne and both protected monomer and PPM strategies

It should be noted that this work was interrupted during a critical time in the evolution of the project (specifically Chapter 3) by the COVID-19 crisis just before the spring of 2020 through the summer of 2020. The completion of work during this time, once research was gradually reopened, was performed safely and under strict adherence to guidelines communicated by the Government of Canada and The University of Western Ontario regarding the COVID-19 situation.

Chapter 2

2 Synthesis of a Masked Strained Alkyne Polymer

2.1 Introduction

In recent years, a plethora of functional polymers have been developed for applications such as drug delivery[40], self-healing materials[41], electronic chemical sensing[42], and biomedical imaging.[45] These systems often require a high degree of control over the polymerization method used. Methods known as "living" polymerizations offer precise control over molecular weight, composition, and architecture and are thus desired in functional polymer synthesis. However, functional polymers often contain sensitive functional groups in their monomers which may limit the control over their polymerization. There are two ways to circumvent this complication. The first involves the protection of sensitive functional groups for the duration of the polymerization. Following polymerization the functional group is then deprotected, exposing the desired functionality. The other way involves the modification of a polymer after polymerization has taken place, known as post-polymerization modification (PPM). PPM is achieved by polymerization of a monomer with a functional group that is inert to polymerization conditions and that can be converted to a desired functionality in a subsequent reaction post-polymerization. Chapter 2 presents the synthesis of a functional polymer template utilizing both the protecting group and PPM strategies.

The synthesis and characterization of a hνDIBO-monomer (**6**) with a masking/unmasking strategy allowing it to be polymerized, unmasked, and the subsequent polymer functionalized via PPM is shown. This strategy involves the protection of a cyclic alkyne with a cyclopropenone moiety, capable of deprotection via exposure to UV light.

The deprotection step only entails the evolution of carbon monoxide gas meaning no purification is required and since UV light exposure can be controlled, the process has spatiotemporal control. The amenability of this strategy has been demonstrated by Popik and coworkers in the synthesis of multifunctional surfaces utilizing surface-bound graft copolymers decorated with hvDIBO moieties.[65] It has also been demonstrated by previous work in the Workentin group, shown by the ability to functionalize small, water-soluble gold nanoparticles using hvDIBO to make functional nanomaterials.[70]

The polymerization of (**6**), yielding hvDIBO-polymer (**13**), is also presented showcasing the ability to make a polymer with a hvDIBO moiety in every repeating unit. The polymerization method used is ring-opening metathesis polymerization (ROMP) using a Grubbs' 3rd generation catalyst derivative. The resulting unmasking and functionalization of this polymer is demonstrated in Chapter 3.

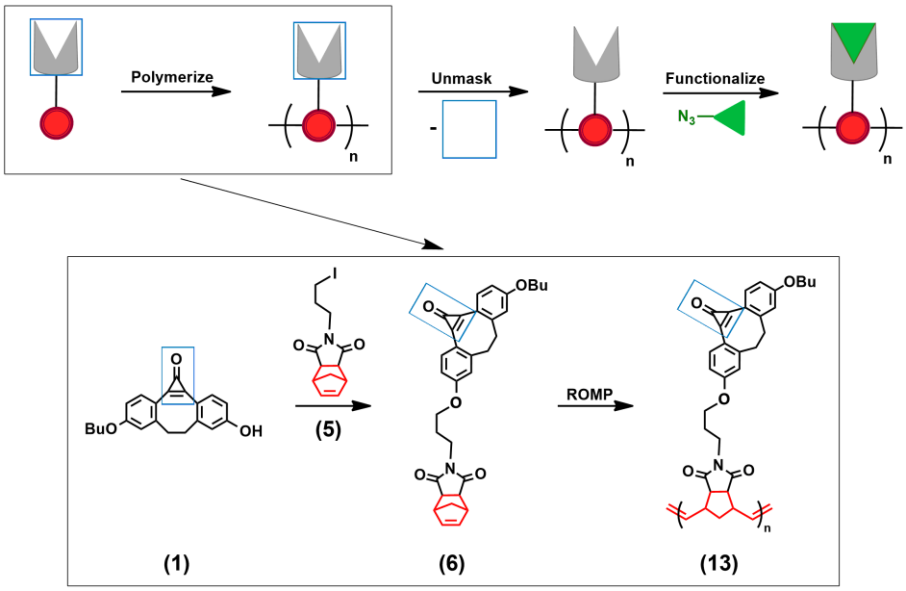

Scheme 17. General scheme of the polymerization, unmasking, and PPM functionalization of masked monomer. Highlighted in the black box is a scheme for the synthesis and polymerization of masked monomer.

2.2 Results and Discussion

2.2.1 Synthesis and characterization of the hvDIBO-monomer

The cyclopropenone-protected strained alkyne, hvDIBO (**1**), was synthesized using a procedure developed by Arnold et al. (**Appendix 2-A)**.[80] To be incorporated into a monomer capable of ROMP, it was envisioned that the phenolic alcohol group would be used to couple hvDIBO to a norbornene derivative. The norbornene derivative chosen, fitted with an imide group, was chosen extending upon work by former group member Rajeshwar Vasdev and based upon published work by Choi and Grubbs.[39]

To synthesize the final monomer, first the norbornene derivative had to be modified for coupling to (**1**). Cis-5-norbornene-exo-1-propanol-2,3-dicarboxylic anhydride (**2**) was modified with a propyl chain terminated in an iodide leaving group (**5**), and condensed with (**1**) via nucleophilic substitution to yield hvDIBO-monomer (**6**) as a white, fluffy, shiny solid (**Scheme 18**).

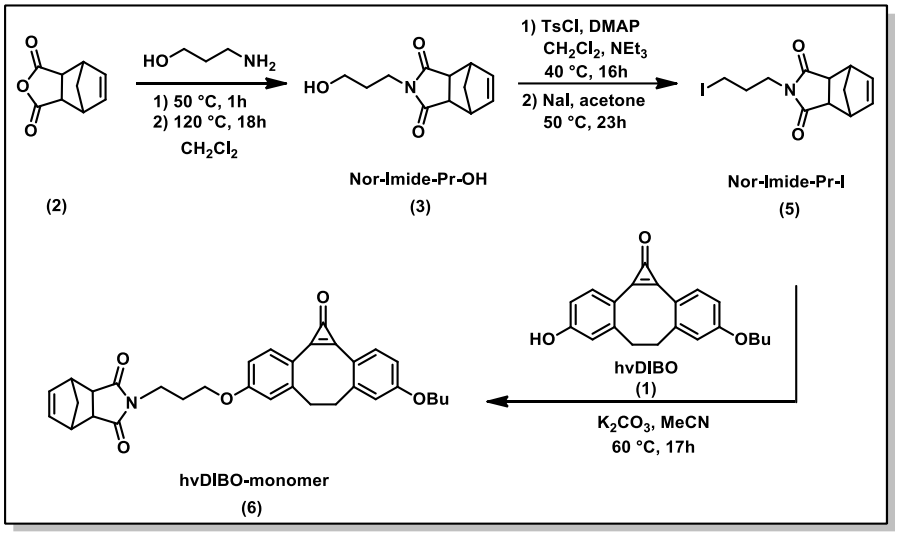

Scheme 18. The synthesis of hvDIBO-monomer (**6**) by the condensation of a norbornene derivative (**5**) and hvDIBO (**1**).

The characterization of (**6**) was completed using ^{1}H and ^{13}C nuclear magnetic resonance (NMR) spectroscopy and high-resolution mass spectrometry (HRMS) (**Appendix 2-D**). The ^{1}H NMR spectrum showed incorporation of signals from (**1**), most notably those from the phenyl rings at 7.93-7.96 ppm and 6.84-6.91 ppm and the cyclooctyl ethane bridge at 3.31-3.35 ppm and 2.58-2.66 ppm. The ^{1}H NMR spectrum also showed incorporation of signals of (**5**), most notably those from the alkene in the bicycle at 6.28-6.30 ppm and the bridgehead positions at 2.68-2.70 ppm. A ^{1}H NMR comparison of hνDIBO (**1**), iodide-functionalized norbornene derivative (**5**), and hνDIBO-monomer (**6**) illustrates the final coupling reaction (**Figure 1**). The signals from the phenyl rings of (**1**) (top, **purple**) at 7.93-7.96 ppm (**purple triangle**) and 6.84-6.91 ppm (**black square**), as well as the diagnostic signals from the alkene in the bicycle of (**5**) (middle, **pink**) at 6.28-6.30 ppm (**pink circle**), were retained in the spectrum of monomer (**6**) (bottom, **gold**).

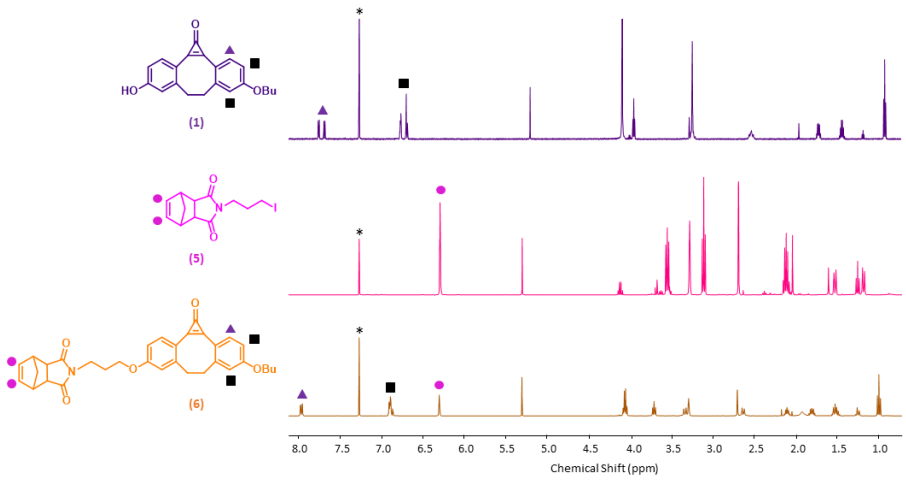

Figure 1. A comparison between ^{1}H NMR spectra ($CDCl_3$) of hνDIBO (**1**) (top, purple), Norbornene derivative (**5**) (middle, pink), and hνDIBO-monomer (**6**) (bottom, gold). Asterisks (*) denote solvent signals.

The ^{13}C NMR spectrum showed the presence of (**1**), most notably from the cyclopropenone alkene and carbonyl signals at 154.2 ppm and 161.9 ppm, respectively. The ^{13}C NMR spectrum also confirmed presence of (**5**), most notably from the imide carbonyl signal at 178.5 ppm. The HRMS spectrum for (**6**) was calculated to have an m/z of 523.2359, which is in agreement with the experimental m/z found to be 523.2356. This characterization data suggests the successful synthesis of the hvDIBO-monomer (**6**).

2.2.2 hvDIBO-catalyst compatibility study

Ring-opening metathesis polymerization proceeds via metathesis of a strained alkene, in this case that of norbornene. This process requires a catalyst, of which a 3-bromopyridine derivative of G-III was chosen for its functional group tolerance, air-stability, and fast initiation and propagation rates.[39] The fast initiation rates of G-III yields the potential to result in a "living" polymerization capable of making polymers with very narrow molecular weight dispersions (< 1.10).[39]

The G-III catalyst reacts rapidly with strained alkenes. The monomer, hvDIBO-monomer (**6**), contains not only the strained alkene of the norbornene group, but also a strained alkene in the cyclopropenone masking group of hvDIBO. It would be undesirable to have the cyclopropenone alkene be metathesized in favour of the norbornene alkene, thus a compatibility study was devised to test the reactivity of G-III catalyst with hvDIBO. Grubbs' catalysts are known to react with primary alcohol groups[81] and since hvDIBO contains a phenol group it was decided that caution should be taken. A modified version of hvDIBO was synthesized to circumvent this potential complication. This compound (**7**) bears an ether with a butoxy group where the original phenol alcohol was, installed via a nucleophilic substitution reaction between (**1**) and butyl bromide. To test reactivity with

G-III, polymerization-like conditions were simulated. Compound (**7**) was subjected to catalyst for 1 hour at 0 °C in DCM under a nitrogen atmosphere. **Scheme 19** shows the synthesis of (**7**) and the subsequent G-III compatibility study:

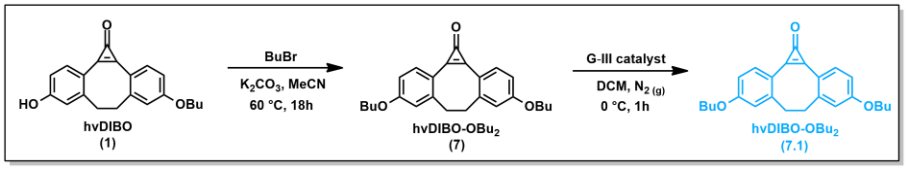

Scheme 19. The synthesis of hvDIBO-OBu_2 (**7**) and the subsequent G-III compatibility study.

To track potential changes in structure FT-IR, UV-Vis, and ^{1}H NMR spectroscopy were performed both before (**7**) and after (**7.1**) G-III exposure (**Appendix 2-E**). It should be noted that the FT-IR and UV-Vis spectra for (**7.1**) were obtained after purification by pipette column chromatography using alumina gel (DCM eluent) to separate the substrate, and/or any byproducts, from the G-III catalyst remaining in solution. The FT-IR spectra of (**7**) (**black**) and (**7.1**) (**cyan**) were identical in features, including diagnostic peaks at 2872-2955 cm^{-1} corresponding to C_{sp^3}-H stretching, 3030-3060 cm^{-1} corresponding to C_{sp^2}-H stretching, 1841 cm^{-1} corresponding to C=O stretching of the cyclopropenone ketone, and 1598 cm^{-1} corresponding to the C=C stretching of the cyclopropenone alkene (**Figure 2**). This confirms that the cyclopropenone remained intact during the course of the experiment.

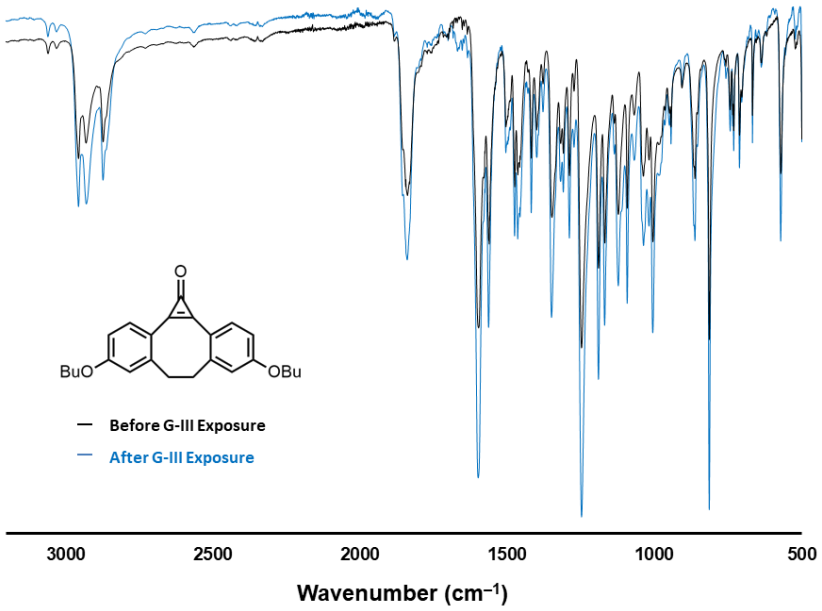

Figure 2. Overlay of FT-IR spectra of hνDIBO-OBu_2 before (**7**) (black) and after (**7.1**) (cyan) G-III exposure.

The UV-Vis spectra of (**7**) (**black**) and (**7.1**) (**cyan**) were also identical in features, including bands at 331-349 nm corresponding to the cyclopropenone group and bands at 240-260 nm corresponding to the two phenyl rings (**Figure 3**). This confirms that the cyclopropenone remained intact during the course of the experiment. The decrease in absorbance can be attributed to the loss of some material during the pipette column.

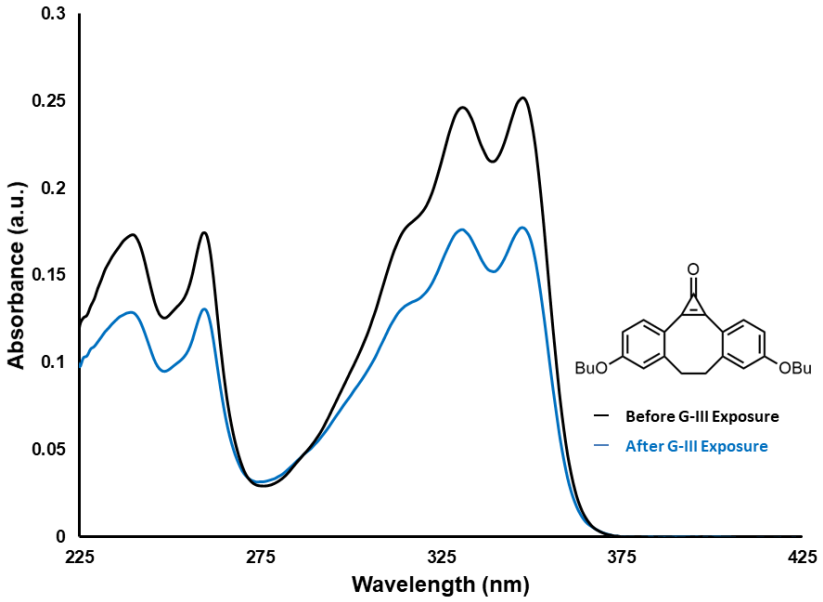

Figure 3. Overlain UV-Vis spectra, obtained in DCM at $1x10^{-5}$ M, of hvDIBO-OBu2 before (**7**) (black) and after (**7.1**) (cyan) G-III exposure.

An impurity, the identity of which could not be determined, was found in the crude ^{1}H NMR of (**7.1**) (<5% by ^{1}H NMR analysis).

2.2.3 Polymerization of the hvDIBO-monomer by ROMP

The first polymerization of hvDIBO-monomer (**6**) was performed to confirm the compatibility of this novel monomer with ROMP and its accompanying conditions. The polymerization was completed under an inert nitrogen atmosphere. The G-III catalyst was dissolved in dry and degassed DCM and added to a solution of stirring hvDIBO-monomer (**6**) at a catalyst loading of 1 mol %. The polymerization was terminated after a reaction time of 60 minutes with ethyl vinyl ether (EVE) to quench the polymerization, purified by alumina gel chromatography, then purified by centrifugation which yielded hvDIBO-polymer (**8**) (**Scheme 20**). The effective quench of the polymerization occurs due to the

formation of a deactivated Fischer carbene (deactivated G-III) when G-III reacts with EVE, resulting in the clean removal of polymer from the catalyst.[https://www.nature.com/articles/nchem.347]

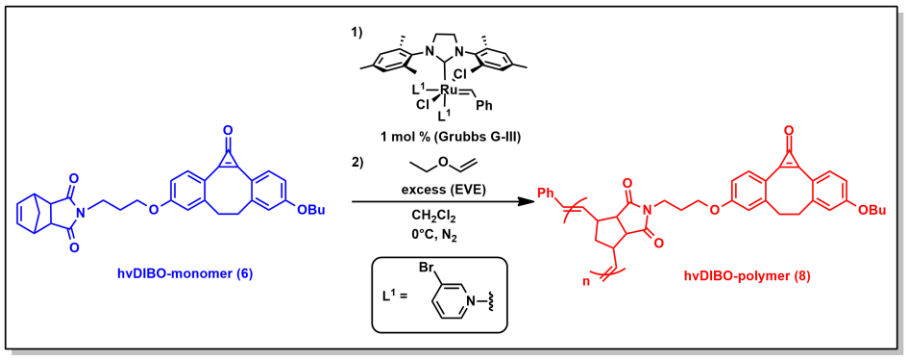

Scheme 20. The synthesis of hvDIBO-polymer (**8**) via ROMP of hvDIBO-monomer (**6**).

The hvDIBO-polymer (**8**) was characterized by ^{1}H NMR spectroscopy and size-exclusion chromatography (SEC) (**Appendix 2-F**). The ^{1}H NMR spectrum of hvDIBO-polymer (**8**) showed retention of all monomer peaks expected to remain unaffected by polymerization, most notably the aromatic signals at 7.80-7.90 ppm and 6.80-6.90 ppm. A comparison between the spectra of monomer (**6**) and hvDIBO-polymer (**8**) also showed both the disappearance of the norbornene alkene signals in the monomer at 6.29 ppm (**Figure 5 – Box A**) and the appearance of new polymer backbone alkene signals at 5.51 ppm and 5.71 ppm (**Figure 5 – Box B**). Finally, all signals could be assigned to the structure of (**8**) and a comparison of spectra showed a broadening of signals expected of a polymer.

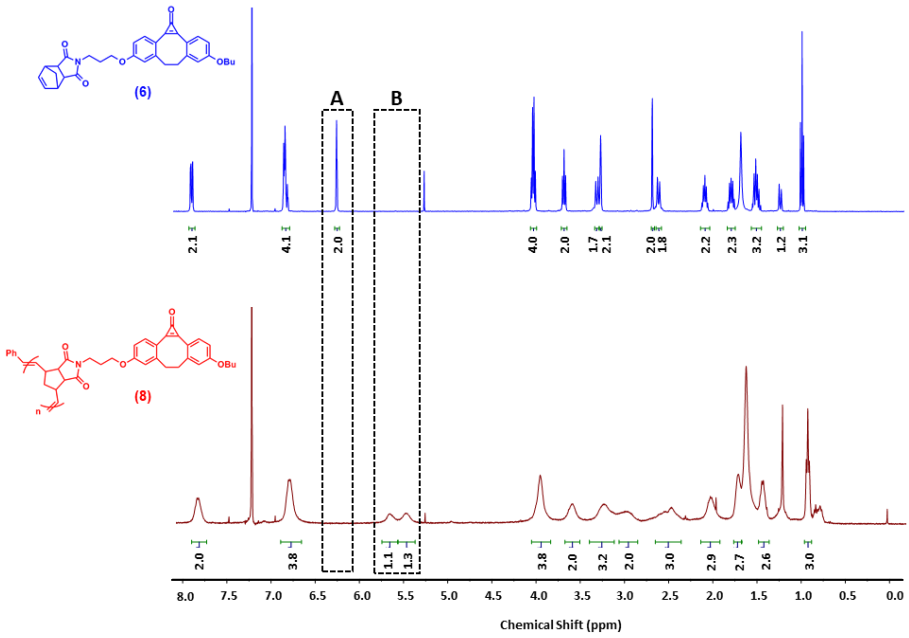

Figure 4. A comparison between ^{1}H NMR spectra ($CDCl_3$) of hνDIBO-monomer (**6**) (top, blue) and hνDIBO-polymer (**8**) (bottom, red). The dotted rectangle (**A**) highlights the disappearance of the norbornene alkene signal. The dotted rectangle (**B**) highlights the appearance of polymer backbone alkene signals.

Molecular weight data (**Table 1**) were obtained from the SEC experiment performed on hνDIBO-polymer (**8**). The theoretical $\bar{M}_n$ for the polymerization, given a catalyst loading of 1 mol %, is 52.4 kg/mol (100 repeating units).

Table 1. Molecular weight data obtained from SEC experiments on hvDIBO-polymer (**8**). *DP_n calculated by dividing experimental $\bar{M}_n$ by monomer molecular weight. Theoretical DP_n is 100 at 1% catalyst loading.

Sample Name	**Polymerization Time (minutes)**	$\bar{M}_n$ **(kg/mol)**	$\bar{M}_w$ **(kg/mol)**	**PDI**	***DP_n**
Polymer **8**	60	64.4	154.6	2.40	123

There was a disparity between the theoretical and experimental $\bar{M}_n$ as well as a high PDI. This suggested the existence of some much higher molecular weight species in the sample. This may have been due to the polymerization finishing before the 60-minute reaction time and the G-III catalyst reacting with alkenes in the polymer backbone once the strained norbornene alkenes were no longer present (chain transfer). The G-III could have crosslinked between polymer chains via the alkenes in their backbones, making crosslinked polymer chains much higher in molecular weight than non-crosslinked chains. This would explain the unusually high $\bar{M}_w$ and PDI.

Several more independent polymerizations (different dates, catalyst batches, solvent batches, monomer batches, etc) were performed following the beforementioned procedure to get an idea of the behavior of this polymerization. This was necessary to make an informed decision in selecting appropriate time points for a final, single behavior study. It is important to note that since these polymerizations were not done under consistent conditions, their comparison is only useful in gaining a general understanding of the polymerization. All polymerizations were characterized and confirmed by ^{1}H NMR and SEC (**Appendix 2-G, 2-H, 2-I**), the results of which are shown in **Table 2**.

Table 2. Table 2. Molecular weight data obtained from SEC experiments on various hνDIBO-polymers. *DPn calculated by dividing experimental $\bar{M}_n$ by monomer molecular weight. Theoretical DPn is 100 at 1% catalyst loading.

Sample Name	Polymerization Time (minutes)	$\bar{M}_n$ (kg/mol)	$\bar{M}_w$ (kg/mol)	PDI	*DP_n
Polymer **9-10**	10	28.2	45.8	1.62	54
Polymer **10**	12	27.6	40.9	1.48	53
Polymer **9-20**	20	24.9	44.6	1.79	48
Polymer **9-30**	30	25.2	46.2	1.84	48
Polymer **11**	40	41.2	87.3	2.12	79
Polymer **8**	60	64.4	154.6	2.40	123

After reflection upon data from **Table 2**, some expected trends were established. The first trend is a general increase in $\bar{M}_n$ with increase in polymerization time. Another trend is a general increase in PDI with increase in polymerization time. To get a more consistent, detailed look at the polymerization of hνDIBO-monomer (**6**), a polymerization behavior study was performed with a single batch of monomer, a single batch of catalyst, a single batch of solvent, on a single day. The study involved preparing a polymerization at 1% catalyst loading where at 5 predetermined time points (10, 20, 40, 80, 120 minutes), aliquots of reaction mixture were removed and added to stirring EVE to terminate. These 5 different polymers were then characterized by ^{1}H NMR and SEC after purification by alumina gel to remove G-III catalyst. Monomer was not separated from polymer samples so as to obtain polymer conversion data (%) via ^{1}H NMR analysis. It should be noted that due to time restrictions imposed by hiatus taken by the UWO Chemistry Department for COVID-19, less time points than desired were collected, and the study was not performed in multiplicate. This means that no error could be accounted for in the data collected for the behavior study. For reasons related to restrictions imposed by COVID-19, an altered

polymerization method was used for the behavior study. The polymerization was still performed under an inert nitrogen atmosphere and using degassed solvents but using different techniques than for all previous polymerizations as noted in the Experimental section of this report.

The polymers synthesized in the behavior study were characterized by ^{1}H NMR and SEC (**Appendix 2-J**). The ^{1}H NMR spectra confirmed successful polymerization of hνDIBO-polymer (**12**) for each of the 10, 20, 40, 80, and 120-minute aliquots (**12-10, 12-20, 12-40, 12-80,** and **12-120**, respectfully). The same results occurred in the ^{1}H NMR spectra of all aliquots of hνDIBO-polymer (**12**) as noted earlier in this chapter for hνDIBO-polymer (**8**), where the aromatic monomer signals (7.80-7.90 ppm, 6.80-6.90 ppm) were retained and the new polymer backbone alkene signals (5.71 ppm, 5.51 ppm) appeared alongside a broadening in signals for peaks originating from the polymer in the sample (**Figure 6**).

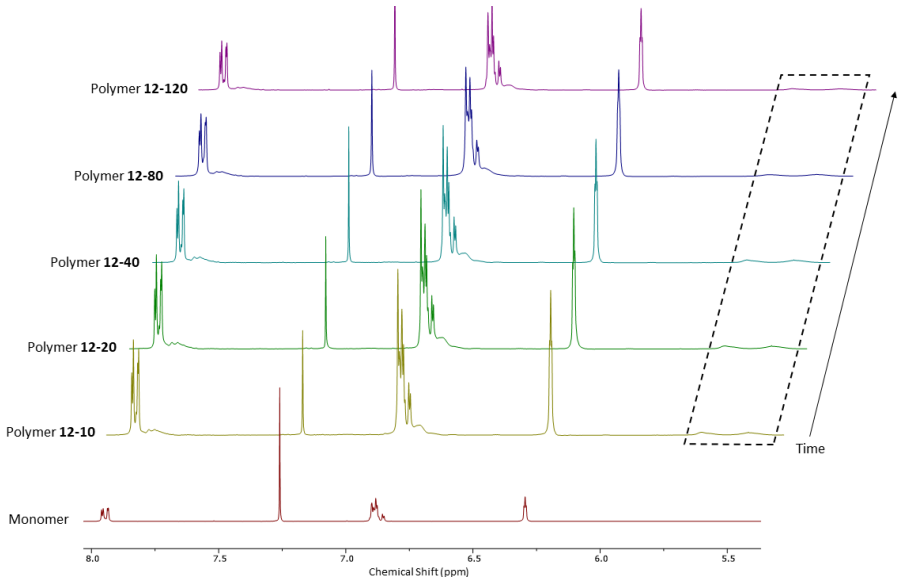

Figure 5. A comparison between ^{1}H NMR spectra of hvDIBO-monomer (**6**) (bottom) and hvDIBO-polymer (**12-10**), (**12-20**), (**12-40**), (**12-80**), and (**12-120**) (increasing time from bottom).

Molecular weight data obtained by SEC for all aliquots of hvDIBO-polymer (**12**) are summarized in **Table 3**. Polymer conversions (%) were determined by comparison of monomer norbornene alkene signals from unreacted monomer to newly appeared polymer alkene backbone signals via ^{1}H NMR analysis.

Table 3. Molecular weight and conversion data obtained from SEC and ^{1}H NMR analysis, respectfully, on hvDIBO-polymers (**12**). *DPn calculated by dividing experimental $\bar{M}_n$ by monomer molecular weight. Theoretical DPn is 100 at 1% catalyst loading.

Sample Name	Polymerization Time (minutes)	$\bar{M}_n$ (kg/mol)	$\bar{M}_w$ (kg/mol)	PDI	*DP_n	Conversion (%)
Polymer **12-10**	10	9.1	19.5	2.15	17	29
Polymer **12-20**	20	27.3	76.9	2.82	52	31
Polymer **12-40**	40	39.5	86.1	2.18	75	33
Polymer **12-80**	80	41.1	87.8	2.13	78	33
Polymer **12-120**	120	36.6	88.9	2.43	70	35

The trends realized from earlier polymerizations (see **Table 2**) were not as well defined in the behavior study. The $\bar{M}_n$ and DP_n values increased over time until 40 minutes after which they plateaued. The $\bar{M}_n$ and DP_n values for polymer (**12-120**) being slightly lower than for polymer (**12-80**) can be attributed to error (instrumental and/or structural mismatch to standard). The PDI did not seem to increase with time, but rather stayed constant from 10 to 80 minutes (if the 20-minute aliquot is ignored as an outlier). It is possible that at some time between 80 and 120 minutes the catalyst started reacting with alkenes in the polymer backbone, potentially causing crosslinking which would cause an increase in PDI. The polymer conversions also appeared to increase very slightly with time but could be considered constant with error (instrumental and/or structural mismatch to standard).

To get a more in-depth look at the polymerization and determine if it is a "living" process, some standard kinetic plots were constructed. The first (**Figure 7**) is a plot of monomer consumption over time. Monomer consumption is expressed as the natural

logarithm of initial monomer concentration ([M_0]) divided by monomer concentration over time ([M]).

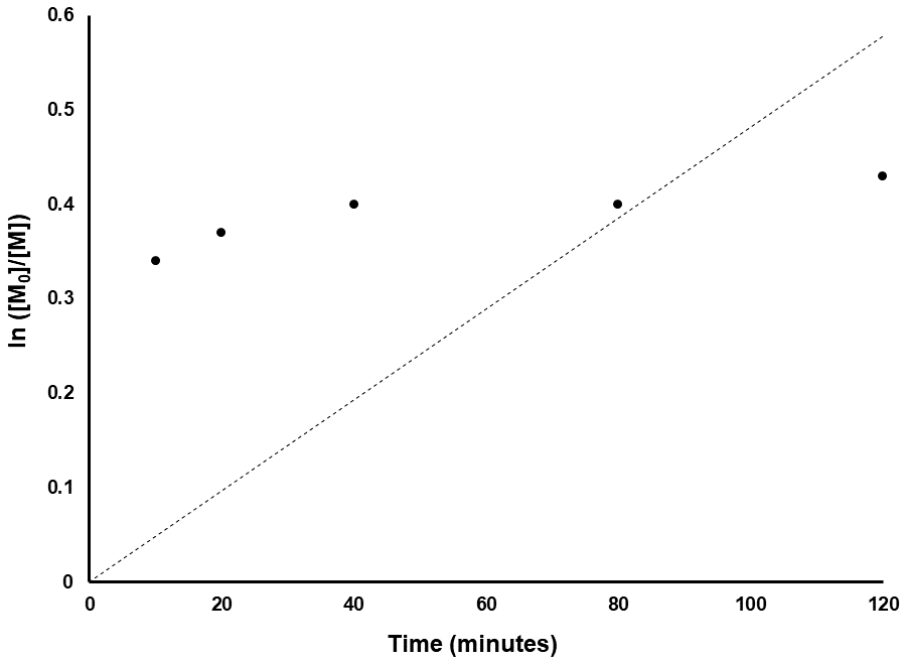

Figure 6. Kinetic plot showing monomer consumption over time of the polymerization of hvDIBO-polymer (**12**).

One characteristic of a "living" polymerization is a linear relationship between reaction time and monomer consumption, which is not seen in **Figure 7**. Monomer consumption over time appears to be rapid under 10 minutes, less steep but positive between 20 and 40 minutes, and plateaued between 40 and 120 minutes. Another kinetic plot (**Figure 8**) was constructed depicting molecular weight versus polymer conversion.

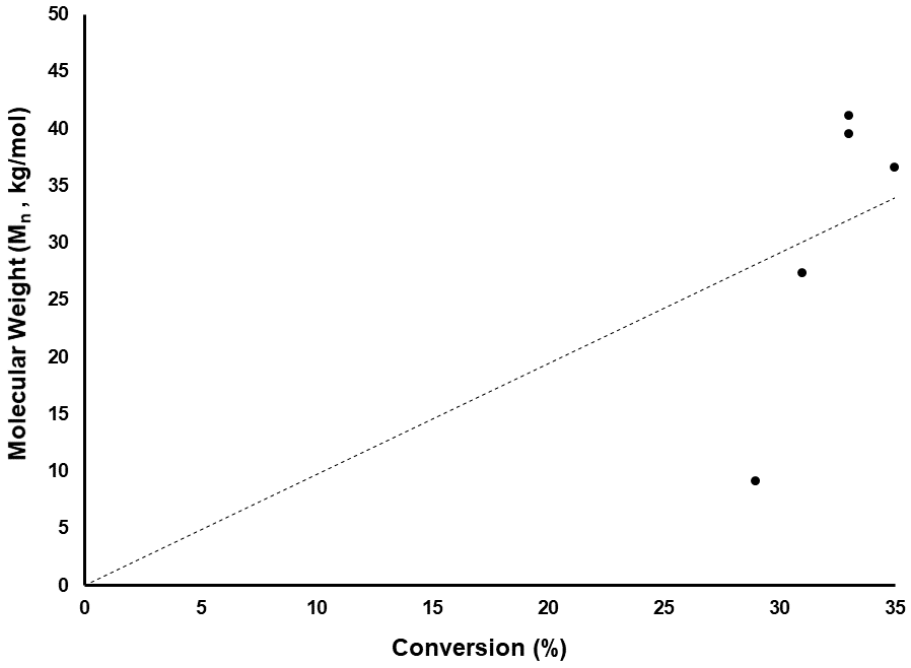

Figure 7. Kinetic plot showing molecular weight ($\bar{M}_n$) as a function of polymer conversion (%). Polymer conversion calculated by ^{1}H NMR analysis.

To be considered "living" this relationship would also have to be linear, which is not seen. Conversion appears to be rapid at molecular weight under 9 kg/mol and very slightly increasing between 9 kg/mol and 40 kg/mol. This very slight increase could be interpreted as roughly constant.

With more knowledge of the how the polymerization behaves, a final bulk polymerization was performed to obtain enough polymer for a full characterization suite and PPM reactions in Chapter 3. This polymerization was performed using the same "altered" method used for the behavior study and 1% catalyst loading. The optimal polymerization time chosen, based upon knowledge gained from the behavior study, was 40 minutes. This is when $\bar{M}_n$ growth started to plateau, PDI had not started to rise yet, and DP_n growth started to plateau. After purification by alumina gel chromatography followed

by centrifugation, pure hvDIBO-polymer (**13**) was obtained. This polymer was characterized by ^{1}H NMR spectroscopy, SEC, FT-IR spectroscopy, and UV-Vis spectroscopy (**Appendix 2-K**). SEC data for (**13**) is summarized in **Table 4**.

Table 4. Table 4. Molecular weight and conversion data obtained from SEC and ^{1}H NMR analysis, respectfully, on hvDIBO-polymer (**13**). *DPn calculated by dividing experimental $\bar{M}_n$ by monomer molecular weight. Theoretical DPn is 100 at 1% catalyst loading.

Sample Name	**Polymerization Time (minutes)**	**$\bar{M}_n$ (kg/mol)**	**$\bar{M}_w$ (kg/mol)**	**PDI**	***DP_n**	**Conversion (%)**
Polymer **13**	40	40.9	71.1	1.74	78	74

The data seen for (**13**) are much more aligned with trends established by the independent polymerizations (see **Table 2**). The $\bar{M}_n$ is around 40 kg/mol as expected for the 40-minute mark, though the $\bar{M}_w$ was considerably lower than seen in the behavior study leading to a much lower PDI of 1.74 as compared to the PDI of 2.18 for polymer (**12-40**). The % conversion of 74% was also much higher than that of polymer (**12-40**) at 33%.

The FT-IR spectra of (**13**) (**red**) and (**6**) (**blue**) were very similar in features, both including diagnostic peaks at ~1840 cm^{-1} corresponding to C=O stretching of the cyclopropenone ketone, ~1695 cm^{-1} corresponding to C=O stretching of the imide carbonyls, and 1600 cm^{-1} corresponding to the C=C stretching of the cyclopropenone alkene (**Figure 8**). The retention of these diagnostic IR signals from monomer to polymer yields proof of a successful polymerization and retention of the cyclopropenone moiety.

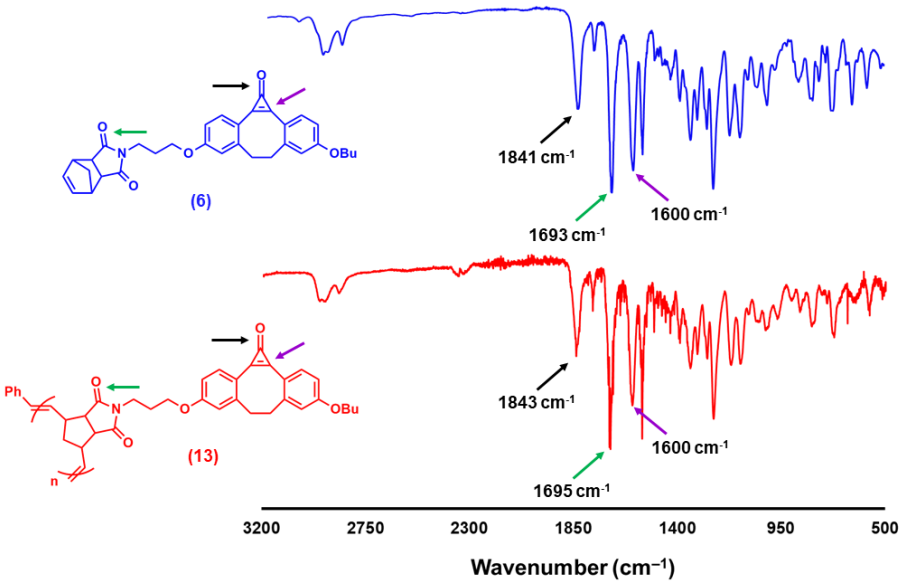

Figure 8. A comparison between FT-IR spectra of hνDIBO-monomer (**6**) (top, blue) and hνDIBO-polymer (**13**) (bottom, red).

The UV-Vis spectra of (**13**) (**red**) and (**6**) (**blue**) were also very similar in features, both including diagnostic bands at 310-350 nm corresponding to the cyclopropenone group and 240-260 nm corresponding to the two phenyl rings of hνDIBO (**Figure 9**). The retention of these diagnostic UV-Vis signals from monomer to polymer also yields proof of a successful polymerization and the retention of the cyclopropenone moiety. The distorted shape of the trace for (**13**) is due to high concentration. For optimal peak shape, see **Figure 11A** in Chapter 3.

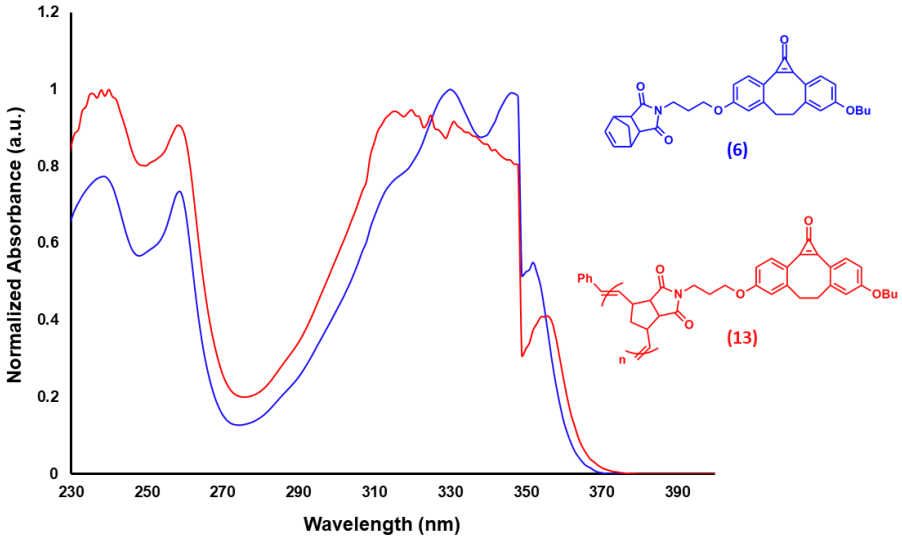

Figure 9. A comparison between UV-Vis spectra of hνDIBO-monomer (**6**) (blue) and hνDIBO-polymer (**13**) (red). The anomaly at ~355 nm and sharp vertical spike at ~350 nm are due to lamp change of the instrument.

2.3 Conclusion

A hνDIBO-monomer (**6**) was successfully synthesized incorporating both a polymerizable group and a reactive handle protected by a unique masking strategy. This monomer was characterized by ^{1}H and ^{13}C NMR spectroscopy, HRMS, FT-IR spectroscopy, and UV-Vis spectroscopy. A control experiment showed the very low reactivity of hνDIBO-OBu_2 with G-III catalyst, meant to mimic the behavior of hνDIBO incorporated into the monomer during polymerization conditions. A minor side reaction occurred yielding an impurity determined to be <5% of the crude sample (**7.1**) by ^{1}H NMR analysis.

Successful polymerization of hνDIBO-monomer was achieved repeatedly, verified via characterization by ^{1}H NMR spectroscopy, SEC, FT-IR spectroscopy, and UV-Vis spectroscopy. A behavior study was then conducted to gain a better understanding of the

polymerization kinetics (**12**). This study showed the successful molecular weight growth over time of the polymerization, though it cannot be considered a “living” polymerization due to non-linear monomer consumption and molecular weight growth. Utilizing information gained from the behavior study, a final bulk polymerization was performed yielding (**13**).

The successful ROMP of a monomer yielding a masked alkyne allowed for a polymer, with this masked alkyne incorporated into every repeating unit, to be synthesized. Upon photo-unmasking, this polymer is capable of decoration with functional azides to yield a functional polymer. The next chapter focuses on the PPM, via SPAAC, of this polymer to introduce functionality — exemplifying its use as a functional polymer template.

2.4 Experimental

2.4.1 Materials and Methods

Reagents were used as received and purchased from Sigma-Aldrich and Alfa Aesar. All common solvents and anhydrous drying agents were purchased from Caledon. Dry solvents were dried using an Innovatice Technologies Inc. solvent purification system, collected under vacuum, and stored under a nitrogen atmosphere over 4 Å molecular sieves.

^{1}H and ^{13}C NMR spectra were recorded on a Mercury 400 MHz or INOVA 600 MHz spectrometer. ^{1}H NMR spectra are reported as δ in units of parts per million (ppm) relative to $CDCl_3$ (δ 7.27, singlet) and DMSO-d6 (δ 2.50, quintet). Multiplicities, if reported in short form, are reported as follows: s (singlet), d (doublet), t (triplet), q (quartet), and m (multiplet). Coupling constants are reported as J values in Hertz (Hz). The number of protons (n) for a given resonance is indicated as nH and is based on spectral integration

values. ^{13}C NMR spectra are reported as δ in units of parts per million (ppm) relative to $CDCl_3$ (δ 77.00, t).

Infrared spectra were recorded using an ATR FT-IR spectrometer by loading sample on to diamond platform. The background was subtracted from each spectrum.

SEC experiments were conducted in chromatography grade DMF at concentrations of 5 mg mL^{-1} using a Waters 2695 separations module equipped with a Waters 2414 differential refractometer and two PLgel 5 m mixed-D (300 x 7.5 mm) columns from Polymer Laboratories connected in series. The calibration was performed using polystyrene standards.

UV-Vis spectra were collected using a Varian UV-Vis spectrophotometer model Cary 300 Bio, by dissolving the sample in spectroscopic grade DCM to obtain a 10^{-5} to 10^{-6} M solution. The background was subtracted from each spectrum.

2.4.2 Preparation and Characterization of Compounds

Synthesis of hvDIBO (1)

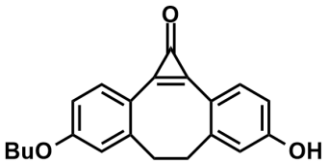

This molecule was synthesized according to a procedure developed by Arnold et al.[80] The compound appeared as a fine white powder (0.977 g, 28%).^{1}H-NMR (600 MHz, DMSO): δ 10.42 (s, 1H), 7.76 (d, J = 8.4 Hz, 1H), 7.69 (d, J = 8.4 Hz, 1H), 7.08 (d, J = 2.4 Hz 1H), 7.00 (dd, J = 8.4 & 2.4 Hz, 1H), 6.89 (d, J = 2.4 Hz, 1H), 6.83 (dd, 8.4 & 2.4 Hz, 1H), 4.06-4.09 (t, J = 6.6 Hz, 2H), 3.34-3.44 (m, 2H), 2.43-2.47 (m, 2H), 1.73 (quintet, *J* = 6.8 Hz, 2H), 1.45 (sextet, *J* = 7.6 Hz, 2H), 0.95 (t, *J* = 7.2 Hz, 3H).

Synthesis of Nor-Imide-Pr-OH (3)

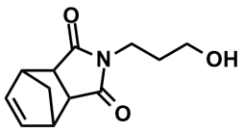

A 25 mL RBF was charged with 3-aminopropanol (0.124 g, 1.65 mmol), cis-5-norbornene-exo-1-propanol-2,3-dicarboxylic anhydride (**2**) (0.246 g, 1.50 mmol) and 5 mL $CHCl_2$. Solution mixture was heated to 50°C in an oil bath and stirred for 60 min. Subsequently, the reaction mixture was heated to 120°C and stirred for 18 h. To the ensuing yellow oil 15 mL $CHCl_2$ and 1 scoop of alumina was added and the mixture was stirred for 30 min. The reaction mixture was filtered over Celite and washed with $CHCl_2$ (5 mL x 3). Clear filtrate was collected and brought to dryness *in vacuo* to yield a clear, yellow oil (0.283 g, 85%). ^{1}H NMR (400 MHz, $CDCl_3$) δ 6.27-6.29 (m, 2H), 3.63 (t, *J* = 6.8 Hz, 2H), 3.54 (quartet, *J* = 6.4 Hz, 2H), 3.26-3.28 (m, 2H), 2.69-2.71 (m, 2H), 2.65 (t, *J* = 6.4 Hz, 1H), 1.73-1.79 (m, 2H), 1.50-1.55 (m, 1H), 1.20-1.24 (m, 1H).

Synthesis of Nor-Imide-Pr-OTs (4)

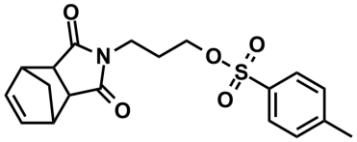

A 100 mL RBF was charged with (**3**) (0.283 g, 1.28 mmol), trimethylamine (0.54 mL, 3.84 mmol), 4-dimethylaminopyridine (0.032 g, 0.26 mmol) and 25 mL $CHCl_2$. The mixture was heated to 40°C in an oil bath and stirred for 5 min, after which *para*-toluenesulfonyl chloride (0.732 g, 3.84 mmol) was slowly added over 1 minute. The reaction mixture was then allowed to stir at 40°C for 16 h. To the resulting yellow solution 10 mL of deionized water was added, then extracted with DCM (25mL x 3), dried over $MgSO_4$, gravity filtered and concentrated *in vacuo*. The crude was moved forward without any further purification.

Synthesis of Nor-Imide-Pr-I (5)

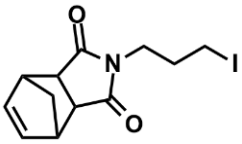

A 100 mL RBF was charged with (**4**) (0.480 g, 1.28 mmol) and 25 mL acetone. The solution was heated to 50°C in an oil bath and stirred for 5 min, after which sodium iodide (0.767 g, 5.12 mmol) was added. The reaction mixture was then allowed to stir at 50°C for 23 h. The resulting crude solution was concentrated *in vacuo* and purified by column chromatography using silica gel (2:1 Hexanes:Ethyl Acetate) and brought to dryness *in vacuo* yielding a white, waxy solid (0.345 g, 81%). ^{1}H NMR (400 MHz, $CDCl_3$) δ 6.27-6.29 (m, 2H), 3.55 (t, *J* = 7.2 Hz, 2H), 3.26-3.28 (m, 2H), 3.11 (t, *J* = 7.2 Hz, 2H), 2.68-2.70 (m, 2H), 2.11 (quintet, *J* = 6.8 Hz, 2H), 1.50-1.54 (m, 1H), 1.16-1.20 (m, 1H).

Synthesis of hνDIBO-monomer (6)

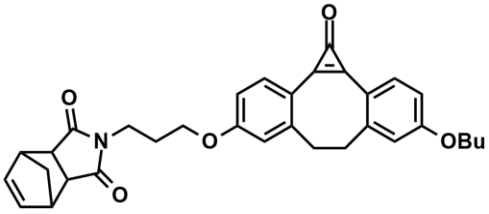

A 50 mL RBF was charged with (**1**) (0.149 g, 0.466 mmol), potassium carbonate (0.322 g, 2.33 mmol), and 15 mL acetonitrile. The solution was heated to 60°C in an oil bath and stirred for 5 min, after which (**5**) (0.170 g, 0.513 mmol) was added. The reaction mixture was then allowed to stir at 60°C for 17 h. The resulting reaction mixture was concentrated *in vacuo* and purified by column chromatography using silica gel (5% MeOH in DCM) and brought to dryness *in vacuo* yielding a white, fluffy, shiny solid (0.213 g, 87%). ^{1}H NMR (400 MHz, $CDCl_3$) δ 7.93-7.96 (m, 2H), 6.84-6.91 (m, 4H), 6.28-6.30 (m, 2H), 4.03-4.09 (m, 4H), 3.71 (t, *J* = 8.0 Hz, 2H), 3.31-3.35 (m, 2H), 3.28-3.30 (m, 2H), 2.69-2.71 (m, 2H), 2.58-2.66 (m, 2H), 2.10 (quintet, *J* = 8.0 Hz, 2H), 1.80 (quintet, *J* = 7.6 Hz, 2H), 1.46-1.56 (m, 3H), 1.22-1.26 (m, 1H), 0.99 (t, *J* = 8.0 Hz,

3H). ^{13}C NMR (74 MHz, $CDCl_3$) δ 178.5, 162.6, 161.9, 154.2, 148.3, 143.0, 142.5, 138.3, 136.2, 117.2, 116.7, 112.7, 68.5, 66.4, 53.9, 48.3, 45.7, 43.3, 37.6, 36.4, 31.6, 28.1, 19.7, 14.3. ESI HRMS: calcd. ($M+Na^+$): $C_{33}H_{33}NO_5$ 523.2359, found 523.2356. IR (ATR, cm^{-1}): 2954, 2877, 1844, 1693, 1597, 1346, 1249, 1175, 1132. UV-Vis in DCM (λ_{max} = 347, 330, 259, 239 nm).

Synthesis of hνDIBO-OBu$_2$ (7)

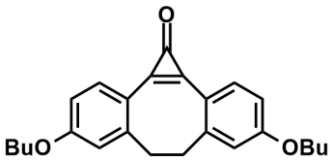

A 25 mL RBF was charged with (**1**) (0.025 g, 0.078 mmol), butyl bromide (0.13 g, 0.93 mmol), and 12 mL acetonitrile. The solution was heated to 60°C in an oil bath and stirred until uniform, after which potassium carbonate (0.108 g, 0.780 mmol) was added. The reaction mixture was allowed to stir at 60°C for 19 h. The resulting mixture was concentrated *in vacuo* and purified by column chromatography using silica gel (5% MeOH in DCM) and brought to dryness *in vacuo* yielding a fine white powder (0.026 g, 90%). ^{1}H-NMR (400 MHz, $CDCl_3$): δ 7.90-7.93 (m, 2H), 6.85-6.89 (m, 4H), 4.03 (t, *J* = 6.8 Hz, 4H), 3.26-3.37 (m, 2H), 2.56-2.67 (m, 2H), 1.79 (quintet, *J* = 6.8 Hz, 4H), 1.50 (sextet, *J* = 7.6 Hz, 4H), 0.98 (t, *J* = 7.2 Hz, 6H). IR (ATR, cm^{-1}): 2954, 2928, 2870, 1838, 1597, 1563, 1346, 1248, 1189, 1169, 1123, 1006, 813. UV-Vis in DCM (λ_{max} = 348, 331, 260, 240 nm).

Synthesis of hνDIBO-polymer (8)

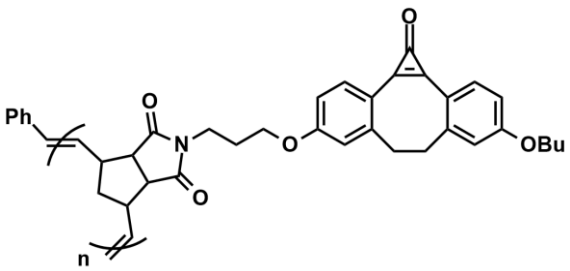

The following is a standard synthesis of hνDIBO-polymer and applies to polymers **8** through **11**. Inside an inert-atmosphere glovebox, a small vial was charged with 3.2mg of Grubbs generation III catalyst. After being brought to atmosphere, a solution of catalyst was made to 1 mg/mL in dry DCM. A separate vial was charged with (**6**) (50.0 mg, 95.5 μmol), 5 mL dry DCM, and a stir bar. Each solution was transferred to separate, purged greaseless Schlenk flasks. Each solution was then degassed via the freeze-pump-thaw method (3 times) using liquid nitrogen, and then refilled with nitrogen. Both flasks were then submerged in a 0 °C ice bath and the monomer-containing flask was wrapped in aluminum foil. From the catalyst flask, 0.84 mL (0.84 mg, 0.954 μmol) was transferred to stirring monomer solution in one, quick plunge. The reaction mixture was allowed to stir for 1 hr at 0 °C. The polymerization was then terminated by the addition of 0.20 mL (0.152 g, 2.11 mol) of ethyl vinyl ether and allowed to stir for 20 min. The reaction mixture was then subjected to atmosphere and loaded onto a pipette alumina plug using dry DCM. The collected liquid was then reduced *in vacuo*, dissolved in a minimum amount of DCM, and added counterclockwise to 40 mL of cold, stirring pentane. The precipitate was then centrifuged and the supernatant decanted (repeated 2 more times). The resulting solid was then dried *in vacuo* to afford a hard, white solid (41.0 mg, 82%). ^{1}H NMR (400 MHz, $CDCl_3$) δ 7.80-7.90 (m, 2H), 6.78-6.87 (m, 4H), 5.64-5.72 (m, 1H), 5.43-5.56 (m, 1H), 3.95-4.05 (m, 4H), 3.59-3.68 (m, 2H), 3.17-3.33 (m, 3H), 2.88-3.08 (m, 2H), 2.35-2.80 (m, 3H), 1.98-2.15 (m, 3H), 1.72-1.79 (m, 2.5H), 1.56-1.69 (m, 7H), 1.44-1.50 (m, 2H), 0.94-

0.99 (m, 3H). SEC (DMF, PS): $\bar{M}_n$ = 64.4 kg/mol, $\bar{M}_w$ = 154.6 kg/mol, PDI = 2.40. IR (ATR, cm^{-1}): 2941, 2872, 1843, 1695, 1598, 1558, 1349, 1249, 1170, 1132. UV-Vis in DCM (λ_{max} = 316, 259, 238 nm).

Synthesis of hνDIBO-polymer (13)

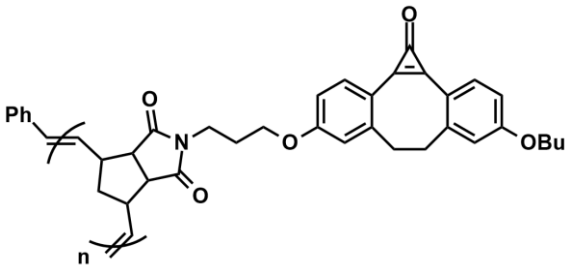

The following is a standard synthesis of hνDIBO-polymer and applies to polymers **12** and **13**. This synthesis was adapted from the method used for polymers **8** through **11** due to restrictions imposed by COVID-19. Inside an inert-atmosphere glovebox, a small vial was charged with 11.1 mg of Grubbs generation III catalyst. After being brought to atmosphere, a solution of catalyst was made to 1 mg/mL in dry DCM. A separate vial was charged with (**6**) (373 mg, 712 μmol), 46.6 mL dry DCM, and a stir bar. Each solution was transferred to separate, clean and dry round bottom flasks fitted with rubber septa and stir bars. Each solution was then degassed via bubbling nitrogen for 15 minutes with a vent needle with stirring, after which the vent needle was removed and the flasks left under positive nitrogen pressure. Both flasks were then submerged in a 0 °C ice bath and the monomer-containing flask was wrapped in aluminum foil. From the catalyst flask, 6.02 mL (6.30 mg, 7.12 μmol) was transferred to stirring monomer solution in one, quick plunge. The reaction mixture was allowed to stir for 40 minutes at 0 °C. The polymerization was then terminated by the addition of 1.35 mL (1.03 g, 14.2 mol) of ethyl vinyl ether and allowed to stir for 20 min. The reaction mixture was then subjected to atmosphere and loaded onto a pipette alumina plug using dry DCM then 5% MeOH in DCM. The collected liquid was then reduced *in vacuo*, dissolved in a minimum amount of DCM, and added

counter-clockwise to 40 mL of cold, stirring pentane. The precipitate was then centrifuged and the supernatant decanted (repeated 2 more times). The resulting solid was then dried *in vacuo* to afford a hard, white solid (40 mg, 11%). ^{1}H NMR (400 MHz, $CDCl_3$) δ 7.80-7.90 (m, 2H), 6.78-6.87 (m, 4H), 5.64-5.72 (m, 1H), 5.43-5.56 (m, 1H), 3.95-4.05 (m, 4H), 3.59-3.68 (m, 2H), 3.17-3.33 (m, 3H), 2.88-3.08 (m, 2H), 2.35-2.80 (m, 3H), 1.98-2.15 (m, 3H), 1.72-1.79 (m, 2.5H), 1.56-1.69 (m, 7H), 1.44-1.50 (m, 2H), 0.94-0.99 (m, 3H). SEC (DMF, PS): $\bar{M}_n$ = 64.4 kg/mol, $\bar{M}_w$ = 154.6 kg/mol, PDI = 2.40. IR (ATR, cm^{-1}): 2941, 2872, 1843, 1695, 1598, 1558, 1349, 1249, 1170, 1132. UV-Vis in DCM (λ_{max} = 316, 259, 238 nm).

Chapter 3

3 Polymer Post-Polymerization Functionalization

3.1 Introduction

Post-polymerization modification (PPM), a method by which polymers are modified by reaction after polymerization has taken place, is a prevalent route to obtain functional polymers. This is due to the ability to construct complex polymers with functionalities that are not compatible with desired polymerization conditions. A reaction type suitable for PPM are “click” reactions, defined by their high efficiency, rapid reaction times, minimal purification, and orthogonality.[46] Presented in this chapter are multiple PPM reactions via SPAAC, a “click” reaction involving a 1,3-dipolar cycloaddition between a strained alkyne and an azide without the necessity for a catalyst.[51,52] For this project, it was envisioned that the alkyne would be incorporated into the polymer and that the functional entity introduced via PPM would contain an azide. Due to the high reactivity of the strained alkyne, a cyclopropenone masking strategy was used to prevent any side reactivity. This strategy, developed by Popik and coworkers, involves the masking of the strained alkyne via a highly inert cyclopropenone group that is unmasked with UV light irradiation.[61] The unmasking of this group only comprises of the evolution of carbon monoxide gas, so no purification is required. In addition, the exposure of UV light may be controlled thus giving the unmasking process spatiotemporal control if desired. This strategy was incorporated in the design of hνDIBO-monomer (**6**) and hνDIBO-polymer (**13**), both successfully synthesized and characterized in Chapter 2. Chapter 3 will entail the unmasking and PPM via SPAAC of (**13**) with benzyl azide as a small molecule model and both (**6**) and (**13**) with Au_{25} azide as a more complex model. The successful

modification and characterization of these monomer/polymers is presented, showcasing the scope of (**13**) as a functional polymer template.

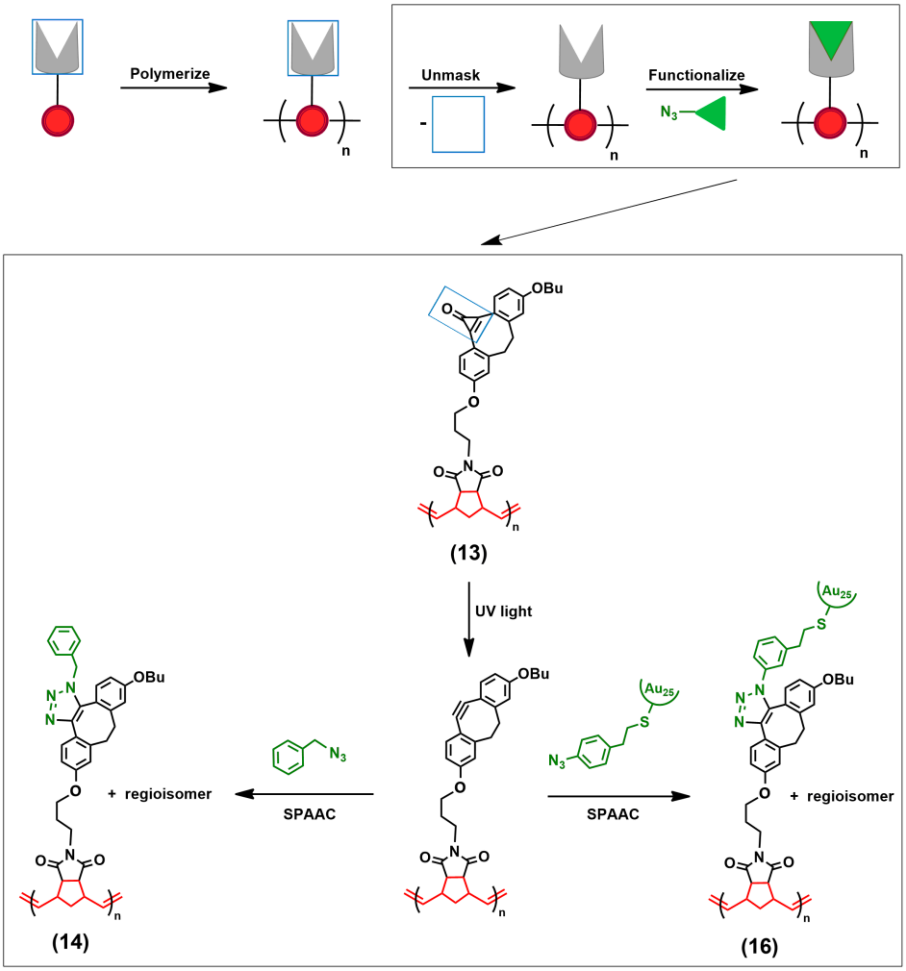

Scheme 21. General scheme of the polymerization, unmasking, and PPM functionalization of masked monomer. Highlighted in the black box is a scheme for the unmasking and SPAAC modification of polymer.

3.2 Results and Discussion

3.2.1 Photo-unmasking and SPAAC reaction of hvDIBO-polymer with benzyl azide

With the successful synthesis of (**13**), PPM via SPAAC was investigated using benzyl azide as a small molecule model. Benzyl azide was chosen for its low cost,

commercial availability, and high reactivity in solution.[5] The first step involved unmasking the alkyne via decarbonylation of the cyclopropenone. Previous work in the Workentin group by Rajeshwar Vasdev showed that a polymer similar in structure to the one presented in this thesis was unstable at some time after the strained alkyne was exposed. This resulted in having to add the azide to the reaction mixture before irradiation with UV light.[79] Thus, the polymer deprotection was performed in the presence of benzyl azide as a one-pot unmask-and-click (**Appendix 3-A**) (**Scheme 21**).

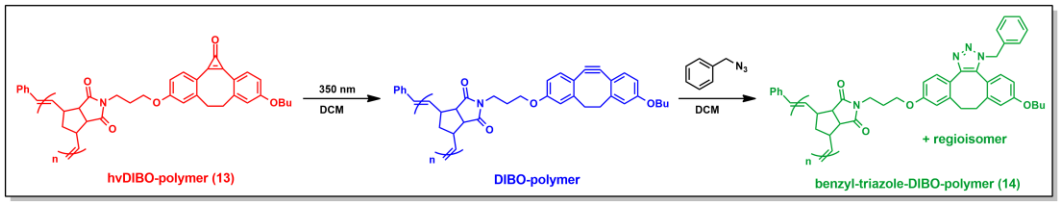

Scheme 22. Photo-unmasking of hvDIBO-polymer (**13**) (red) to give DIBO-polymer (blue) in-situ and resulting SPAAC reaction with benzyl azide yielding benzyl-triazole-DIBO-polymer (**14**) (green).

Before attempting the unmasking reaction with benzyl azide in solution, the unmasking of (**13**) was attempted as a stand-alone reaction and monitored by UV-Vis spectroscopy (**Figure 11A**). An initial spectrum of (**13**) was taken, showing bands at 331–349 nm corresponding to the cyclopropenone group (**red**). The solution was then placed in the Luzchem reactor fitted with 350 nm lamps and irradiated for 15 minutes. A UV-Vis spectrum was then collected which showed the disappearance of the bands corresponding to the cyclopropenone and the appearance of bands at 304–322 nm corresponding to the formation of unmasked strained alkyne (**blue**).

After the success of the unmasking reaction with only polymer in solution, the one-pot unmask-and-click was monitored by UV-Vis spectroscopy (**Figure 11B**). First, (**13**)

and excess benzyl azide were dissolved in DCM and an initial spectrum was taken that showed bands at 331–349 nm corresponding to the cyclopropenone group (**red**). The reaction mixture was then placed in the Luzchem reactor fitted with 350 nm lamps and irradiated for 15 minutes. A UV-Vis spectrum was collected which showed the disappearance of the bands corresponding to the cyclopropenone and the appearance of bands at 304–322 nm corresponding to the formation of unmasked strained alkyne (**blue**). The reaction mixture was then removed from the Luzchem reactor, concentrated, and allowed to stir at room temperature for 7 h. Following purification by precipitation and then centrifugation, a UV-Vis spectrum was obtained showing the disappearance of bands at 304–322 nm corresponding to the consumption of the strained alkyne, suggesting the success of the reaction to yield benzyl-triazole-DIBO-polymer (**14**) (**green**).

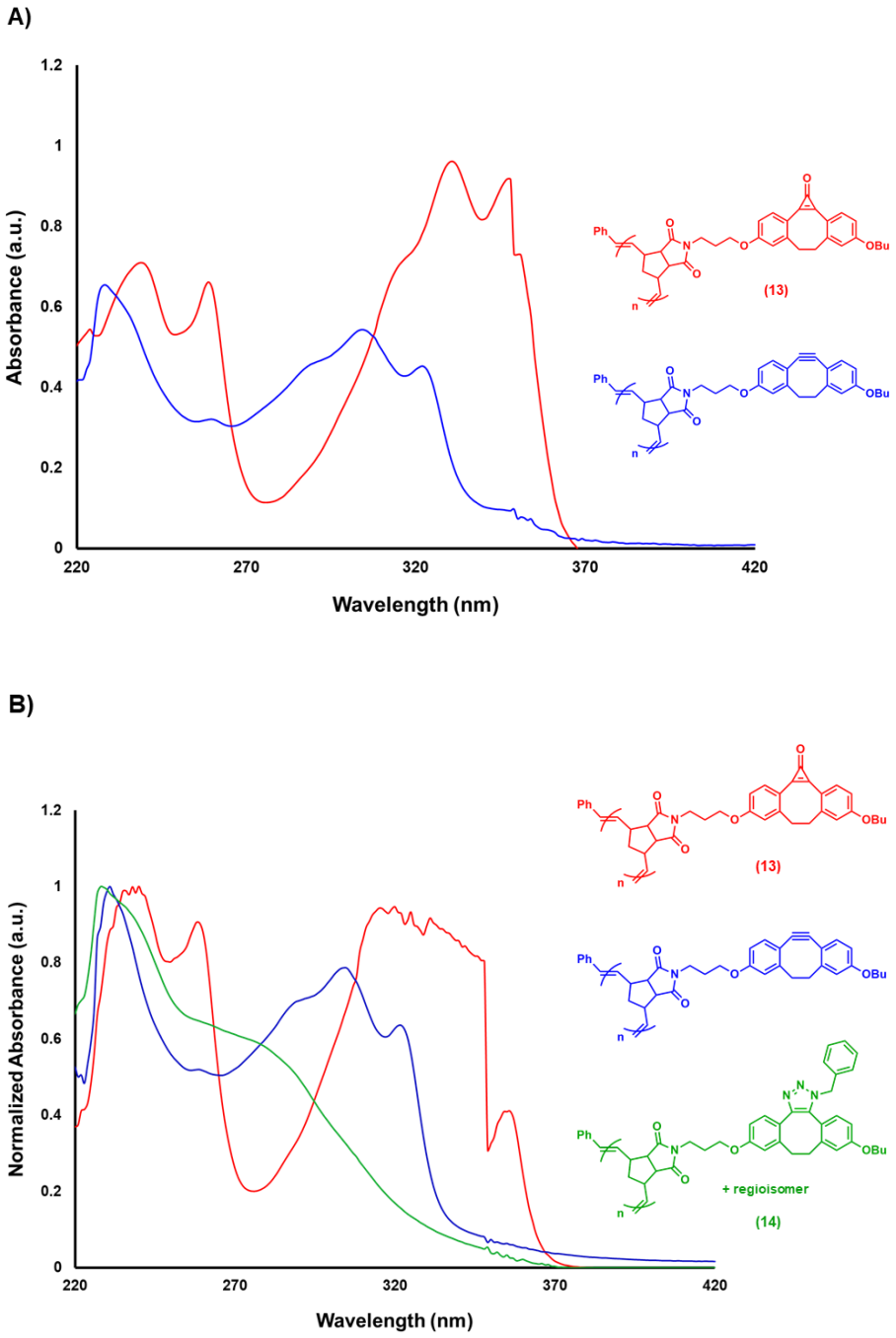

Figure 10. UV-Vis spectra of A) hvDIBO-polymer (**13**) (red) and DIBO-polymer (blue) and B) hvDIBO-polymer (**13**) (red), DIBO-polymer (blue), and benzyl-triazole-DIBO-polymer (**14**) (green) highlighting the unmasking and SPAAC reactions. The difference in shape of (**13**) in A) and B) is due to difference in concentration. The anomaly at ~355 nm in B) and sharp vertical spike at ~350 nm in both A) and B) are due to lamp change of the instrument.

The success of the synthesis of (**14**) was also confirmed by FT-IR spectroscopy (**Figure 12**). The loss of the peak at ~1840 cm^{-1} corresponding to C=O stretching of the cyclopropenone ketone (black checkered box) indicates the successful decarbonylation of the cyclopropenone masking group. Signals at ~1695 cm^{-1} corresponding to C=O stretching of the imide carbonyls and ~1600 cm^{-1} corresponding to C=C stretching of the cyclopropenone alkene were retained. The loss/retention of these diagnostic signals from (**13**) (**red**) before reaction to (**14**) (**green**) after reaction lends proof of a successful SPAAC.

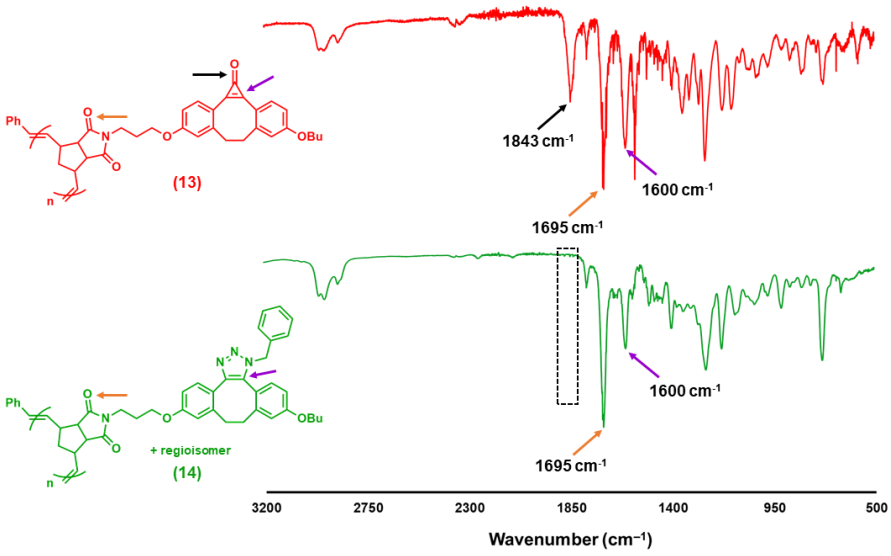

Figure 11. FT-IR spectra of hvDIBO-polymer (**13**) (red) and benzyl-triazole-DIBO-polymer (**14**) (green) highlighting the unmasking and SPAAC reactions.

^{1}H NMR spectroscopy was also used to provide confirmation of a successful SPAAC reaction (**Figure 13**). The aromatic protons corresponding to the phenyl rings of (**13**) (**red**) appear as two broad signals centered at 7.88 and 6.83 ppm, integrating to 2 and 4 protons respectively. The alkene protons in the backbone appear at 5.50–5.70 ppm, integrating to 2 protons. The spectrum of (**14**) (**green**) shows the upfield shift of the 2 protons from the signal centered at 7.88 ppm from the spectrum of (**13**). The spectrum also

shows the appearance of 5 new aromatic protons by integration, suggesting the inclusion of the benzyl group from the SPAAC reaction. Finally, the retention of the integration of 2 alkene protons from the backbone of the polymer as well as the addition of 2 new protons corresponding to the methylene protons of the benzyl group are seen at 5.50–5.70 ppm.

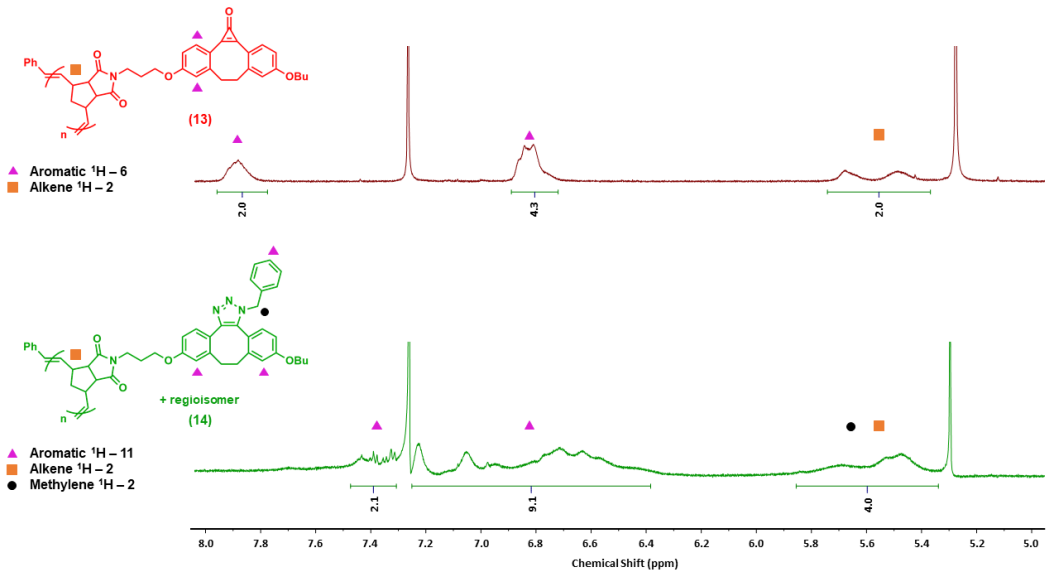

Figure 12. ^{1}H NMR of hvDIBO-polymer (**13**) (red) and benzyl-triazole-DIBO-polymer (**14**) (green) in $CDCl_3$ highlighting the unmasking and SPAAC reactions.

Finally, molecular weight data obtained by SEC for (**14**) are summarized in **Table 5** below. The molecular weight data ($\bar{M}_n$ and $\bar{M}_w$) observed for this experiment are lower than that of (**13**). This is likely due to the increase in non-polar character from (**13**) to (**14**) after the loss of cyclopropenone and introduction of benzyl groups. The SEC experiment was run in DMF, a polar solvent, which would cause the very nonpolar (**14**) to prefer interaction with itself over solvent, causing it to contract and appear smaller during the SEC experiment. These results could also be due to chain scission or chain linking during reaction.

Table 5. Molecular weight data obtained from SEC on benzyl-triazole-DIBO-polymer (**14**).

Sample Name	$\bar{M}_n$ (kg/mol)	$\bar{M}_w$ (kg/mol)	PDI
Polymer **14**	17.2	46.1	2.69

3.2.2 Photo-unmasking and SPAAC reaction of hvDIBO-polymer with Au_{25} azide

With the successful decoration of (**13**) with a small molecule via PPM, a more complex system was desired to be tested to display the breadth of (**13**) as a functional polymer template. The system chosen was one recently developed by the Workentin group — a Au_{25} nanocluster with 18 azide-appended ligands (Au_{25} azide), capable of interfacial surface SPAAC.[78] These novel Au_{25} nanoclusters are ultrasmall (<2 nm), atomically precise, and allow for all surface azide moieties to be functionalized. Due to the likelihood of Au_{25} azide being altered in the presence of UV light, the azide was added immediately after the deprotection of (**6**) as opposed to the in-situ approach taken for the synthesis of (**14**). Before attempting the PPM reaction with polymer, the SPAAC reaction between Au_{25} azide and (**6**) was performed (**Appendix 3-B**) (**Scheme 22**).

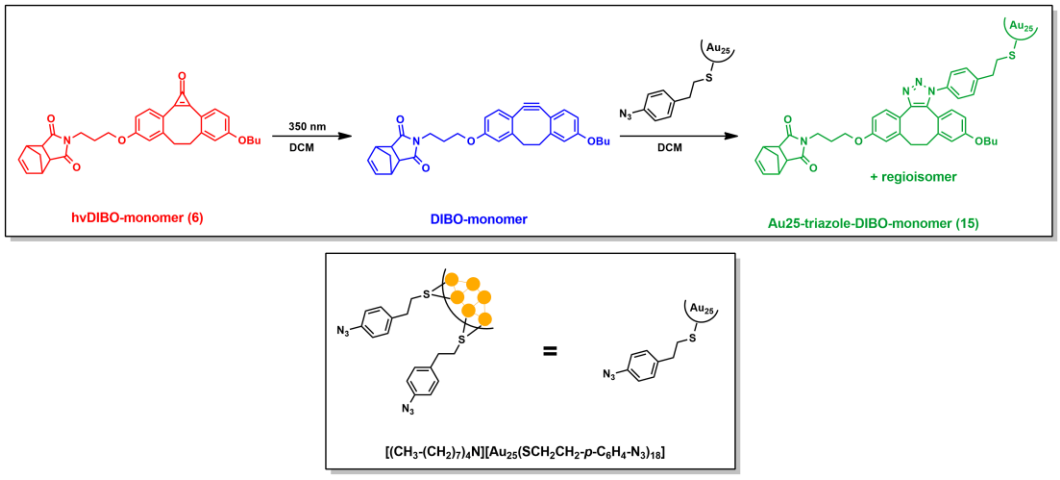

Scheme 23. Photo-unmasking of hvDIBO-monomer (**6**) (red) to give DIBO-monomer (blue) in-situ and resulting SPAAC reaction with Au_{25} azide yielding Au_{25}-triazole-DIBO-monomer (**15**) (green).

The unmasking of (**6**) was monitored by UV-Vis spectroscopy (**Figure 13**). First, (**6**) was dissolved in DCM and an initial spectrum was taken that showed bands at 331–347 nm corresponding to the cyclopropenone group (**red**). The solution was then placed in the Luzchem reactor fitted with 350 nm lamps and irradiated for 15 minutes. A UV-Vis spectrum was collected which showed the disappearance of the bands corresponding to the cyclopropenone and the appearance of bands at 304–322 nm corresponding to the formation of unmasked strained alkyne (**blue**). The reaction mixture was then removed from the Luzchem reactor and immediately a solution of ~1/19 equivalents of Au_{25} azide in DCM was added. This mixture was concentrated and allowed to stir at room temperature for 5 h. Following multiple washes with tetrahydrofuran, a UV-Vis spectrum was obtained showing the disappearance of bands at 304–322 nm corresponding to the consumption of the strained alkyne, suggesting the success of the reaction to yield Au_{25}-triazole-DIBO-monomer (**15**) (**green**).

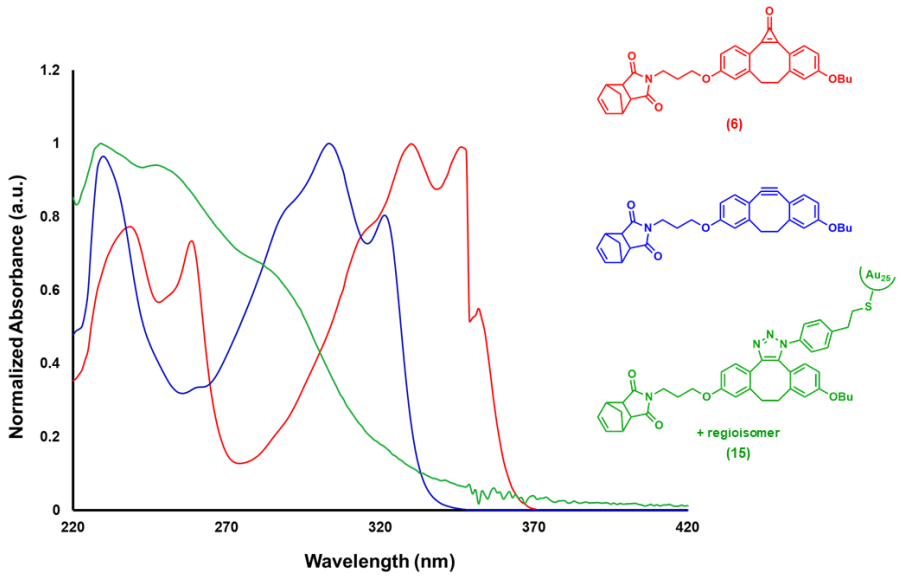

Figure 13. UV-Vis spectra of hvDIBO-monomer (**6**) (red), DIBO-monomer (blue), and Au_{25}-triazole-DIBO-monomer (**15**) (green) in DCM highlighting the unmasking and SPAAC reactions. The anomaly at ~355 nm and sharp vertical spike at ~350 nm are due to lamp change of the instrument.

The success of the synthesis of (**15**) was also confirmed by FT-IR spectroscopy (**Figure 14**). The loss of the peak at ~1840 cm^{-1} corresponding to C=O stretching of the cyclopropenone ketone (black checkered box) indicates the successful decarbonylation of the cyclopropenone masking group. Signals at ~1695 cm^{-1} corresponding to C=O stretching of the imide carbonyls of (**6**), ~1600 cm^{-1} corresponding to C=C stretching of the cyclopropenone alkene of (**6**), and at ~2110 cm^{-1} corresponding to N=N=N stretching of unreacted azide of Au_{25} azide were retained. The loss/retention of these diagnostic signals from (**6**) (**red**) and Au_{25} azide (**gold**) before reaction to (**15**) (**green**) after reaction lends proof of a successful SPAAC.

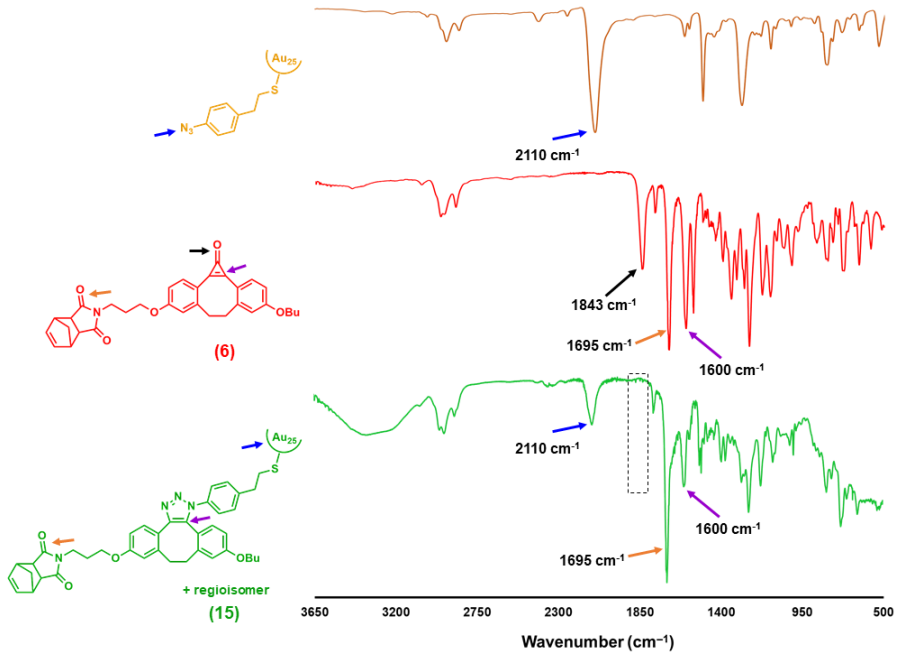

Figure 14. FT-IR spectra of hvDIBO-monomer **(6)** (red), Au_{25} azide (gold), and Au_{25}-triazole-DIBO-monomer (**15**) (green) highlighting the unmasking and SPAAC reactions.

Due to poor solubility, likely due to the potential for polymer cross-linking, a quality ^{1}H NMR spectrum of (**15**) was unable to be collected. After the confirmation of a successful SPAAC reaction between (**6**) and Au_{25} azide, the post-polymerization SPAAC of (**13**) and Au_{25} azide was performed (**Appendix 3-C**) (**Scheme 24**). Due to the likelihood of Au_{25} azide being altered in the presence of UV light, the azide was added immediately after the deprotection of (**13**) as opposed to the in-situ approach taken for the synthesis of (**14**).

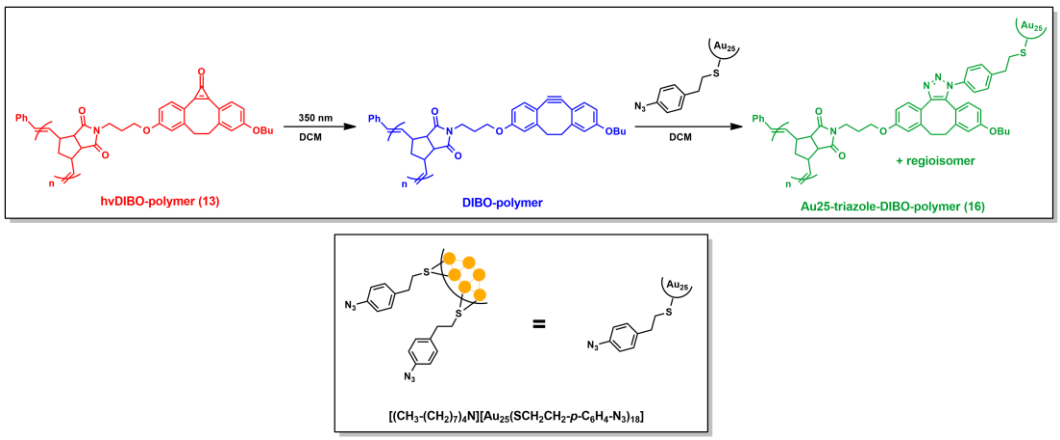

Scheme 24. Photo-unmasking of hvDIBO-polymer (**13**) (red) to give DIBO-polymer (blue) in-situ and resulting SPAAC reaction with Au25 azide yielding Au25-triazole-DIBO-polymer (**16**) (green).

The unmasking of (**13**) was monitored by UV-Vis spectroscopy (**Figure 15**). First, (**13**) was dissolved in DCM and an initial spectrum was taken that showed bands at 315–348 nm corresponding to the cyclopropenone group (**red**). The solution was then placed in the Luzchem reactor fitted with 350 nm lamps and irradiated for 15 minutes. A UV-Vis spectrum was collected which showed the disappearance of the bands corresponding to the cyclopropenone and the appearance of bands at 305–322 nm corresponding to the formation of unmasked strained alkyne (**blue**). The reaction mixture was then removed from the Luzchem reactor and immediately a solution of ~1/21 equivalents of Au_{25} azide in DCM was added. This mixture was concentrated and allowed to stir at room temperature for 4 h. It should be noted that the reaction mixture appeared to become insoluble after ~30 minutes of stirring. Following multiple washes with tetrahydrofuran, a UV-Vis spectrum was obtained showing the disappearance of bands at 305–322 nm corresponding to the consumption of the strained alkyne, suggesting the success of the reaction to yield Au_{25}-triazole-DIBO-polymer (**16**) (**green**).

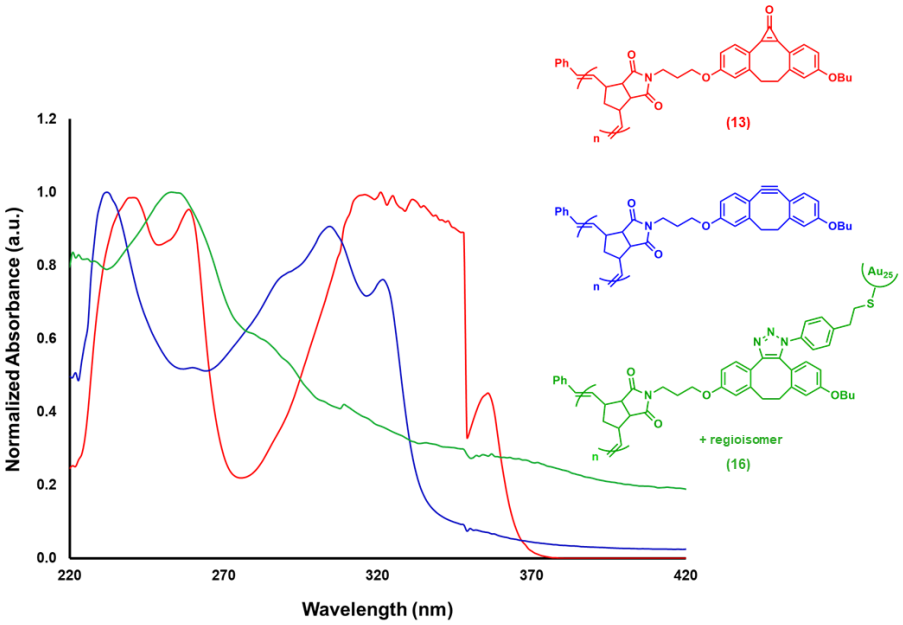

Figure 15. UV-Vis spectra of hνDIBO-polymer (**13**) (red), DIBO-polymer (blue), and Au_{25}-triazole-DIBO-polymer (**16**) (green) in DCM highlighting the unmasking and SPAAC reactions. The obscure shape of the trace for (**13**) (red) at 315–348 nm is due to overly high concentration (hit the instrument absorbance maximum) — see **Figure 11A** for optimal peak shape. The anomaly at ~355 nm and sharp vertical spike at ~350 nm are due to lamp change of the instrument.

The success of the synthesis of (**16**) was also confirmed by FT-IR spectroscopy (**Figure 16**). The loss of the peak at ~1840 cm^{-1} corresponding to C=O stretching of the cyclopropenone ketone (black checkered box) indicates the successful decarbonylation of the cyclopropenone masking group. Signals at ~1695 cm^{-1} corresponding to C=O stretching of the imide carbonyls of (**13**), ~1600 cm^{-1} corresponding to C=C stretching of the cyclopropenone alkene of (**13**), and at ~2110 cm^{-1} corresponding to N=N=N stretching of unreacted azide of Au_{25} azide were retained. The loss/retention of these diagnostic signals from (**13**) (**red**) and Au_{25} azide (**gold**) before reaction to (**16**) (**green**) after reaction lends proof of a successful SPAAC.

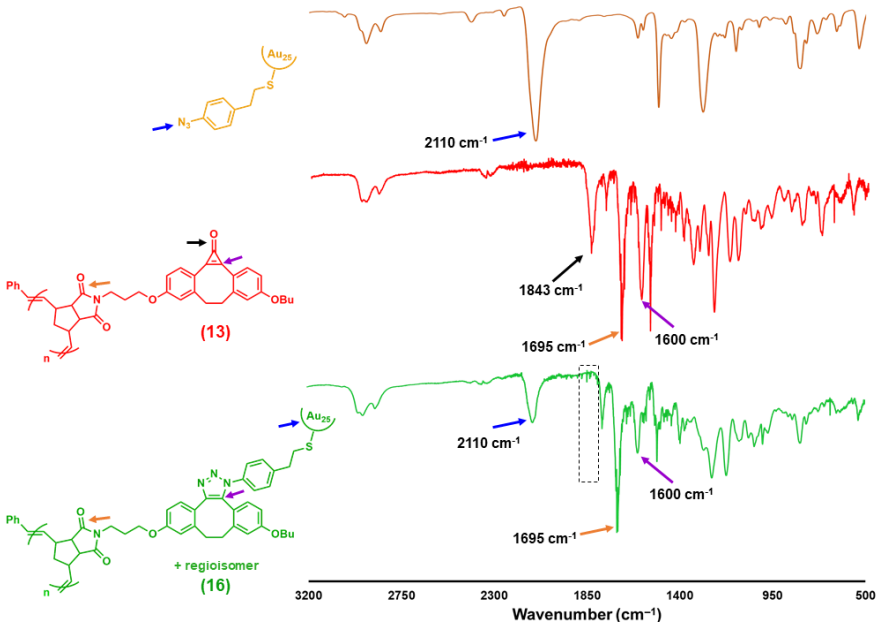

Figure 16. FT-IR spectra of hvDIBO-polymer (**13**) (red), Au25 azide (gold), and Au25-triazole-DIBO-polymer (**16**) (green) highlighting the unmasking and SPAAC reactions.

Finally, (**16**) was characterized by X-ray photoelectron spectroscopy (XPS). A comparison between survey scans of (**13**) and (**16**) showed a relative increase in N_{1s} and decrease in O_{1s} character (**Table 6**). This corresponds to the introduction of a triazole ring from the Au_{25} azide SPAAC and the loss of the cyclopropenone during unmasking of (**13**).

Table 6. XPS survey scan data of hvDIBO-polymer (**13**) and Au_{25}-triazole-DIBO-polymer (**16**).

Sample Name	**N_{1s} (atom %)**	**O_{1s} (atom %)**	**S_{2p} (atom %)**	**Au_{4f} (atom %)**
Polymer **13**	2.5	11.1	-	-
Polymer **16**	3.1	10.5	1.6	2.1

A comparison between high-resolution scans of the N_{1s} region of both (**13**) and (**16**) showed the appearance of triazole N_{1s} character in addition to the existing imide N_{1s}

character (**Table 7, Figure 17**). This corresponds to the introduction of a triazole ring from the Au_{25} azide SPAAC reaction.

Table 7. XPS high-resolution N_{1s} scan data of hνDIBO-polymer (**13**) and Au25-triazole-DIBO-polymer (**16**).

Sample Name	**(O=C)-N-(C=O) (area %)**	**N=N=N (area %)**
Polymer **13**	100	-
Polymer **16**	71.6	28.4

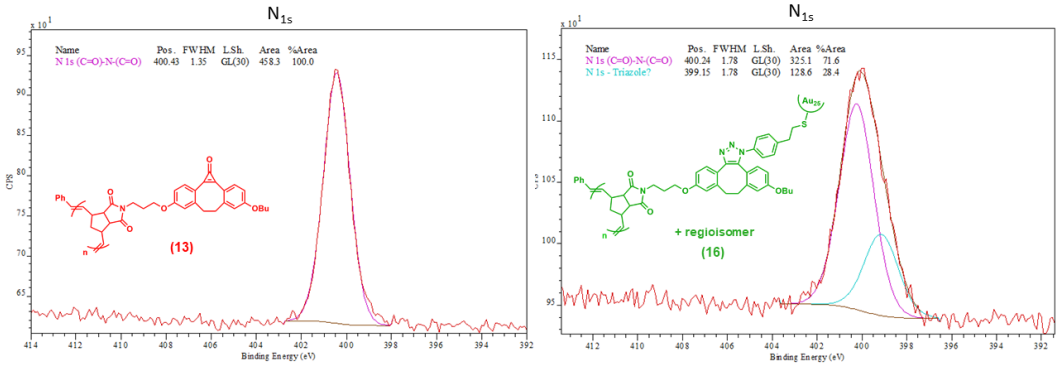

Figure 17. Comparison between XPS high-resolution N_{1s} scan spectra for (**13**) and (**16**).

Finally, a high-resolution scan in the S_{2p} and Au_{4f} regions of (**16**) revealed their character to be of $S_{2p3/2}$ C-S-Au and $Au_{4f7/2}$ nature, confirming the presence of Au_{25} triazole in the sample (**Figure 18**).

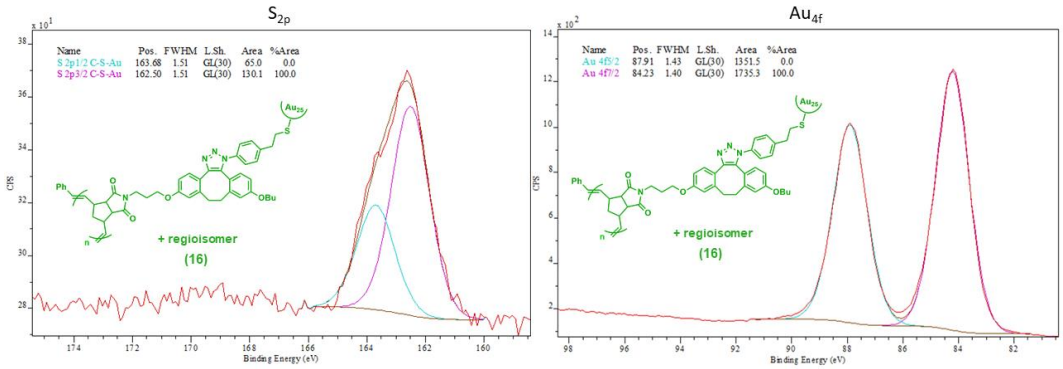

Figure 18. XPS high-resolution Au_{4f} and S_{2p} scan spectra for (**16**).

Due to the insolubility of (**16**), ^{1}H NMR and SEC experiments were unable to be performed.

3.3 Conclusion

The deprotection of (**13**) via irradiation with UV light was successfully performed, monitored by UV-Vis spectroscopy. A one-pot unmask-and-click was then performed on (**13**) with benzyl azide, chosen as a small molecule model. This new polymer (**14**) was characterized by UV-Vis, FT-IR, and ^{1}H NMR spectroscopy and SEC. This experiment showed the successful PPM of (**13**) with a small molecule model via SPAAC.

With the success of the PPM via SPAAC of (**13**) with a small molecule model, reaction with Au_{25} azide was desired to be performed to demonstrate a more complex system. First, the unmasking of (**6**) and subsequent reaction with Au_{25} azide was performed and monitored by UV-Vis spectroscopy. The reaction was also characterized by IR spectroscopy. Next, the unmasking of (**13**) and subsequent reaction with Au_{25} azide was performed and monitored by UV-Vis spectroscopy. The reaction was also

characterized by FT-IR and XPS. This study showed the successful PPM of (**13**) with a more complex model via SPAAC, demonstrated first by a test with (**6**).

The successful decoration of (**13**) with both a small molecule and more complex system post-polymerization demonstrates the breadth of this system as a functional polymer template.

3.4 Experimental

3.4.1 Materials and Methods

Reagents were used as received and purchased from Sigma-Aldrich and Alfa Aesar. All common solvents and anhydrous drying agents were purchased from Caledon. Dry solvents were dried using an Innovatice Technologies Inc. solvent purification system, collected under vacuum, and stored under a nitrogen atmosphere over 4 Å molecular sieves.

^{1}H and ^{13}C NMR spectra were recorded on a Mercury 400 MHz or INOVA 600 MHz spectrometer. ^{1}H NMR spectra are reported as δ in units of parts per million (ppm) relative to $CDCl_3$ (δ 7.27, singlet) and DMSO-d6 (δ 2.50, quintet). Multiplicities, if reported in short form, are reported as follows: s (singlet), d (doublet), t (triplet), q (quartet), and m (multiplet). Coupling constants are reported as J values in Hertz (Hz). The number of protons (n) for a given resonance is indicated as nH, and is based on spectral integration values. ^{13}C NMR spectra are reported as δ in units of parts per million (ppm) relative to $CDCl_3$ (δ 77.00, t).

Infrared spectra were recorded using an ATR IR spectrometer by loading sample on to diamond platform. The background was subtracted from each spectrum.

SEC experiments were conducted in chromatography grade DMF at concentrations of 5 mg mL^{-1} using a Waters 2695 separations module equipped with a Waters 2414 differential refractometer and two PLgel 5 m mixed-D (300 x 7.5 mm) columns from Polymer Laboratories connected in series. The calibration was performed using polystyrene standards.

UV-Vis spectra were collected using a Varian UV-Vis spectrophotometer model Cary 300 Bio, by dissolving the sample in spectroscopic grade DCM to obtain a 10-5 M solution. The background was subtracted from each spectrum.

XPS samples were analyzed using a Kratos AXIS Supra X-ray photoelectron spectrometer. XPS can detect all elements except hydrogen and helium, probes the surface of the sample to a depth of 7 - 10 nanometres, and has detection limits ranging from 0.1 - 0.5 atomic percent depending on the element. The survey scan analyses were carried out with an analysis area of 300 x 700 microns and a pass energy of 160 eV. The high-resolution analyses were carried out with an analysis area of 300 x 700 microns and a pass energy of 20 eV.

3.4.2 Preparation and Characterization of Compounds

Synthesis of benzyl-triazole-DIBO-polymer (14)

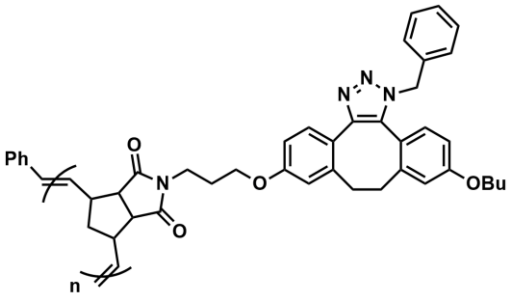

Polymer (**13**) (10 mg, 19 µmol) and benzyl azide (4.0 mg, 29 µmol) were dissolved in glass distilled DCM (80 mL) in a 250 mL round-bottomed flask and purged with nitrogen gas for 15 minutes. The mixture was then irradiated in

the Luzchem reactor with 350 nm UV light for 15 minutes (monitored by UV-Vis spectroscopy). The mixture was removed from the reactor, concentrated to 1 mL, and allowed to stir at room temperature for 7 hours. The crude mixture was then precipitated into stirring pentane (12 mL) at 0 ^{o}C, centrifuged, and dried *in vacuo* to afford (**14**) as a yellow solid (10 mg, 83%). ^{1}H NMR (600 MHz, $CDCl_3$) δ 7.50-7.30 (m, 2H), 7.25-7.16 (m, 1H), 7.15-6.88 (m, 2H), 6.88-6.34 (m, 6H), 5.87-5.35 (m, 4H), 4.05-3.72 (m, 6H), 3.72-3.51 (m, 3H), 3.51-3.38 (m, 3H), 3.38-3.29 (m, 1H), 3.12-2.83 (m, 5H), 2.98-2.47 (m, 3H), 2.13-1.85 (m, 3H), 1.81-1.50 (m, 11H), 1.50-1.10 (m, 15H), 1.02-0.70 (m, 9H). SEC (DMF, PS): $\bar{M}_n$ = 17.2 kg/mol, $\bar{M}_w$ = 46.1 kg/mol, Đ = 2.69. IR (ATR, cm^{-1}): 2955, 2928, 2870, 1771, 1695, 1598, 1396, 1244, 1172, 1114, 910, 738. UV-Vis in DCM (λ_{max} = 229 nm).

Synthesis of Au25-triazole-DIBO-monomer (15)

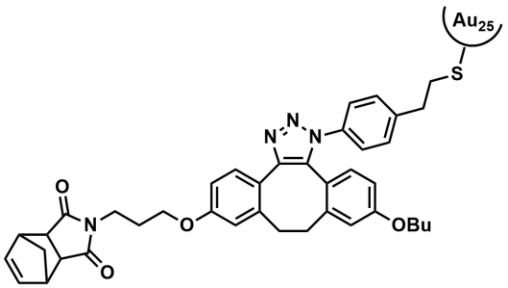

Monomer (**6**) (12 mg, 23 µmol) was dissolved in glass distilled DCM (250 mL) in a 500 mL round-bottomed flask and purged with nitrogen gas for 15 minutes. The solution was then irradiated in the Luzchem reactor with 350 nm UV light for 15 minutes (monitored by UV-Vis spectroscopy). Immediately after removing the solution out of the Luzchem reactor, a solution of Au_{25} azide (10 mg, 1.2 µmol) in glass distilled DCM (1 mL) was added. This mixture was then concentrated to 1.5 mL and allowed to stir at room temperature for 5 hours. The crude mixture was then washed with THF (2 mL) and the supernatant was decanted off with a Pasteur pipette. This process was repeated 2 more times. The compound (**15**) was allowed to air dry before drying *in vacuo* to afford a brown solid (22 mg). IR

(ATR, cm^{-1}): 3336, 2956, 2930, 2872, 2111, 1771, 1695, 1603, 1506, 1396, 1371, 1280, 1243, 1175, 1110.

Synthesis of Au25-triazole-DIBO-polymer (16)

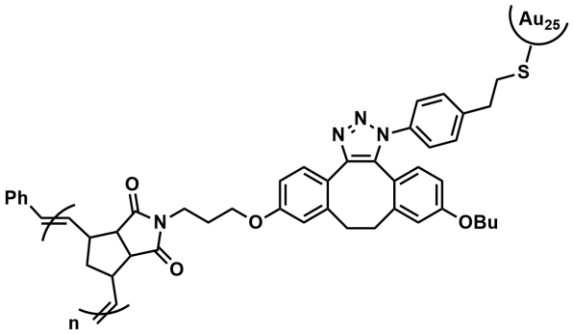

Polymer (**13**) (15 mg, 29 µmol) was dissolved in glass distilled DCM (120 mL) in a 250 mL round-bottomed flask and purged with nitrogen gas for 15 minutes. The solution was then irradiated in the Luzchem reactor with 350 nm UV light for 15 minutes (monitored by UV-Vis spectroscopy). Immediately after removing the solution out of the Luzchem reactor, a solution of Au_{25} azide (11 mg, 1.4 µmol) in glass distilled DCM (1 mL) was added. This mixture was then concentrated to 1 mL and allowed to stir at room temperature for 4 hours. The crude mixture was then washed with THF (2 mL) and the supernatant was decanted off with a Pasteur pipette. This process was repeated 2 more times. The compound (**16**) was allowed to air dry before drying *in vacuo* to afford a brown solid (19 mg). IR (ATR, cm^{-1}): 3335, 2928, 2871, 2108, 1771, 1699, 1599, 1505, 1393, 1371, 1279, 1239, 1171, 1110, 810. UV-Vis in DCM (λ_{max} = 255 nm).

Chapter 4

4 Conclusions and Future Work

4.1 Conclusions

Post-polymerization modification (PPM) is a powerful method by which polymers are modified by reaction after polymerization has taken place and provides a way obtain functional polymers. The power of PPM comes from the ability to construct complex polymers with functionalities that may not be compatible with desired polymerization conditions. “Click” reactions provide a fast, clean, and efficient way to introduce functionality to a polymer post-polymerization, an example of which includes the catalyst-free strain-promoted azide-alkyne cycloaddition (SPAAC). In this thesis, it was envisioned that the alkyne would be incorporated into the polymer and that the functional entity introduced via PPM would contain an azide. The SPAAC reaction requires a strained alkyne to be present, which is a highly reactive functional group. Thus, a cyclopropenone masking strategy was used to prevent any side reactivity. This strategy involves the masking of the strained alkyne via a highly inert cyclopropenone group that is unmasked by UV light irradiation. Benefits of this strategy include: the unmasking process only involves the evolution of carbon monoxide gas and the exposure of UV light may be controlled thus giving the unmasking process spatiotemporal control if desired.

In chapter 2, the synthesis and characterization of a monomer (**6**) with a cyclopropenone-masked strained alkyne (hνDIBO-monomer) was described. The monomer was synthesized via condensation of the cyclopropenone-masked strained alkyne, hνDIBO (**1**), with a norbornene derivative (**5**) via nucleophilic substitution. This

monomer was characterized by ^{1}H and ^{13}C NMR spectroscopy, HRMS, FT-IR spectroscopy, and UV-Vis spectroscopy. The ^{1}H NMR showed incorporation of signals from (**1**), most notably those from the phenyl rings at 7.93-7.96 ppm and 6.84-6.91 ppm and the cyclooctyl ethane bridge at 3.31-3.35 ppm and 2.58-2.66 ppm. The ^{1}H NMR spectrum also showed incorporation of signals of (**5**), most notably those from the alkene in the bicycle at 6.28-6.30 ppm and the bridgehead positions at 2.68-2.70 ppm. The ^{13}C NMR spectrum showed the presence of (**1**), most notably from the cyclopropenone alkene and carbonyl signals at 154.2 ppm and 161.9 ppm, respectively. The ^{13}C NMR spectrum also confirmed presence of (**5**), most notably from the imide carbonyl signal at 178.5 ppm. The HRMS spectrum for (**6**) was calculated to have an m/z of 523.2359, which is in agreement with the experimental m/z found to be 523.2356. The FT-IR spectrum of (**6**) showed diagnostic peaks at ~1840 cm^{-1} corresponding to C=O stretching of the cyclopropenone ketone, ~1695 cm^{-1} corresponding to C=O stretching of the imide carbonyls, and 1600 cm^{-1} corresponding to the C=C stretching of the cyclopropenone alkene. The UV-Vis spectrum of (**6**) showed diagnostic bands at 310-350 nm corresponding to the cyclopropenone group and 240-260 nm corresponding to the two phenyl rings of hνDIBO. Before polymerization, a control experiment was run to test the compatibility of hνDIBO with the catalyst used for polymerization, a derivative of Grubbs' third generation catalyst. The study involved subjecting a hνDIBO derivative to catalyst in DCM under a nitrogen atmosphere for 1 hour, meant to mimic polymerization conditions. This study showed that a reaction occurred yielding an impurity, though it was determined to be <5% of the crude sample by ^{1}H NMR analysis. The subsequent ring-opening metathesis polymerization of (**6**) yielding hνDIBO-polymer (**13**) (**Scheme 24**) was also a

success, confirmed by ^{1}H NMR spectroscopy, SEC, IR spectroscopy, and UV-Vis spectroscopy. The ^{1}H NMR spectrum of hvDIBO-polymer (**13**) showed retention of all monomer peaks expected to remain unaffected by polymerization, most notably the aromatic signals at 7.80-7.90 ppm and 6.80-6.90 ppm. It also showed polymer backbone alkene peaks at 5.51 and 5.71 ppm and a broadening of signals expected of a polymer ^{1}H NMR spectrum. The SEC data for (**13**) revealed a $\bar{M}_n$ of 40.9 kg/mol, a $\bar{M}_w$ of 71.1, a PDI of 1.74, a DP_n of 78, and a polymer conversion of 74%. The FT-IR spectrum of (**13**) included diagnostic peaks at ~1840 cm^{-1} corresponding to C=O stretching of the cyclopropenone ketone, ~1695 cm^{-1} corresponding to C=O stretching of the imide carbonyls, and 1600 cm^{-1} corresponding to the C=C stretching of the cyclopropenone alkene. The UV-Vis spectrum of (**13**) showed diagnostic bands at 310-350 nm corresponding to the cyclopropenone group and 240-260 nm corresponding to the two phenyl rings of hvDIBO. A polymerization behavior study was also performed, which revealed that the polymerization process cannot be deemed "living", though it is a successful method of polymerization.

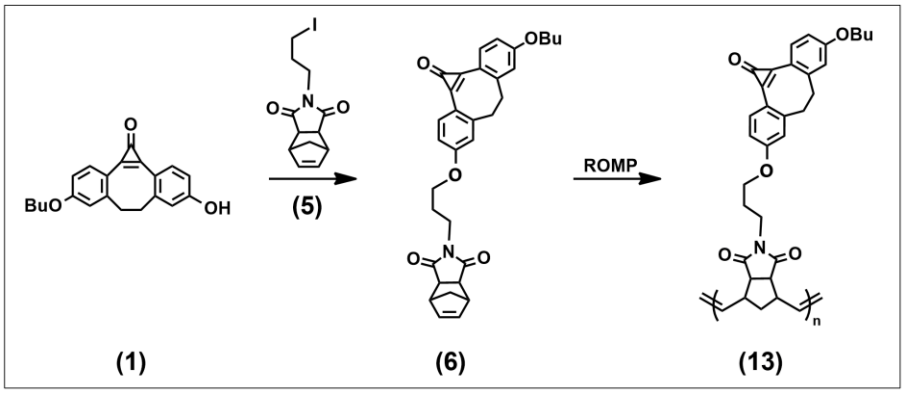

Scheme 25. General scheme of the synthesis of hvDIBO-monomer (**6**) and subsequent ring-opening metathesis polymerization yielding hvDIBO-polymer (**13**).

Chapter 3 focused upon the PPM via SPAAC of (**13**) to show the ability of this system to serve as a functional polymer template (**Scheme 25**). First, the PPM of (**13**) was performed using benzyl azide as a small molecule model. The unmasking reaction of (**13**) was first tested as a stand-alone reaction and monitored via UV-Vis spectroscopy. An initial spectrum of (**13**) was taken, showing bands at 331–349 nm corresponding to the cyclopropenone group. The solution was then placed in the Luzchem reactor fitted with 350 nm lamps and irradiated for 15 minutes. A UV-Vis spectrum was then collected which showed the disappearance of the bands corresponding to the cyclopropenone and the appearance of bands at 304–322 nm corresponding to the formation of unmasked strained alkyne. After success of the unmasking reaction of (**13**), the reaction with benzyl azide was performed. The same process as mentioned above was repeated, but with excess benzyl azide in solution. After the unmasking reaction the solution was concentrated, allowed to react, and purified by precipitation yielding benzyl-triazole-DIBO-polymer (**14**). Polymer (**14**) was characterized by SEC and UV-Vis, FT-IR, and ^{1}H NMR spectroscopy. The UV-Vis spectrum of (**14**) showed the disappearance of bands at 304–322 nm corresponding to the consumption of the strained alkyne. The FT-IR spectrum of (**14**) showed the loss of the peak at ~1840 cm^{-1} corresponding to C=O stretching of the cyclopropenone ketone and signals at ~1695 cm^{-1} corresponding to C=O stretching of the imide carbonyls and ~1600 cm^{-1} corresponding to C=C stretching of the cyclopropenone alkene. The ^{1}H NMR spectrum of (**14**) showed an integration of 11 protons in the aromatic region, an additional 5 beyond that of the spectrum for (**13**) suggesting the inclusion of the benzyl group from the SPAAC reaction. Also, the integration of 2 alkene protons from the backbone of the polymer seen in the spectrum of (**13**) as well as the addition of 2 new protons corresponding

to the methylene protons of the benzyl group are seen at 5.50–5.70 ppm. The SEC experiment yielded results that would suggest that the molecular weight of the polymer decreased after the reaction. This is likely due to an unfavourable solvent-polymer interaction between (**14**) and the SEC solvent DMF, causing the polymer to contract in solution and appear smaller. The increased non-polar character introduced by the benzyl groups are the probable cause of this phenomenon. To demonstrate a more complex system, a gold-25 nanocluster decorated with 18 azide-appended ligands (Au_{25} azide) was introduced via PPM. First, the SPAAC of Au_{25} azide (1/19 equivalents) was attempted with monomer (**6**), yielding Au_{25}-triazole-DIBO-monomer (**15**), and characterized by UV-Vis and FT-IR spectroscopy. This reaction was monitored via UV-Vis and appeared very similar to the monitoring of (**14**), showing a successful deprotection and click reaction. The FT-IR of (**15**) also appeared very similar to that of (**14**), but with the addition of N=N=N stretching appearing at ~2110 cm^{-1} due to unreacted azide from Au_{25} azide. After the success of reaction of Au_{25} azide with monomer (**6**), the reaction was performed with polymer (**13**) but with 1/21 equivalents of azide yielding Au_{25}-triazole-DIBO-polymer (**16**). The SPAAC reaction was characterized by UV-Vis and FT-IR spectroscopy with almost identical results for that of (**15**), showing a successful reaction. The reaction was also characterized by XPS, which showed a relative increase in N_{1s} and decrease in O_{1s} character when comparing the XPS spectra from (**13**) to (**16**). This corresponds to the introduction of a triazole ring from the Au_{25} azide SPAAC and the loss of the cyclopropenone during unmasking of (**13**). Also, a N_{1s} high-resolution scan revealed the appearance of triazole N_{1s} character and a relative decrease in imide N_{1s} character when

comparing the XPS spectra from (**13**) to (**16**). This corresponds to the introduction of a triazole ring from the Au_{25} azide SPAAC reaction.

Overall, this work demonstrated a synthetic route to a novel polymer which contained a strained alkyne, protected via a cyclopropenone, in each repeating unit. After polymerization, the cyclopropenone could then easily and efficiently be removed via UV light irradiation with no purification required. This method of deprotection also allows for spatiotemporal control, as exposure of UV light to the polymer could be controlled if desired. PPM could then be performed via SPAAC reaction with functional azides, both of a small molecule and more complex nature. This system as a whole demonstrates the ability of this polymer to serve as a functional polymer/material template with the ability to synthesize entire libraries of functional polymers with ease.

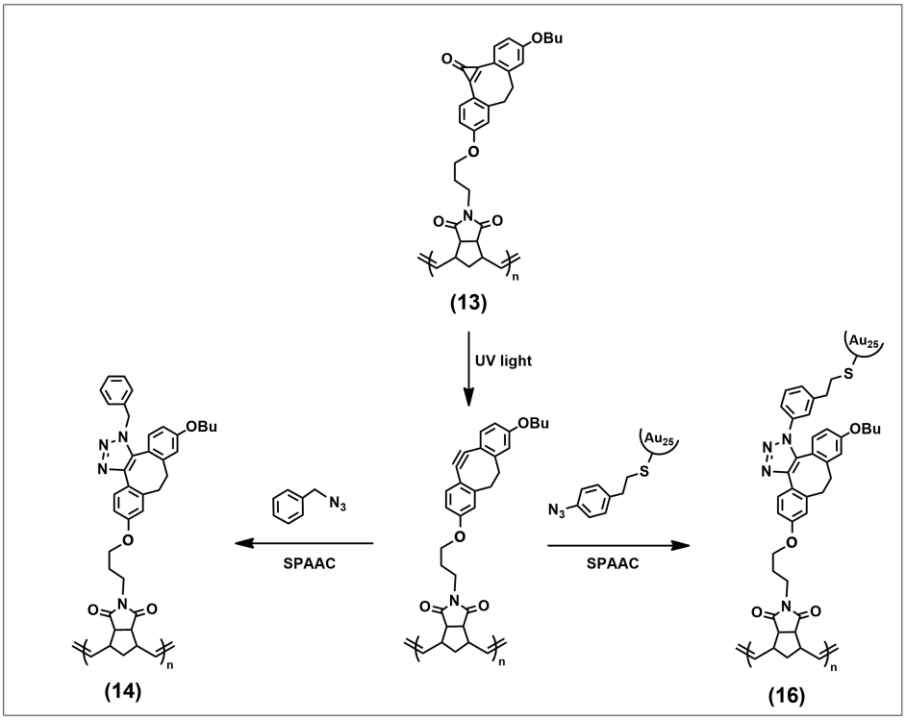

Scheme 26. General scheme of the synthesis of functional polymers via SPAAC post-polymerization. Shown are the simplified schemes of the syntheses of (14) and (16).

4.2 Future Work

Future work on this system would involve further polymerization behavior studies. This would allow for a more comprehensive data set to analyze polymerization behavior and allow for the polymerization to be optimized for higher consistency in molecular weight targeting and distribution (PDI). Demonstrated in this work is the ability to modify polymers with Au_{25} nanoclusters. Next steps include testing properties of this polymer-nanocluster hybrid for applications such as chemical sensing[75], catalysis[76], and optical imaging.[77] In addition, the ability to control the unmasking of the cyclopropenone via selective irradiation would allow for photopatterning applications to be explored. This would involve spin-coating a thin film of masked polymer and covering portions of the film, allowing for the selective irradiation of exposed portions of film. The exposed

portions of the film could then be introduced to azide and allowed to react. This process could then be repeated as desired, yielding the ability to make multifunctional polymers.

An array of functional azides could be introduced to this system to create a library of functional polymers (**Scheme 26**). This could include emissive molecules such as Rhodamine B as a model for applications in chemical sensing.[73] This could also include polymers adapted with azides to create graft copolymers for self-assembly.

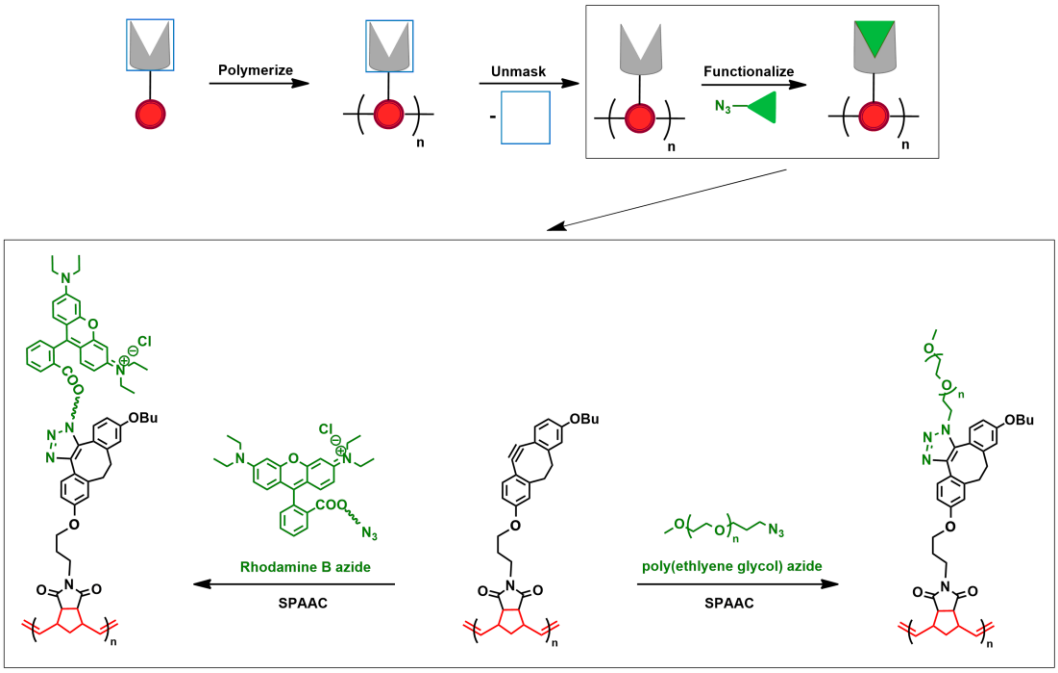

Scheme 27. General scheme of the synthesis of a library of functional polymers using the functional polymer template presented in this thesis.

5 References

(1) Mülhaupt, R. *Angew. Chem. Int. Ed.* **2004**, *43* (9), 1054–1063.

(2) Jensen, W. B. *J. Chem. Educ.* **2008**, *85* (5), 624–625.

(3) Jenkins, A. D.; Stepto, R. F. T.; Kratochvíl, P.; Suter, U. W. *Pure Appl. Chem.* **1996**, *68* (12), 2287–2311.

(4) Jaeger, W.; Bohrisch, J.; Laschewsky, A. *Prog. Polym. Sci.* **2010**, *35* (5), 511–577.

(5) Fan, B.; Trant, J. F.; Wong, A. D.; Gillies, E. R. *J. Am. Chem. Soc.* **2014**, *136* (28), 10116–10123.

(6) Wang, Y.; Zhang, J.; Wang, X.; Antonietti, M.; Li, H. *Angew. Chem. Int. Ed.* **2010**, *49* (19), 3356–3359.

(7) Manners, I. *Synthetic Metal-Containing Polymers*; Wiley-VCH: Weinham, 2003.

(8) Puddephatt, R. J. *Chem. Commun.* **1998**, *0* (10), 1055–1062.

(9) Aboudzadeh, M. A.; Muñoz, M. E.; Santamaría, A.; Marcilla, R.; Mecerreyes, D. *Macromol. Rapid Commun.* **2012**, *33* (4), 314–318.

(10) Heeger, A. J. *J. Phys. Chem. B* **2001**, *105* (36), 8475–8491.

(11) Nicholson, J. W. *The Chemistry of Polymers*, 5th ed.; Royal Society of Chemistry: London, 2017.

(12) Clark, M.-A.; Choi, J.; Douglas, M. *Biology 2e*; OpenStax, 2018.

(13) Ebdon, J. R. *Polym. Int.* **1992**, *27* (2), 10–13.

(14) Yokozawa, T.; Yokoyama, A. *Polym. J.* **2004**, *36* (2), 65–83.

(15) Flory, P. J. *Principles of Polymer Chemistry*; Cornell University Press: Ithaca, 1953.

(16) Billiet, L.; Fournier, D.; Du Prez, F. *Polym. J.* **2009**, *50* (16), 3877–3886.

(17) Palmer, R. J. Polyamides, Plastics. In *Encyclopedia of Polymer Science and Technology*, 4th ed.; John Wiley & Sons, Inc.: Hoboken, 2001.

(18) Szwarc, M. *Nature* **1956**, *178* (4543), 1168–1169.

(19) Cowie, J. M. G.; Arrighi, V. *Polymers: Chemistry and Physics of Modern Materials*, 3rd ed.; CRC Press: New York, 2007.

(20) Matyjaszewski, K. *Macromolecules* **1993**, *26* (7), 1787–1788.

(21) Calderon, N. *J. Macromol. Sci. Part C* **1972**, *7* (1), 105–159.

(22) Ivin, K. J.; Mol, J. C. *Olefin Metathesis and Metathesis Polymerization*, 2nd ed.; Academic Press: San Diego, 1997.

(23) Grubbs, R. H. *Handbook of Metathesis*; Wiley-VCH: Weinham, Germany, 2003; Vol. 3.

(24) Calderon, N. *Acc. Chem. Res.* **1972**, *5* (4), 127–132.

(25) Bielawski, C. W.; Grubbs, R. H. *Prog. Polym. Sci.* **2007**, *32* (1), 1–29.

(26) Benson, S. W.; Golden, D. M.; Haugen, G. R.; Shaw, R.; Cruickshank, F. R.; Rodgers, A. S.; O'neal, H. E.; Walsh, R. *Chem. Rev.* **1969**, *69* (3), 279–324.

(27) Tebbe, F. N.; Parshall, G. W.; Ovenall, D. W. *J. Am. Chem. Soc.* **1979**, *101* (17), 5074–5075.

(28) Wallace, K. C.; Schroch, R. R. *Macromolecules* **1987**, *20* (2), 448–450.

(29) Schrock, R. R.; Feldman, J.; Cannizzo, L. F.; Grubbs, R. H. *Macromolecules* **1987**, *20* (5), 1169–1172.

(30) Oskam, J. H.; Schrock, R. R. *J. Am. Chem. Soc.* **1993**, *115* (25), 11831–11845.

(31) Nguyen, S. B. T.; Johnson, L. K.; Grubbs, R. H.; Ziller, J. W. *J. Am. Chem. Soc.* **1992**, *114* (10), 3974–3975.

(32) Bielawski, C. W.; Benitez, D.; Morita, T.; Grubbs, R. H. *Macromolecules* **2001**, *34* (25), 8610–8618.

(33) Schwab, P.; Grubbs, R. H.; Ziller, J. W. *J. Am. Chem. Soc.* **1996**, *118* (1), 100–108.

(34) Lynn, D. M.; Kanaoka, S.; Grubbs, R. H. *J. Am. Chem. Soc.* **1996**, *118* (4), 784–789.

(35) Scholl, M.; Ding, S.; Lee, C. W.; Grubbs, R. H. *Org. Lett.* **1999**, *1* (6), 953–956.

(36) Scholl, M.; Trnka, T. M.; Morgan, J. P.; Grubbs, R. H. *Tetrahedron Lett.* **1999**, *40* (12), 2247–2250.

(37) Bielawski, C. W.; Grubbs, R. H. *Angew. Chemie Int. Ed.* **2000**, *39* (16), 2903–2906.

(38) Love, J. A.; Morgan, J. P.; Trnka, T. M.; Grubbs, R. H. *Angew. Chemie Int. Ed.* **2002**, *41* (21), 4035–4037.

(39) Choi, T.-L.; Grubbs, R. H. *Angew. Chemie Int. Ed.* **2003**, *42* (15), 1743–1746.

(40) Liechty, W. B.; Kryscio, D. R.; Slaughter, B. V.; Peppas, N. A. *Annu. Rev. Chem. Biomol. Eng.* **2010**, *1* (1), 149–173.

(41) Yang, Y.; Urban, M. W. *Chem. Soc. Rev.* **2013**, *42* (17), 7446–7467.

(42) Janata, J.; Josowicz, M. *Nat. Mater.* **2003**, *2* (1), 19–24.

(43) Noga, D. E.; Petrie, T. A.; Kumar, A.; Weck, M.; García, A. J.; Collard, D. M. *Biomacromolecules* **2008**, *9* (7), 2056–2062.

(44) Gauthier, M. A.; Gibson, M. I.; Klok, H.-A. *Angew. Chemie Int. Ed.* **2009**, *48* (1), 48–58.

(45) Raycraft, B. M.; MacDonald, J. P.; McIntosh, J. T.; Shaver, M. P.; Gillies, E. R. *Polym. Chem.* **2017**, *8* (3), 557–567.

(46) Kolb, H. C.; Finn, M. G.; Sharpless, K. B. *Angew. Chemie Int. Ed.* **2001**, *40* (11), 2004–2021.

(47) Rostovtsev, V. V.; Green, L. G.; Fokin, V. V.; Sharpless, K. B. *Angew. Chemie Int. Ed.* **2002**, *41* (14), 2596–2599.

(48) Lutz, J.-F. *Angew. Chemie Int. Ed.* **2007**, *46* (7), 1018–1025.

(49) Lutz, J. F.; Zarafshani, Z. *Adv. Drug Deliv. Rev.* **2008**, *60* (9), 958–970.

(50) Li, S.; Cai, H.; He, J.; Chen, H.; Lam, S.; Cai, T.; Zhu, Z.; Bark, S. J.; Cai, C. *Bioconjug. Chem.* **2016**, *27* (10), 2315–2322.

(51) Agard, N. J.; Prescher, J. A.; Bertozzi, C. R. *J. Am. Chem. Soc.* **2004**, *126* (46), 15046–15047.

(52) Shea, K. J.; Kim, J. S. *J. Am. Chem. Soc.* **1992**, *114* (12), 4846–4855.

(53) Patterson, D. M.; Nazarova, L. A.; Prescher, J. A. *ACS Chem. Biol.* **2014**, *9* (3), 592–605.

(54) Krebs, A.; Wilke, J. *Top. Curr. Chem.* **1983**, *109*, 189–233.

(55) Dommerholt, J.; Rutjes, F. P. J. T.; van Delft, F. L. *Top. Curr. Chem.* **2016**, *374* (2).

(56) Turner, R. B.; Jarrett, A. D.; Goebel, P.; Mallon, B. J. *J. Am. Chem. Soc.* **1973**, *95* (3), 790–792.

(57) Bach, R. D. *J. Am. Chem. Soc.* **2009**, *131* (14), 5233–5243.

(58) Wang, S.; Yang, X.; Zhu, W.; Zou, L.; Zhang, K.; Chen, Y.; Xi, F. *Polymer (Guildf).* **2014**, *55* (19), 4812–4819.

(59) McNelles, S. A.; Pantaleo, J. L.; Meichsner, E.; Adronov, A. *Macromolecules* **2019**, *52* (19), 7183–7187.

(60) Li, K.; McNelles, S. A.; Adronov, A. *Synlett* **2018**, *29* (19), 2535–2541.

(61) Poloukhtine, A. A.; Mbua, N. E.; Wolfert, M. A.; Boons, G. J.; Popik, V. V. *J. Am. Chem. Soc.* **2009**, *131* (43), 15769–15776.

(62) Poloukhtine, A.; Popik, V. V. *J. Org. Chem.* **2003**, *68* (20), 7833–7840.

(63) Urdabayev, N. K.; Poloukhtine, A.; Popik, V. V. *Chem. Commun.* **2006**, No. 4, 454–456.

(64) McNitt, C. D.; Popik, V. V. *Org. Biomol. Chem.* **2012**, *10* (41), 8200–8202.

(65) Orski, S. V.; Poloukhtine, A. A.; Arumugam, S.; Mao, L.; Popik, V. V.; Locklin, J. *J. Am. Chem. Soc.* **2010**, *132* (32), 11024–11026.

(66) Lallana, E.; Fernandez-Megia, E.; Riguera, R. *J. Am. Chem. Soc.* **2009**, *131* (16), 5748–5750.

(67) Bernardin, A.; Cazet, A.; Guyon, L.; Delannoy, P.; Vinet, F.; Bonnaffé, D.; Texier, I. *Bioconjug. Chem.* **2010**, *21* (4), 583–588.

(68) Fong, D.; Andrews, G. M.; McNelles, S. A.; Adronov, A. *Polym. Chem.* **2018**, *9* (35), 4460–4467.

(69) Wang, C. F.; Mäkilä, E. M.; Kaasalainen, M. H.; Liu, D.; Sarparanta, M. P.; Airaksinen, A. J.; Salonen, J. J.; Hirvonen, J. T.; Santos, H. A. *Biomaterials* **2014**, *35* (4), 1257–1266.

(70) Luo, W.; Gobbo, P.; McNitt, C. D.; Sutton, D. A.; Popik, V. V.; Workentin, M. S. *Chem. - A Eur. J.* **2017**, *23* (5), 1052–1059.

(71) Li, K.; Kardelis, V.; Adronov, A. *J. Polym. Sci. Part A Polym. Chem.* **2018**, *56* (18), 2053–2058.

(72) Ledin, P. A.; Kolishetti, N.; Boons, G. J. *Macromolecules* **2013**, *46* (19), 7759–7768.

(73) Orski, S. V.; Sheppard, G. R.; Arumugam, S.; Arnold, R. M.; Popik, V. V.; Locklin, J. *Langmuir* **2012**, *28* (41), 14693–14702.

(74) Kardelis, V.; Chadwick, R. C.; Adronov, A. *Angew. Chemie Int. Ed.* **2016**, *55* (3), 945–949.

(75) Pu, K. Y.; Luo, Z.; Li, K.; Xie, J.; Liu, B. *J. Phys. Chem. C* **2011**, *115* (26), 13069–13075.

(76) Li, G.; Abroshan, H.; Liu, C.; Zhuo, S.; Li, Z.; Xie, Y.; Kim, H. J.; Rosi, N. L.; Jin, R. *ACS Nano* **2016**, *10* (8), 7998–8005.

(77) Polavarapu, L.; Manna, M.; Xu, Q. H. *Nanoscale* **2011**, *3* (2), 429–434.

(78) Gunawardene, P. N.; Corrigan, J. F.; Workentin, M. S. *J. Am. Chem. Soc.* **2019**, *141* (30), 11781–11785.

(79) Vasdev, R. Strategies for the Preparation of Functional Pendant Group Polymer Materials via Click Chemistry. M.Sc. Thesis, The University of Western Ontario, London, ON, 2019.

(80) Arnold, R. M.; McNitt, C. D.; Popik, V. V.; Locklin, J. *Chem. Commun*. **2014**, *50*, 5307–5309.

(81) Dinger, M.B.; Mol, J.C. *Eur. J. Inorg. Chem.* **2003**, *15*, 2827-2833.

(82) Partyka, D. V.; Gao, L.; Teets, T. S.; Updegraff, J. B.; Deligonul, N.; Gray, T. G., *Organometallics* **2009,** *28*, 6171-6182.

Appendices

Appendix 1 - Supporting Information for Chapter 2

2-A. Characterization of hvDIBO (1)

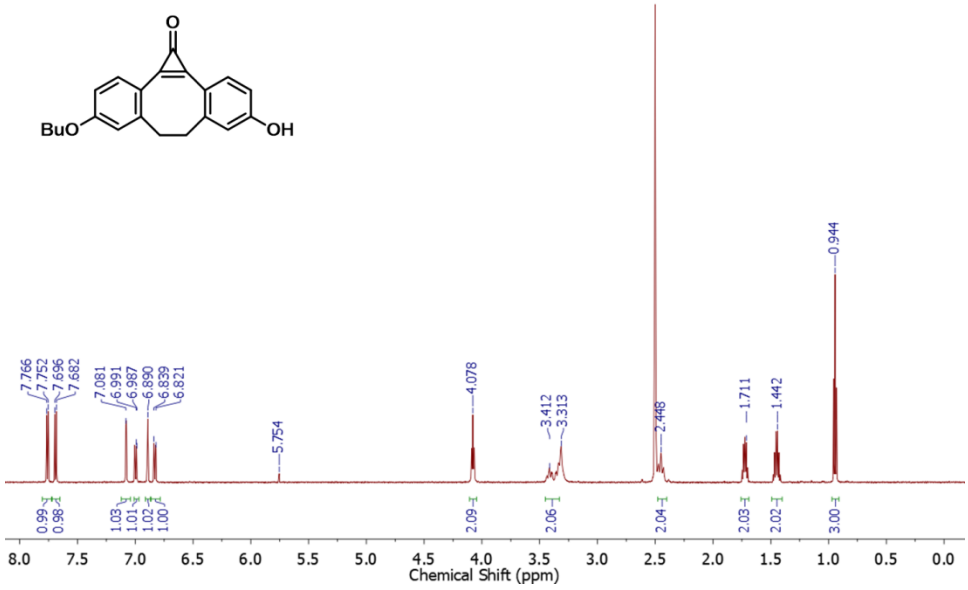

Figure A1. ^{1}H NMR spectrum of compound (**1**) in $CDCl_3$.

2-B. Characterization of Nor-Imide-Pr-OH (3)

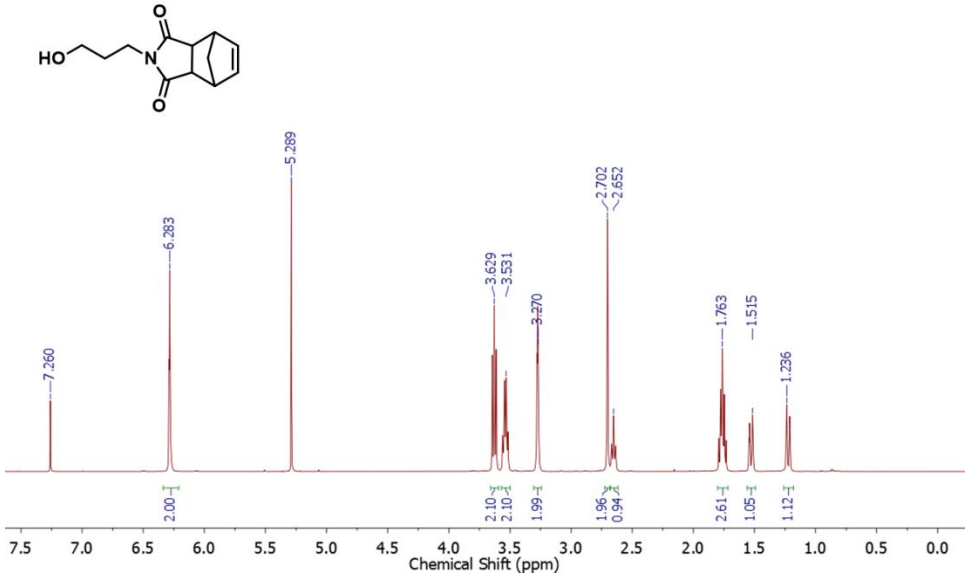

Figure B1. ^{1}H NMR spectrum of compound (**3**) in $CDCl_3$.

2-C. Characterization of Nor-Imide-Pr-I (5)

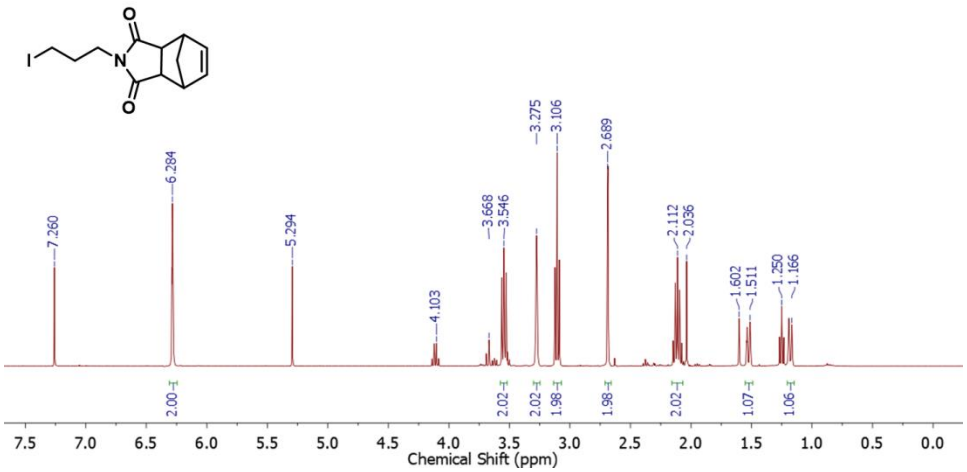

Figure C1. ^{1}H NMR spectrum of compound (**5**) in $CDCl_3$.

2-D. Characterization of hvDIBO-monomer (6)

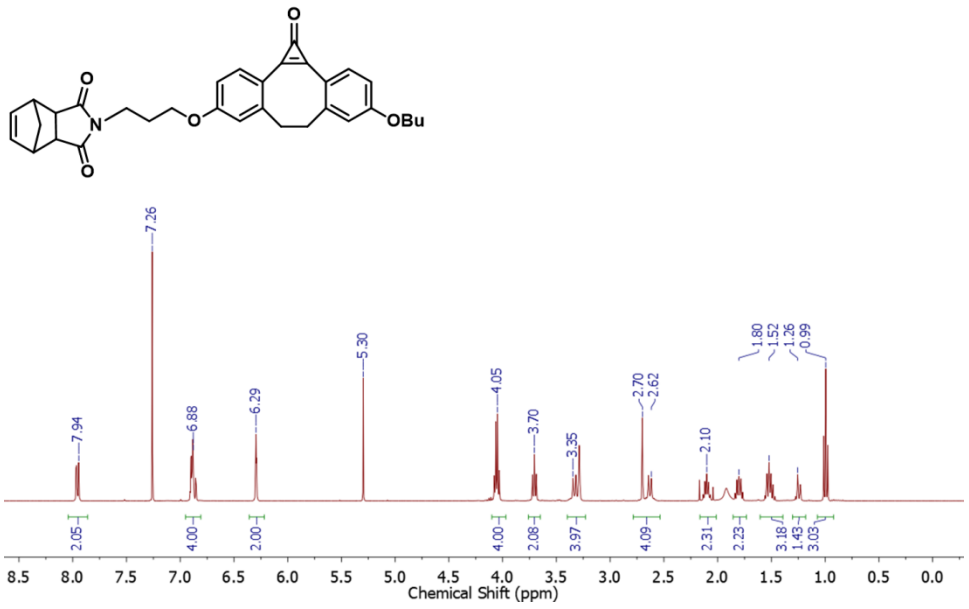

Figure D1. ^{1}H NMR spectrum of compound (**6**) in $CDCl_3$.

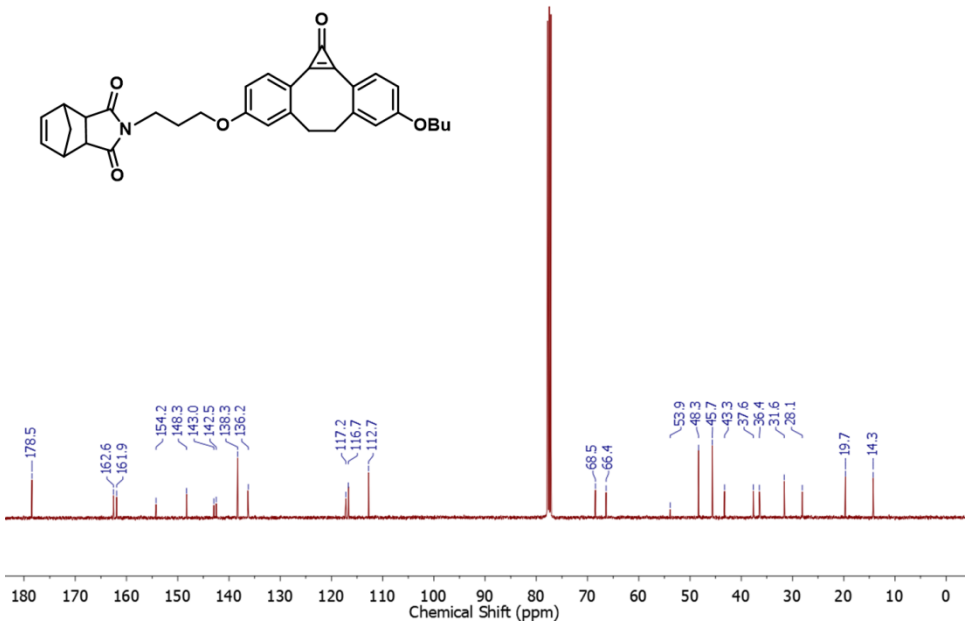

Figure D2. $^{13}C\{^{1}H\}$ NMR spectrum of compound (**6**) in $CDCl_3$.

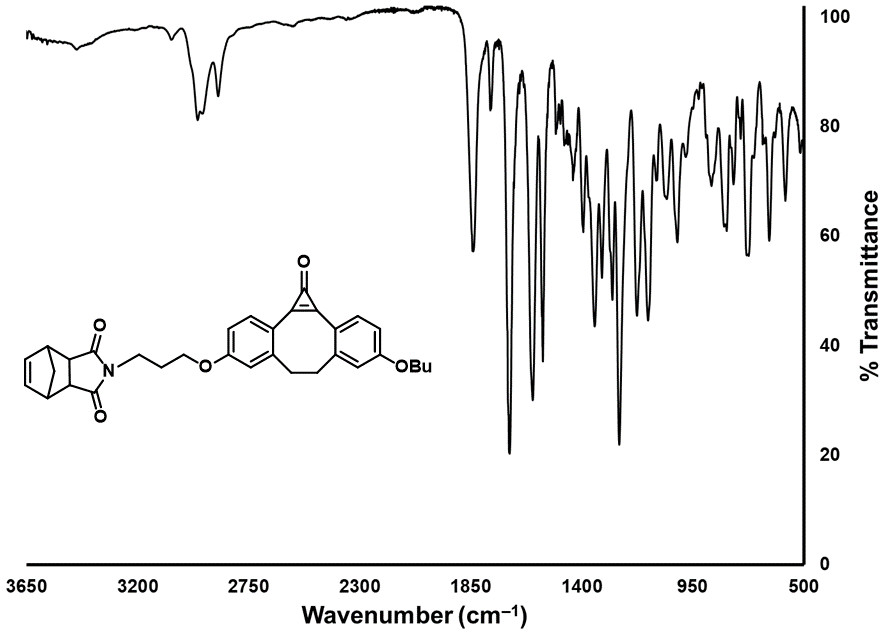

Figure D3. FT-IR spectrum of compound (**6**).

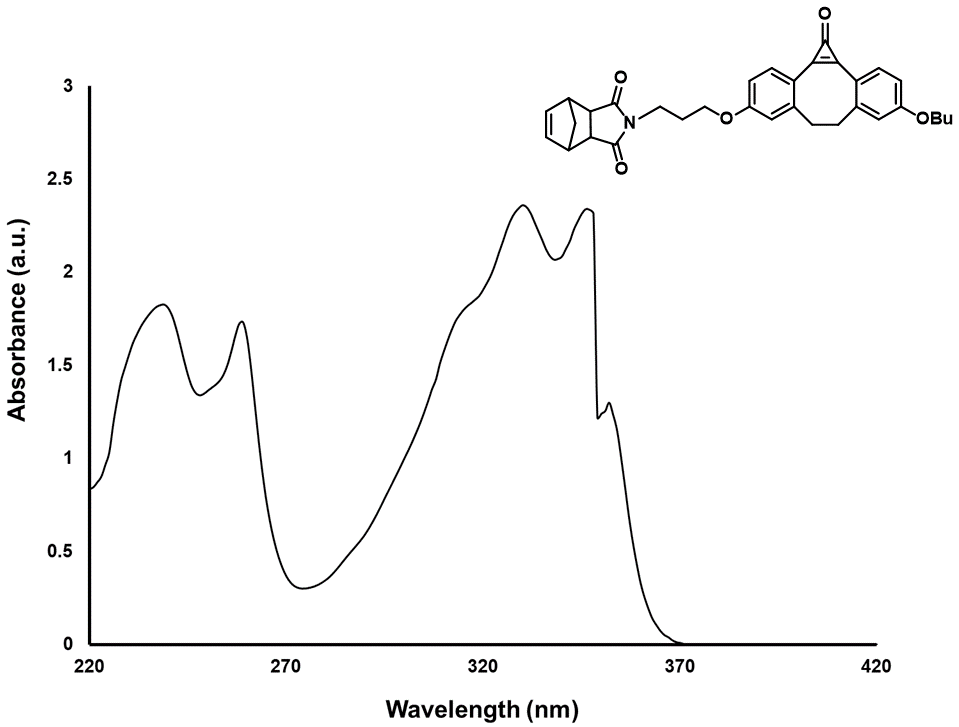

Figure D4. UV-Vis spectrum of compound (**6**) in DCM.

2-E. Characterization of hνDIBO-OBu$_2$ (7)

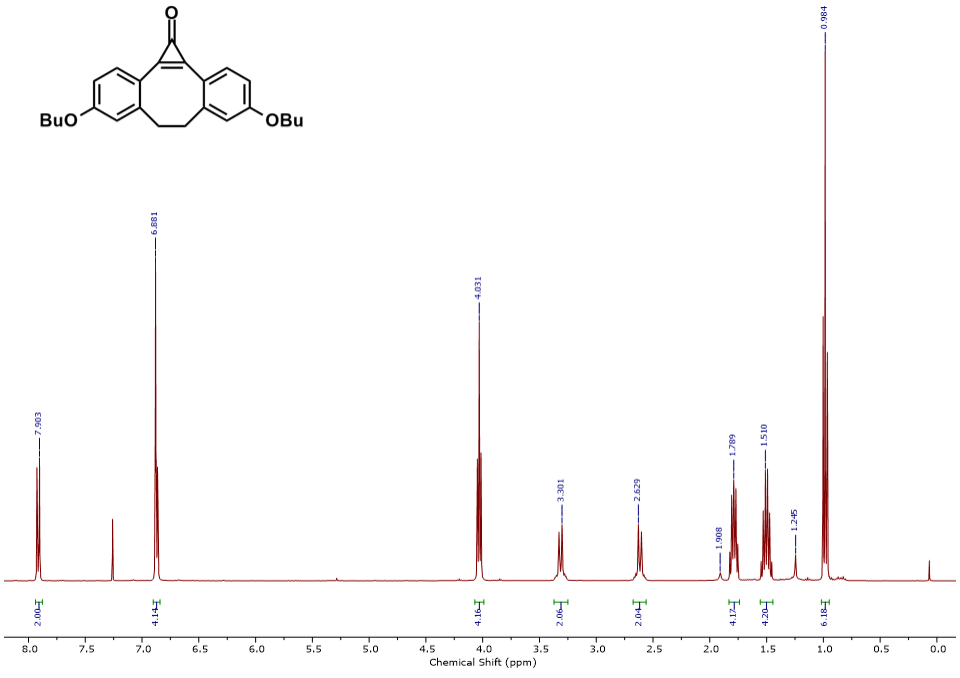

Figure E1. ^{1}H NMR spectrum of (**7**) in $CDCl_3$ before reaction with catalyst.

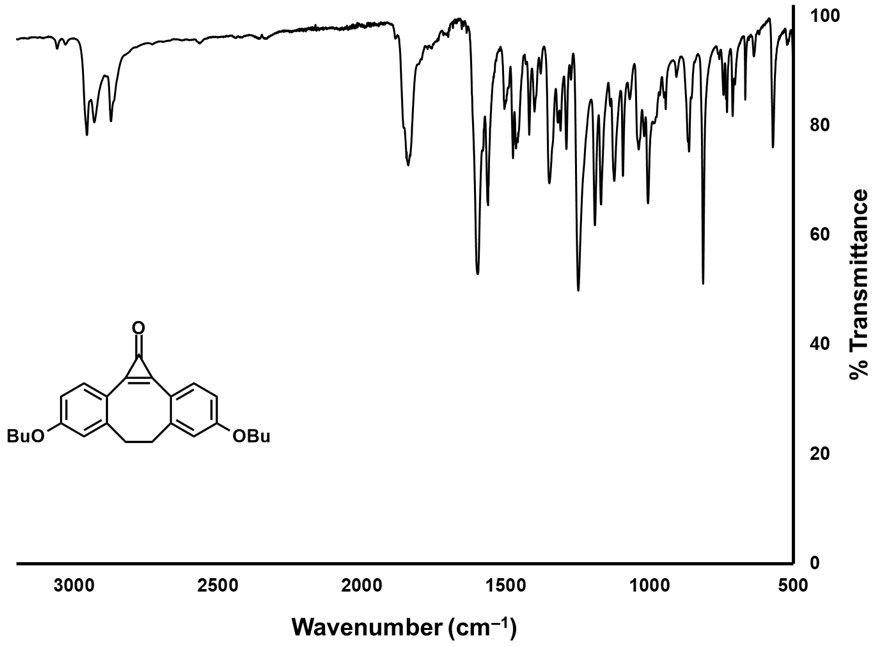

Figure E2. FT-IR spectrum of (**7**) before reaction with catalyst.

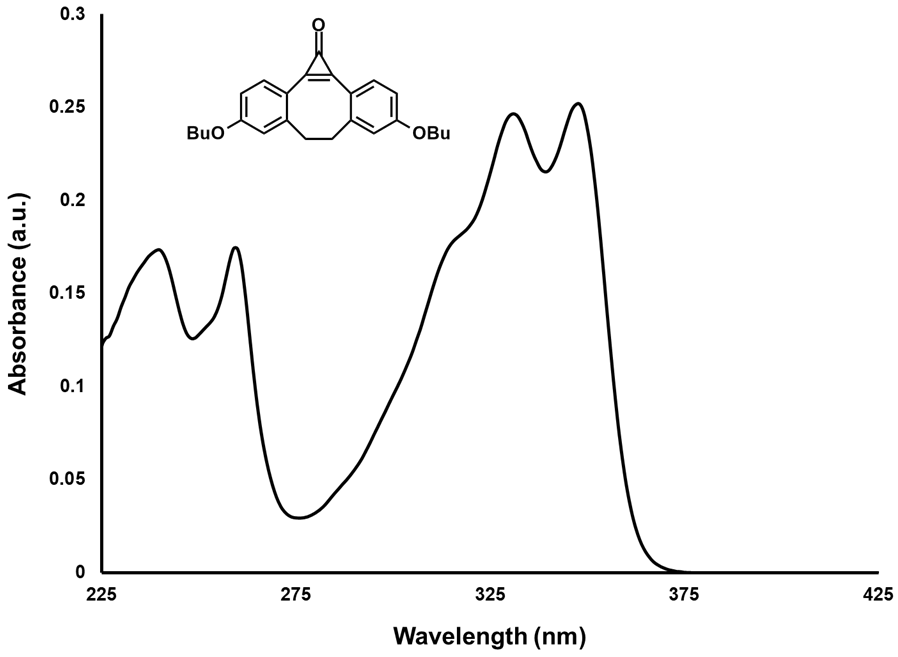

Figure E3. UV-Vis spectrum of (**7**) in DCM before reaction with catalyst.

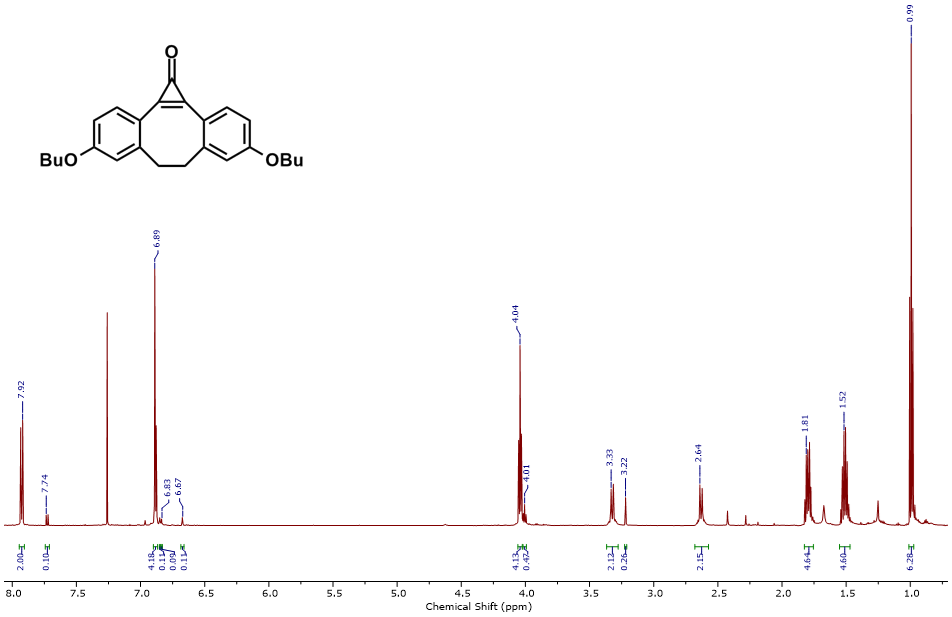

Figure E4. ^{1}H NMR spectrum of (**7.1**) in $CDCl_3$ after reaction with catalyst (crude).

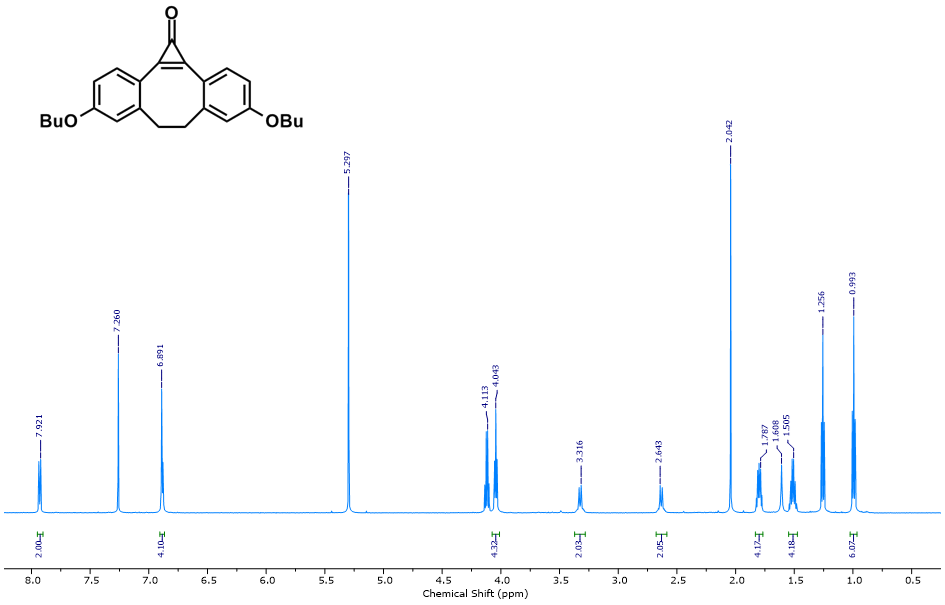

Figure E5. ^{1}H NMR spectrum of (**7.1-A**) in $CDCl_3$ after reaction with catalyst (pure).

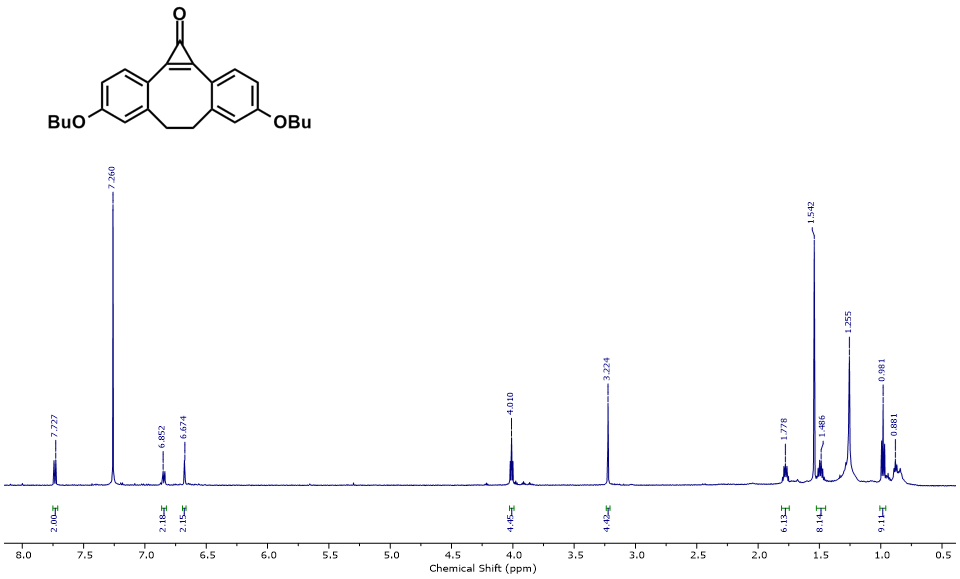

Figure E6. ^{1}H NMR spectrum of (**7.1-B**) in $CDCl_3$ after reaction with catalyst (impurity).

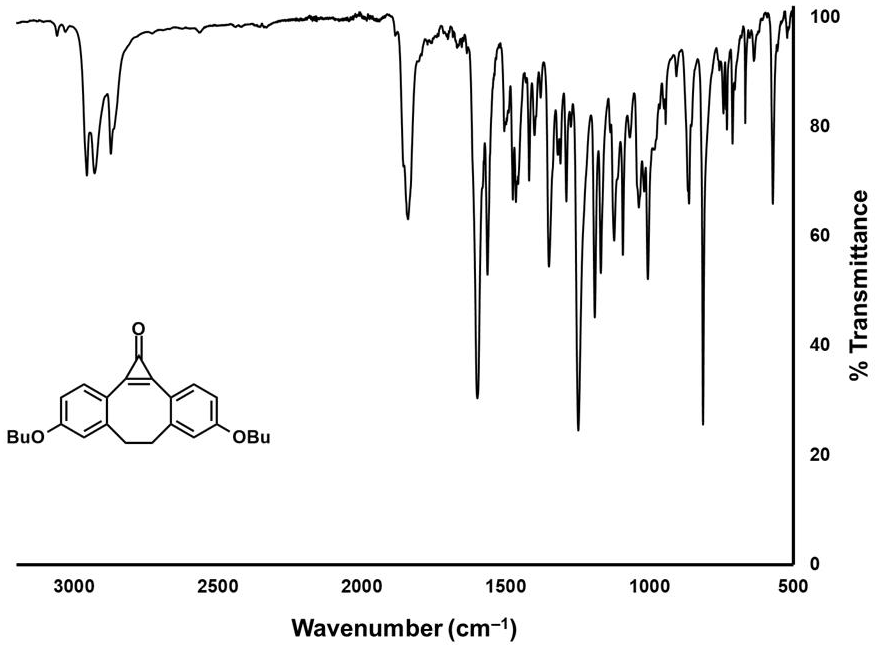

Figure E7. FT-IR spectrum of (**7.1**) after reaction with catalyst (crude).

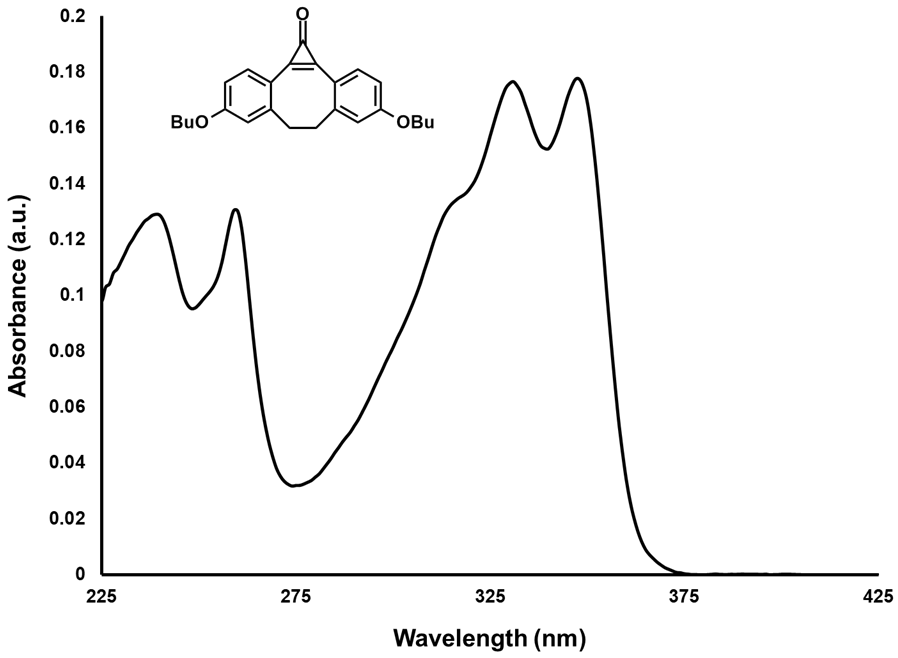

Figure E8. UV-Vis spectrum of (**7.1**) in DCM after reaction with catalyst (crude).

2-F. Characterization of hvDIBO-polymer (8)

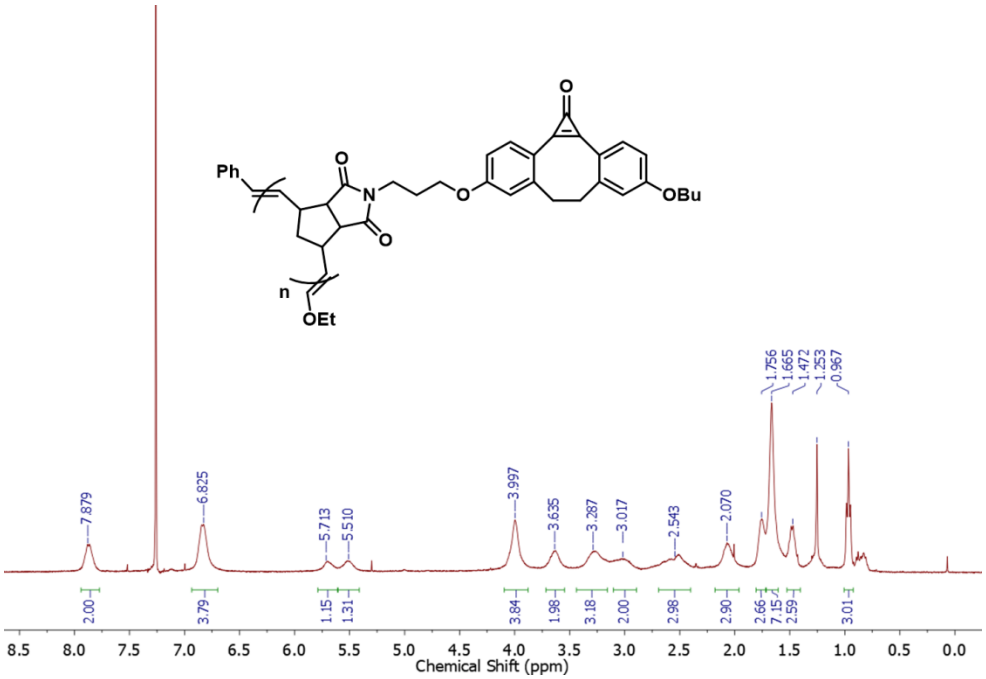

Figure F1. ^{1}H NMR spectrum of polymer (**8**) in $CDCl_3$.

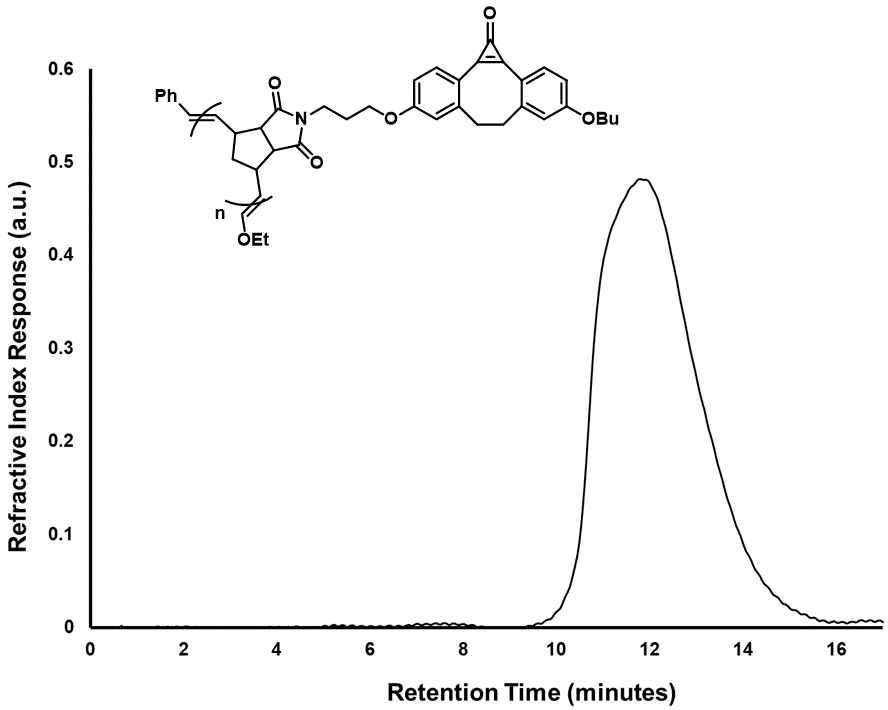

Figure F2. SEC trace of polymer (**8**) in DMF against a PS standard.

2-G. Characterization of hvDIBO-polymer (9)

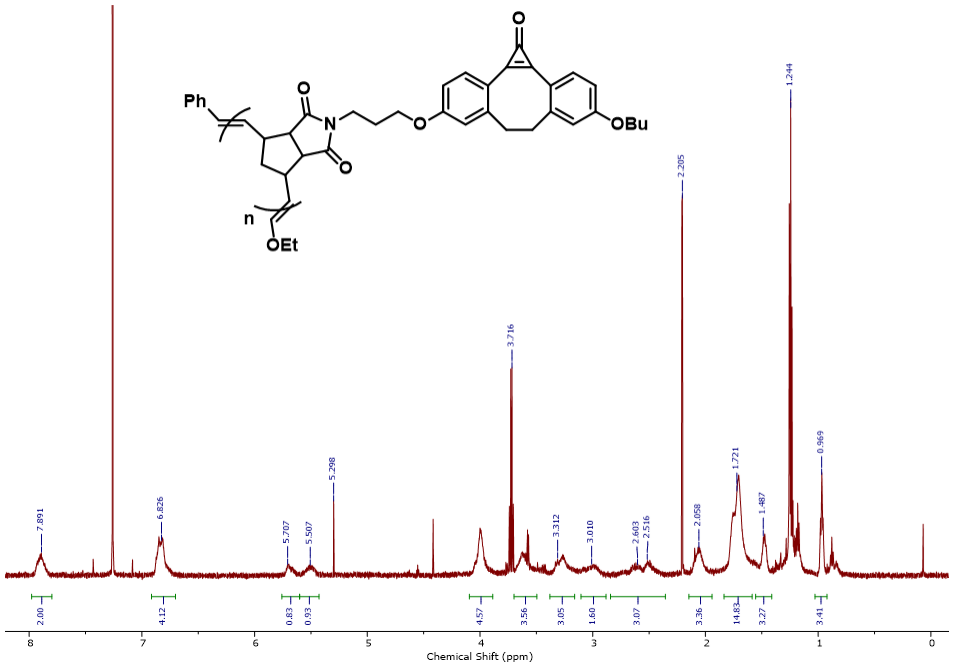

Figure G1. ^{1}H NMR spectrum of polymer (**9-10**) in $CDCl_3$.

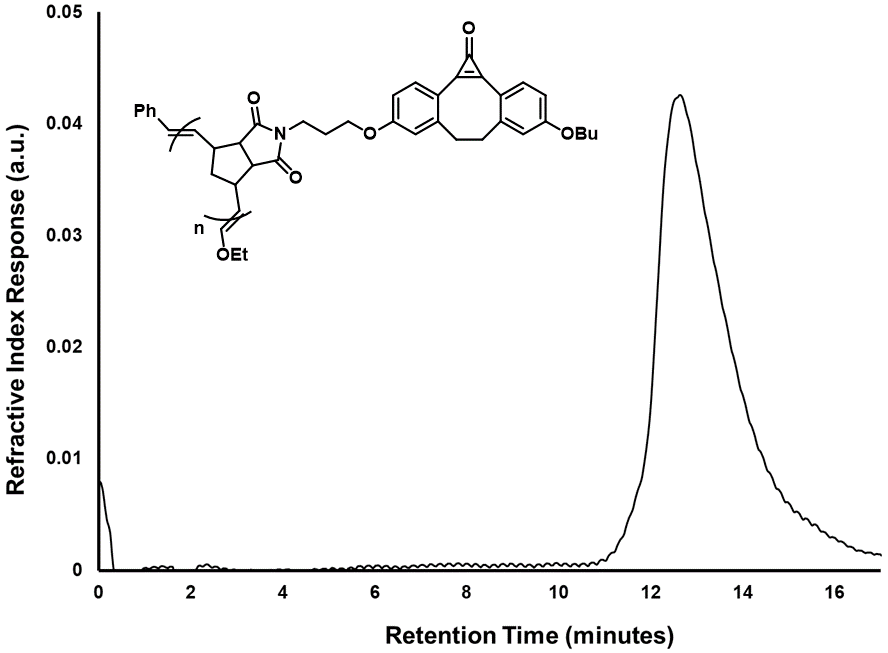

Figure G2. SEC trace of polymer (**9-10**) in DMF against a PS standard.

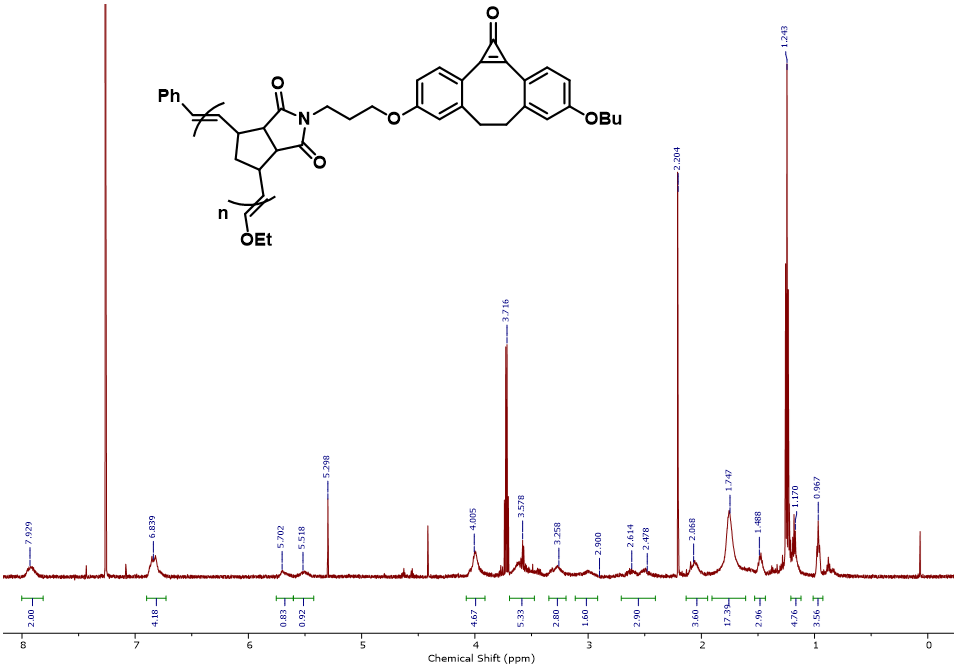

Figure G3. ^{1}H NMR spectrum of polymer (**9-20**) in $CDCl_3$.

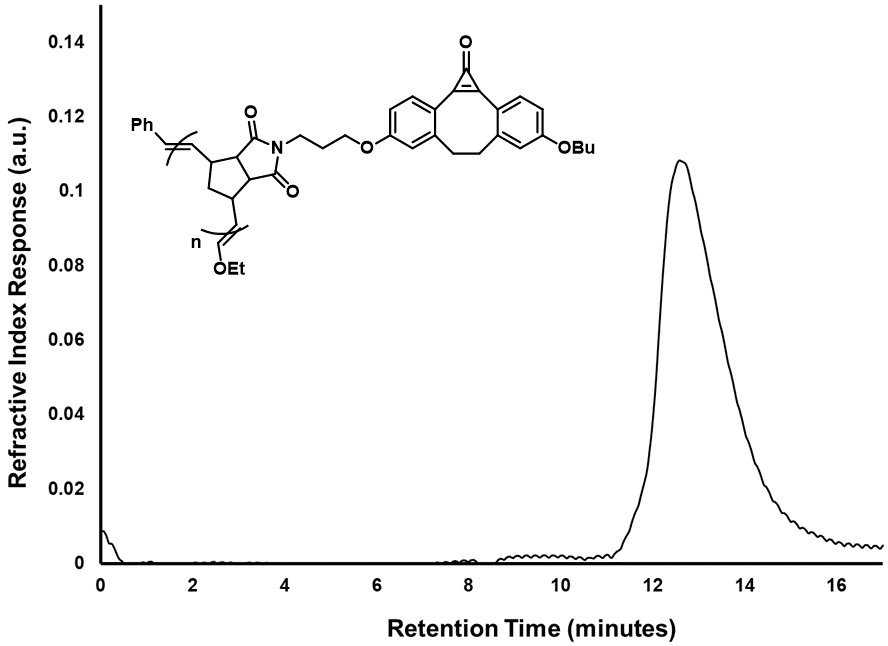

Figure G4. SEC trace of polymer (**9-20**) in DMF against a PS standard.

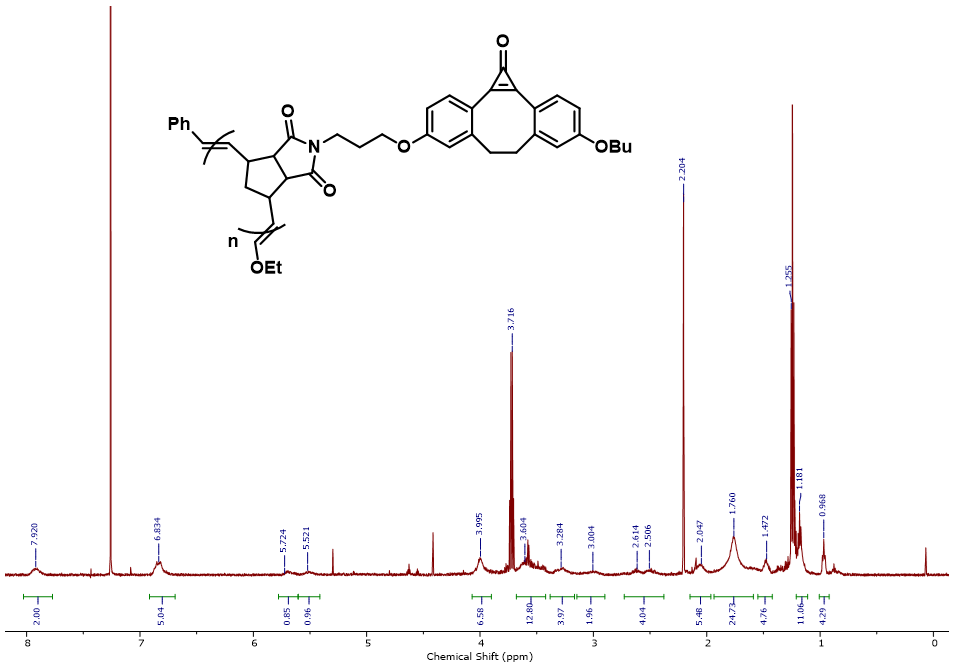

Figure G5. ^{1}H NMR spectrum of polymer (**9-30**) in $CDCl_3$.

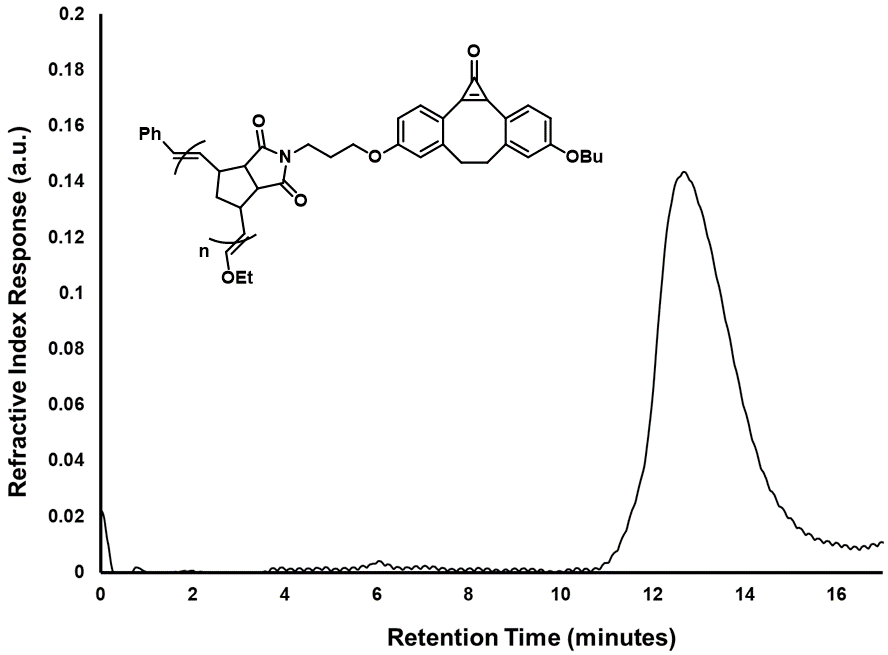

Figure G6. SEC trace of polymer (**9-30**) in DMF against a PS standard.

2-H. Characterization of hvDIBO-polymer (10)

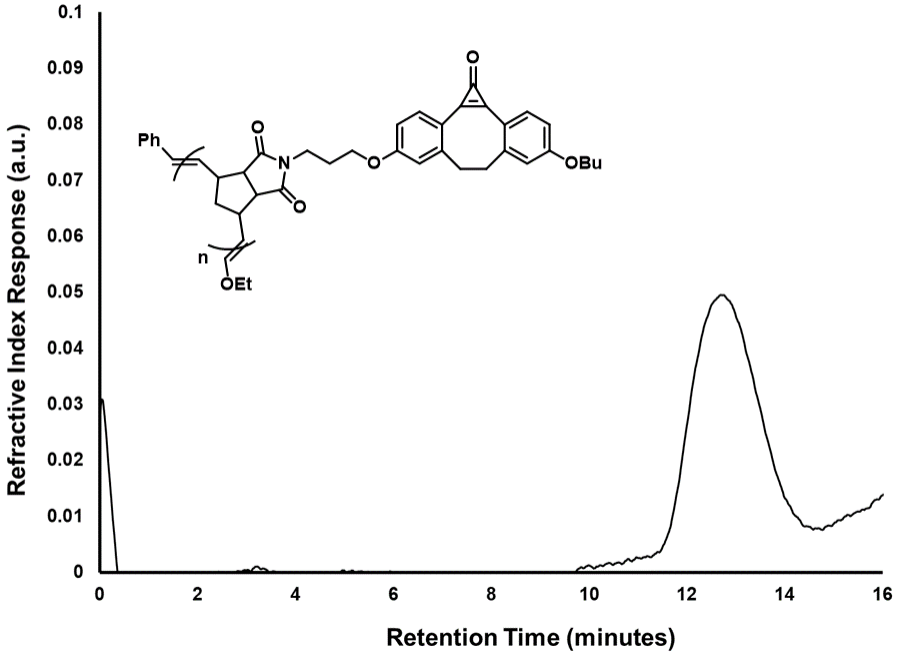

Figure H1. SEC trace of polymer (**10**) in DMF against a PS standard.

2-I. Characterization of hvDIBO-polymer (11)

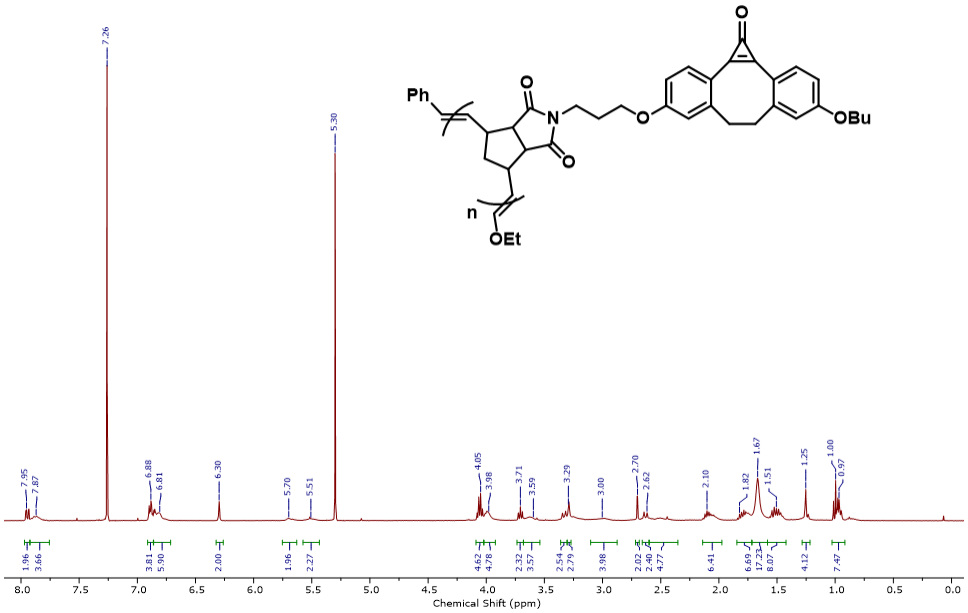

Figure I1. ^{1}H NMR spectrum of polymer (**11**) in $CDCl_3$.

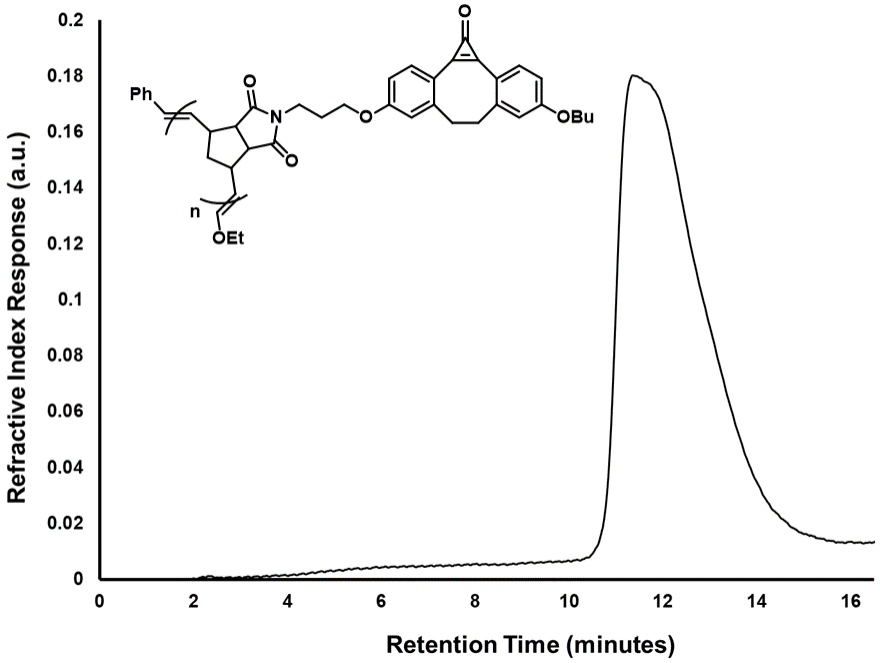

Figure I2. SEC trace of polymer (**11**) in DMF against a PS standard.

2-J. Characterization of hvDIBO-polymer (12)

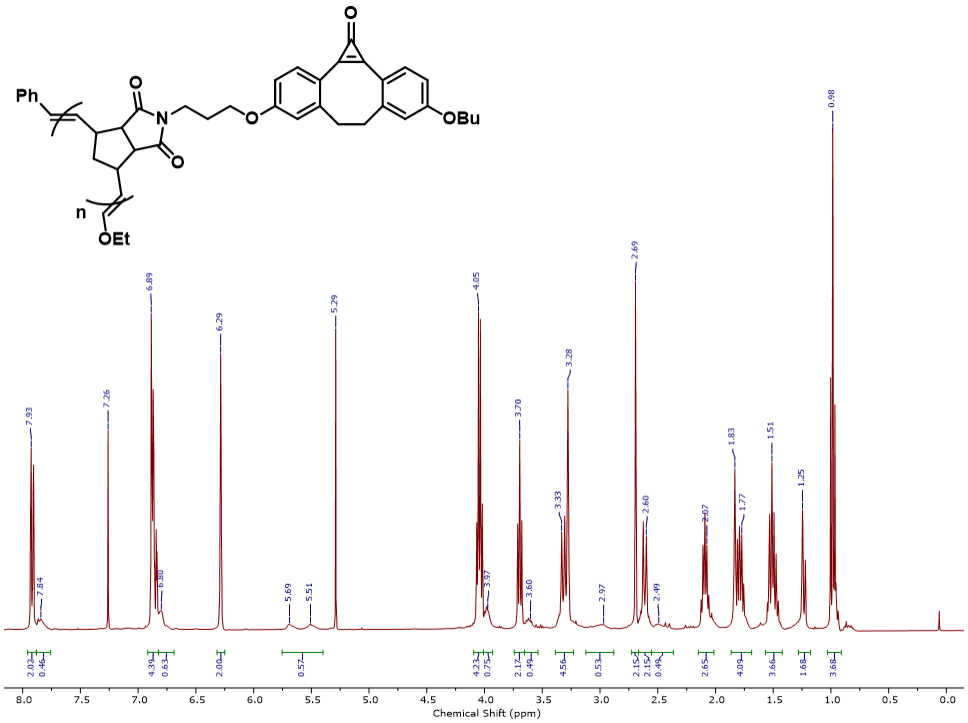

Figure J1. ^{1}H NMR spectrum of polymer (**12-10**) in $CDCl_3$.

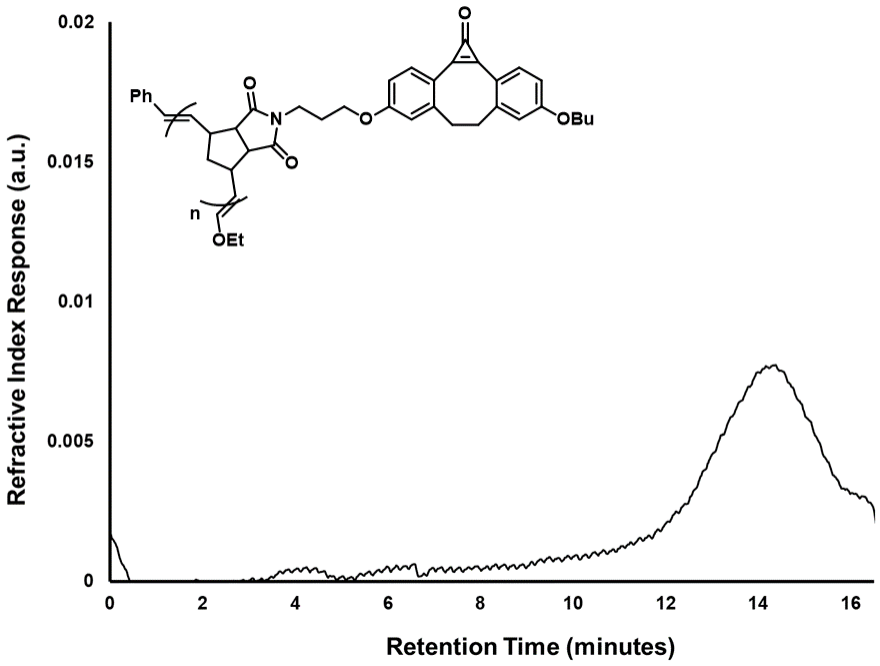

Figure J2. SEC trace of polymer (**12-10**) in DMF against a PS standard.

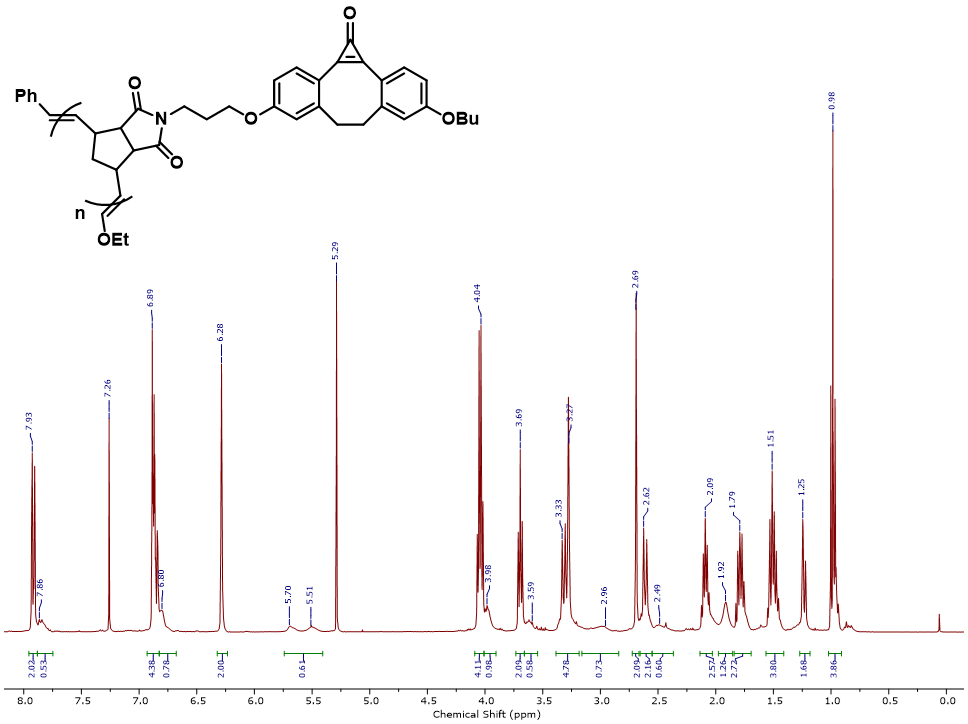

Figure J3. ^{1}H NMR spectrum of polymer (**12-20**) in $CDCl_3$.

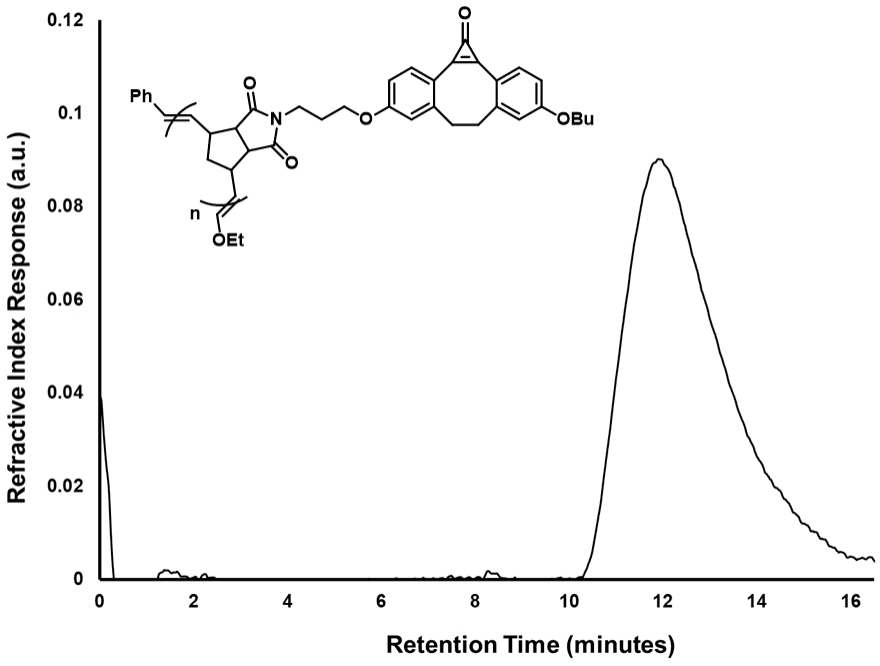

Figure J4. SEC trace of polymer (**12-20**) in DMF against a PS standard.

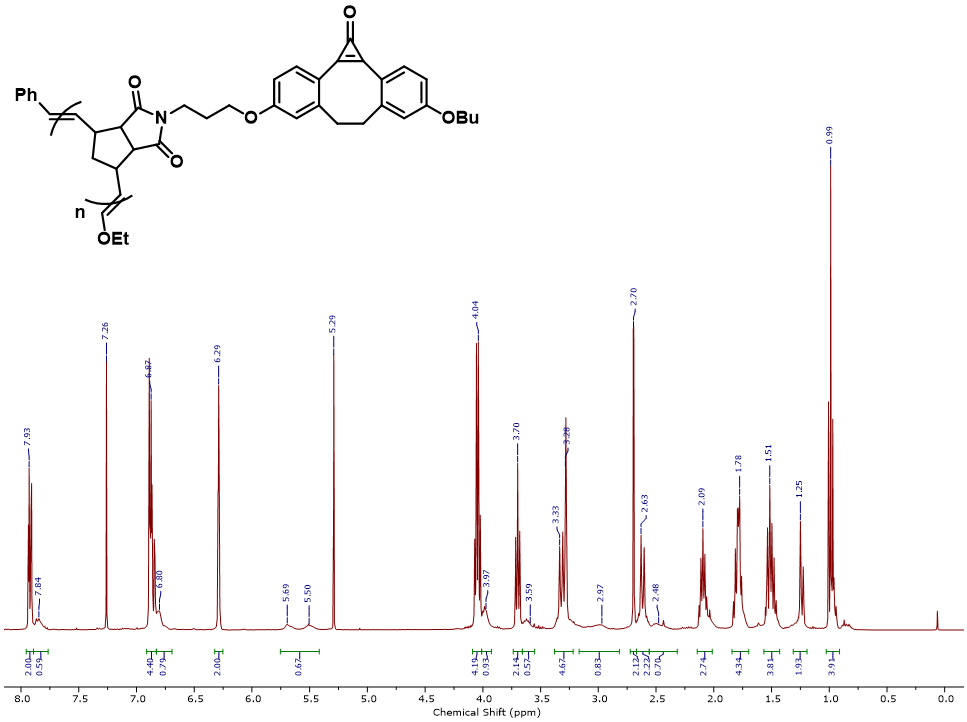

Figure J5. ^{1}H NMR spectrum of polymer (**12-40**) in $CDCl_3$.

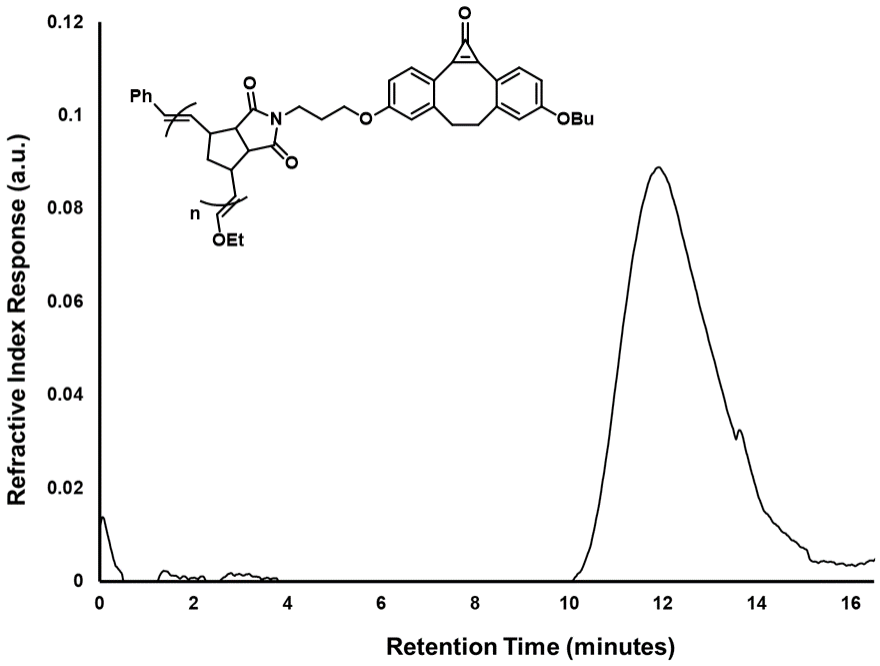

Figure J6. SEC trace of polymer (**12-40**) in DMF against a PS standard.

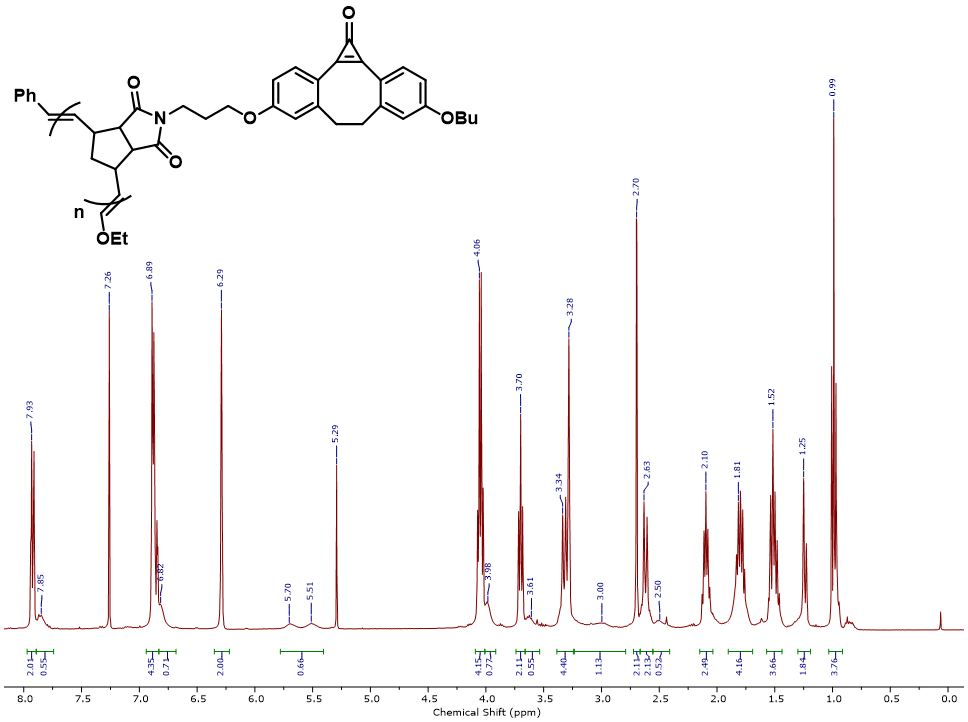

Figure J7. ^{1}H NMR spectrum of polymer (**12-80**) in $CDCl_3$.

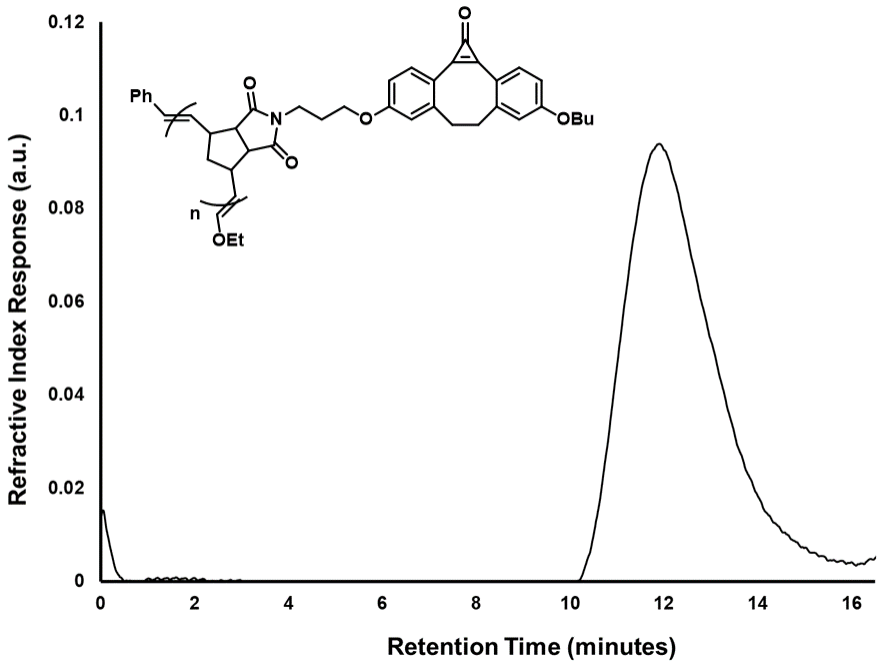

Figure J8. SEC trace of polymer (**12-80**) in DMF against a PS standard.

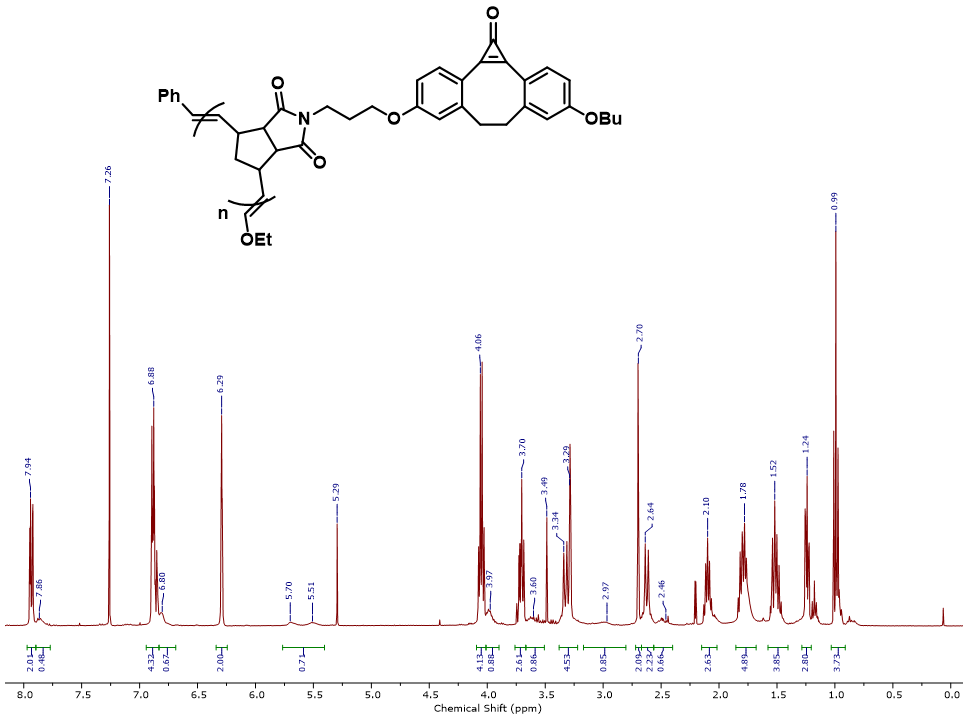

Figure J9. ^{1}H NMR spectrum of polymer (**12-120**) in $CDCl_3$.

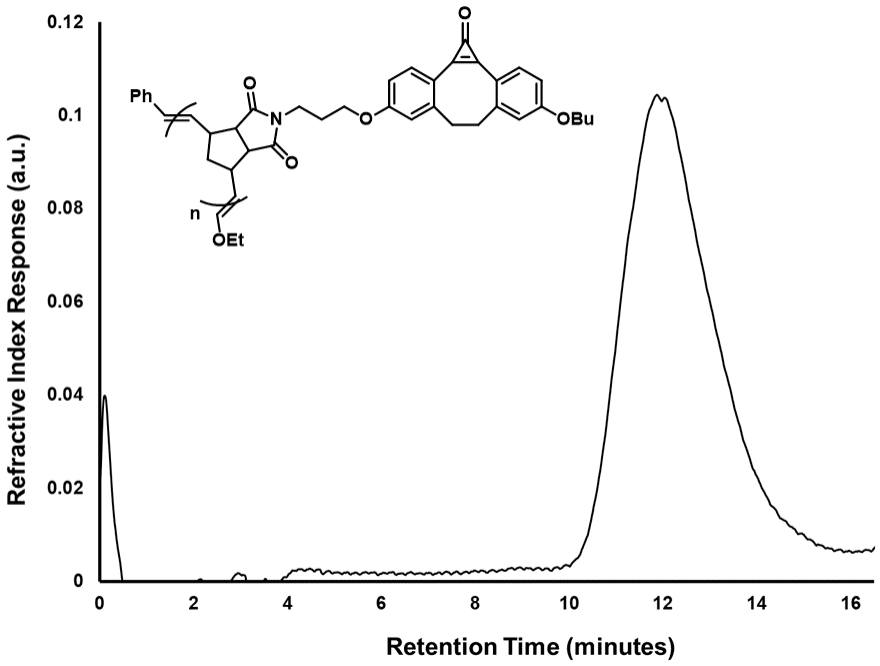

Figure J10. SEC trace of polymer (**12-120**) in DMF against a PS standard.

2-K. Characterization of hvDIBO-polymer (13)

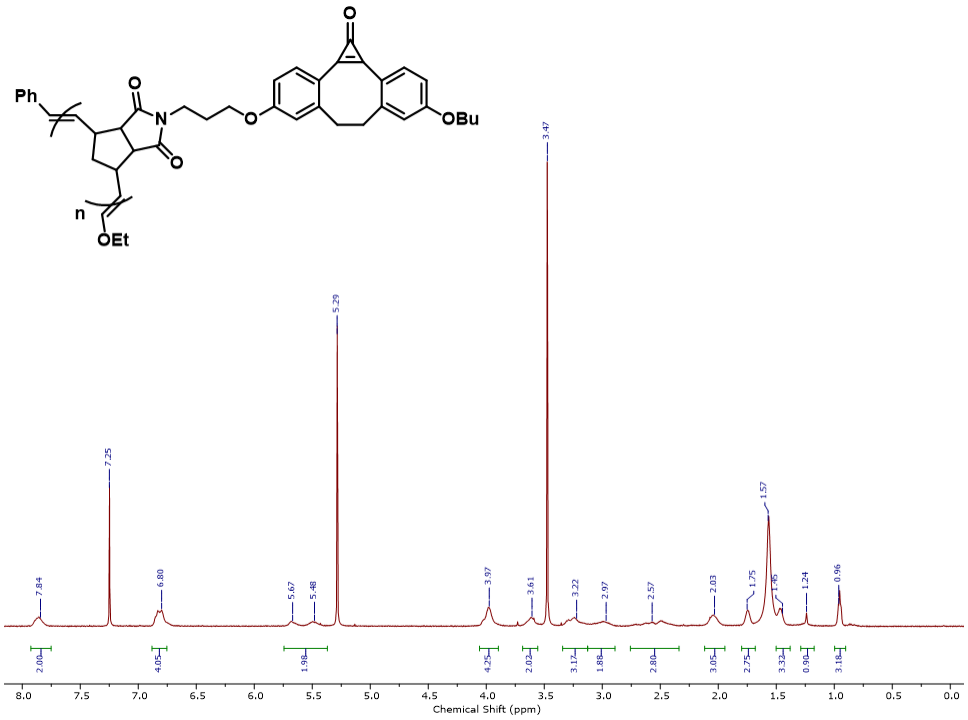

Figure K1. ^{1}H NMR spectrum of polymer (**11**) in $CDCl_3$.

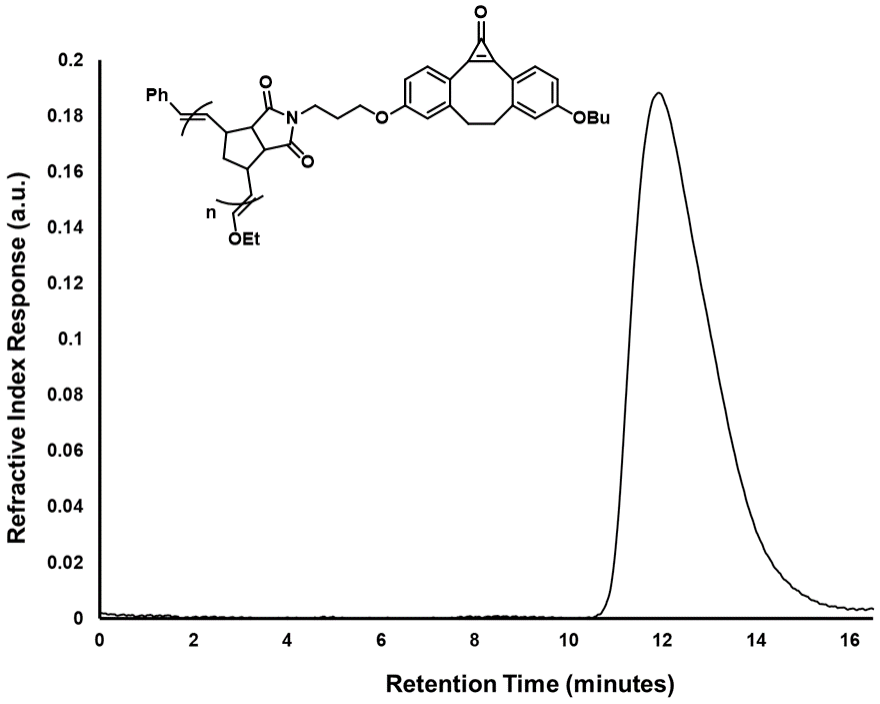

Figure K2. SEC trace of polymer (**11**) in DMF against a PS standard.

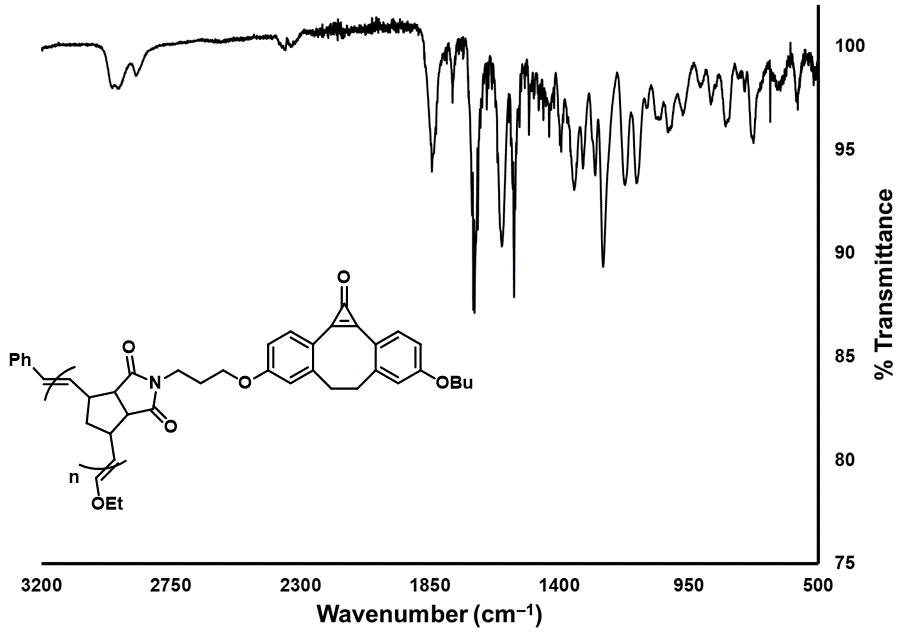

Figure K3. FT-IR spectrum of polymer (**13**).

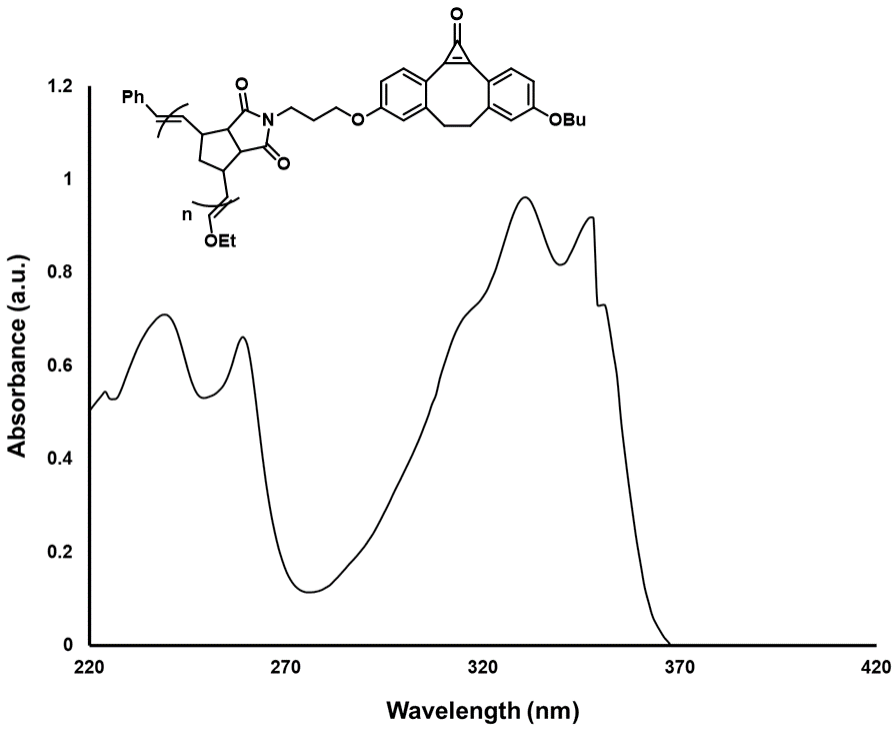

Figure K3. UV-Vis spectrum of polymer (**13**) in DCM.

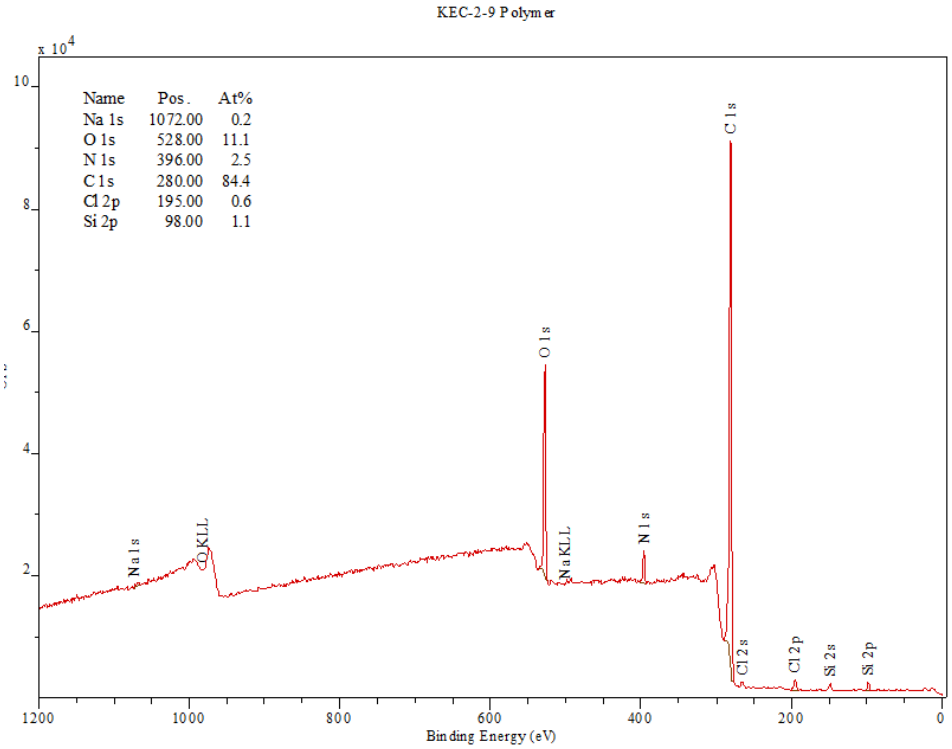

Figure K4. XPS survey scan of polymer (**13**).

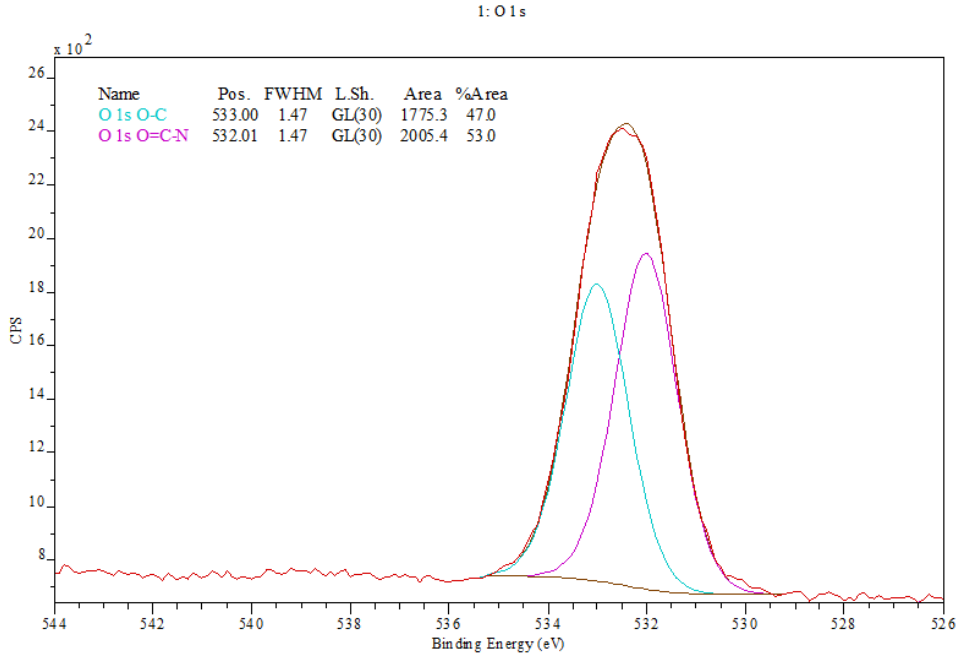

Figure K5. XPS O_{1s} high-resolution scan of (**13**).

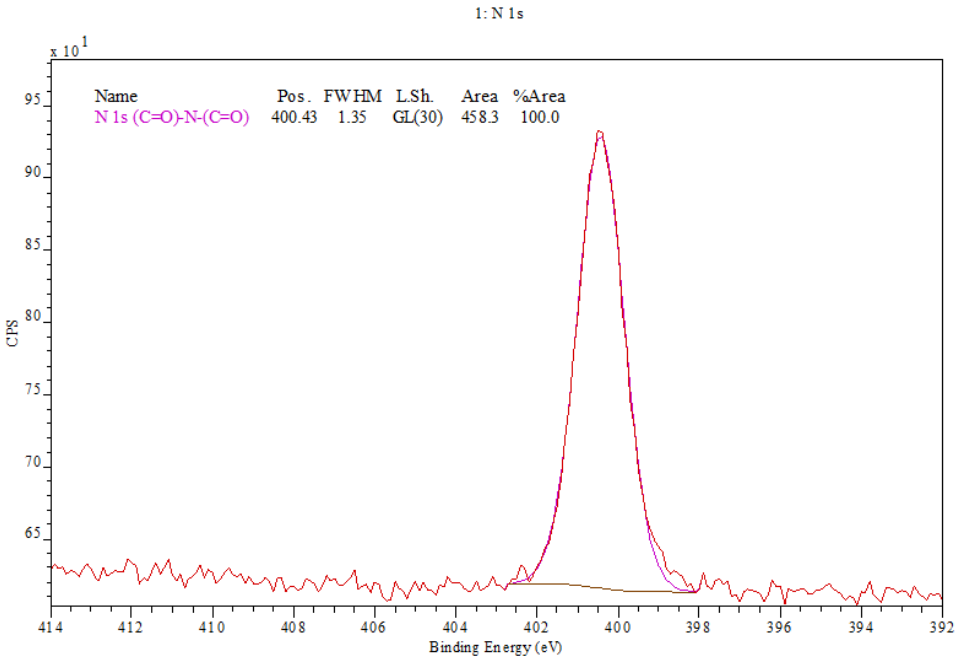

Figure K6. XPS N_{1s} high-resolution scan of (**13**).

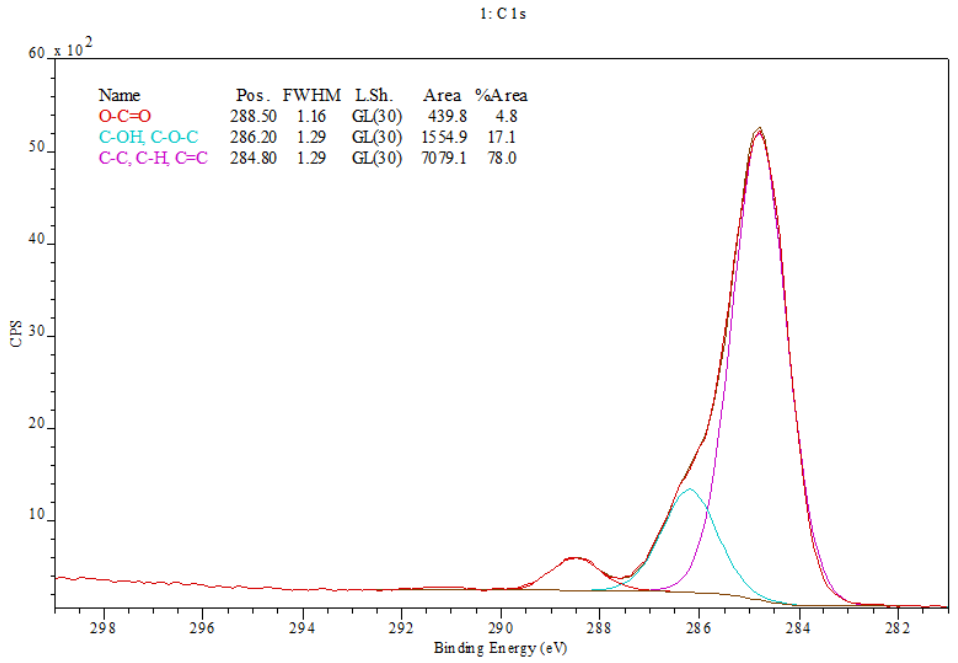

Figure K7. XPS C_{1s} high-resolution scan of (**13**).

Appendix 2 - Supporting Information for Chapter 3

3-A. Characterization of benzyl-triazole-DIBO-polymer (14)

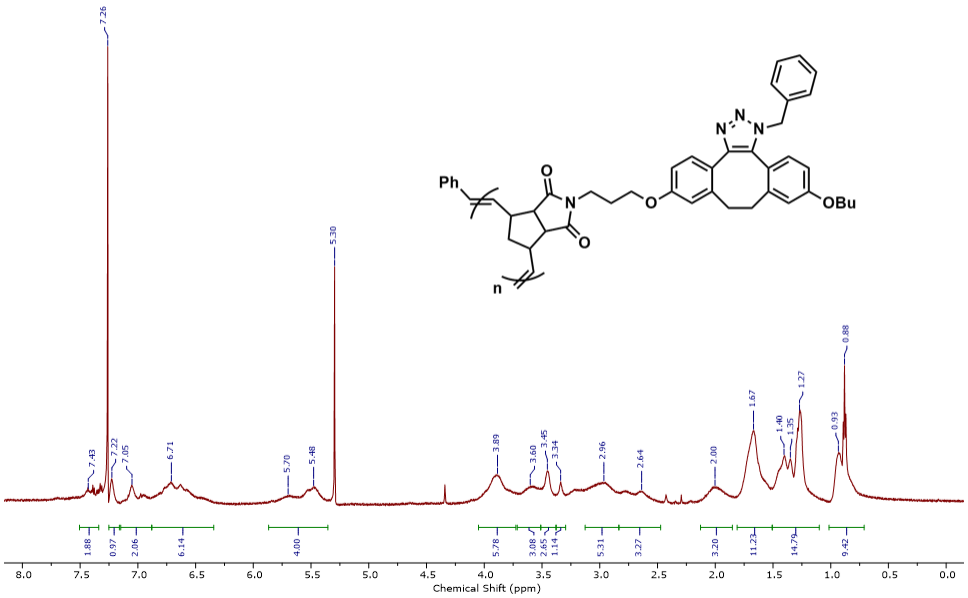

Figure A1. ^{1}H NMR spectrum of polymer (**14**) in $CDCl_3$.

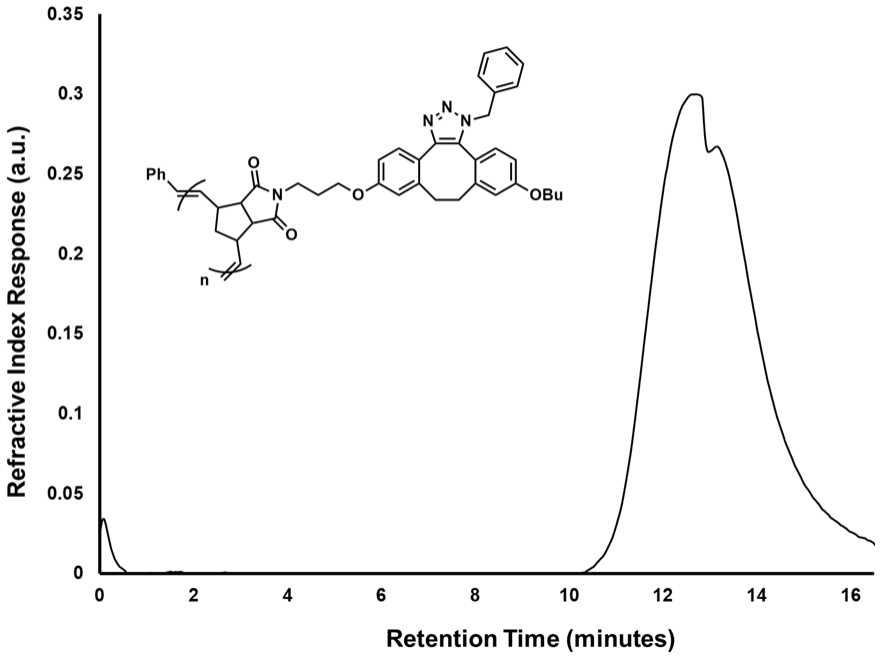

Figure A2. SEC trace of polymer (**14**) in DMF against a PS standard.

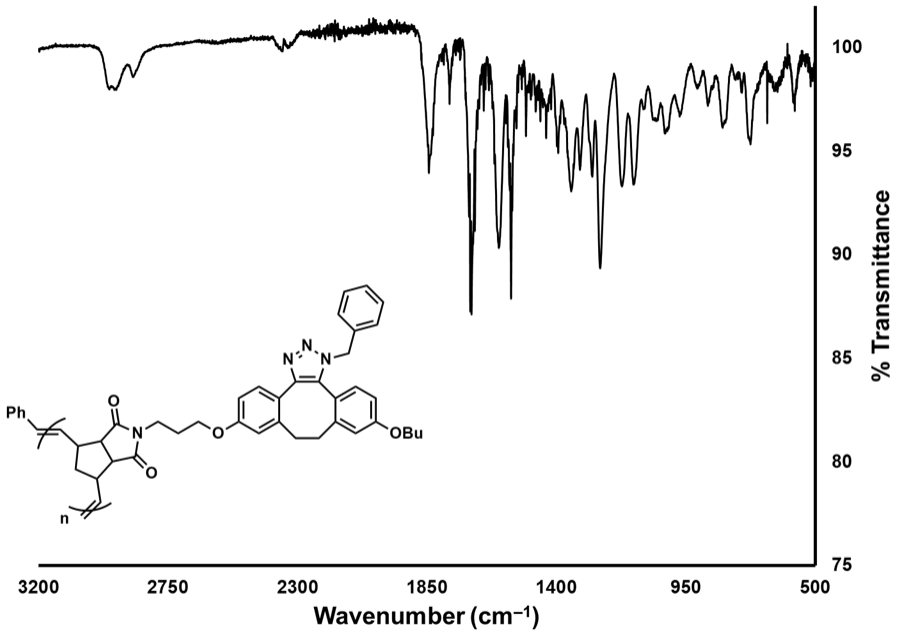

Figure A3. FT-IR spectrum of polymer (**14**).

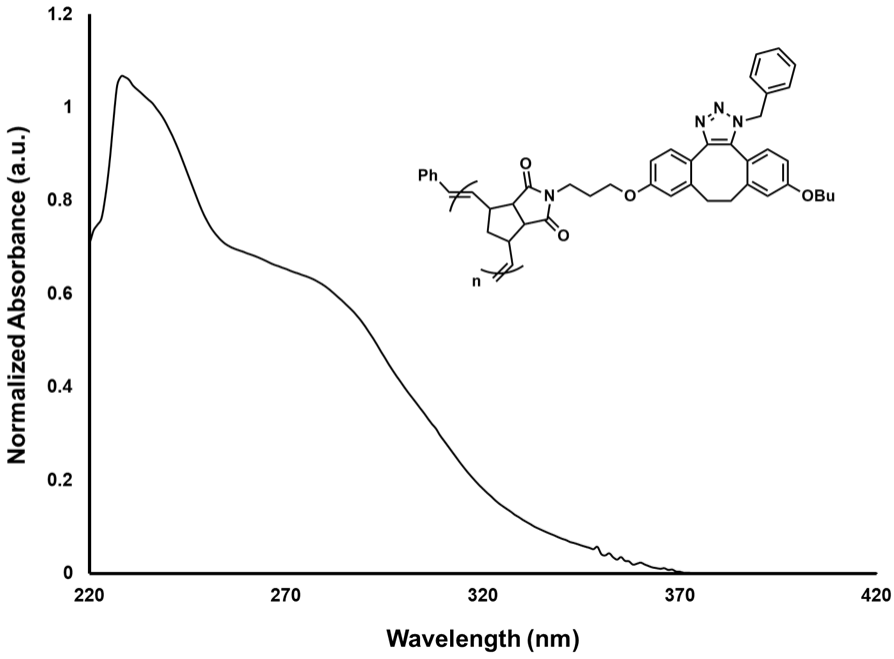

Figure A4. UV-Vis spectrum of polymer (**14**) in DCM.

3-B. Characterization of Au_{25}-triazole-DIBO-monomer (15).

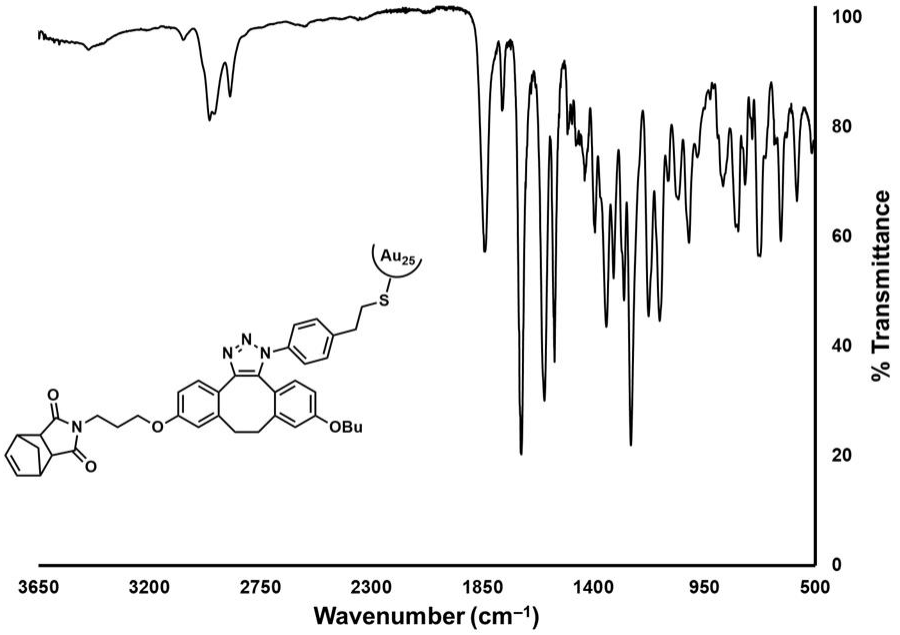

Figure B1. FT-IR spectrum of compound (**15**).

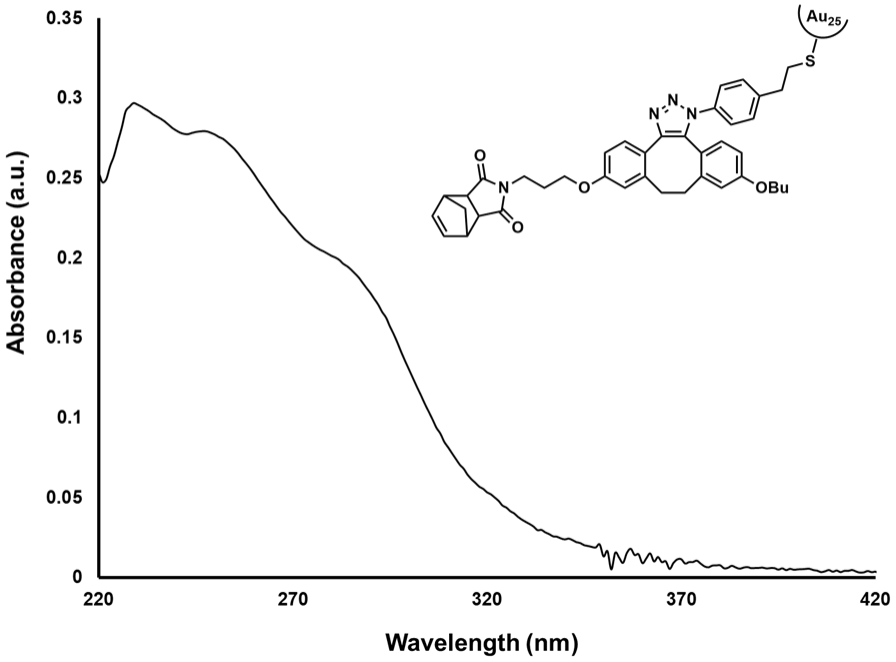

Figure B2. UV-Vis spectrum of compound (**15**) in DCM.

3-C. Characterization of Au_{25}-triazole-DIBO-polymer (16)

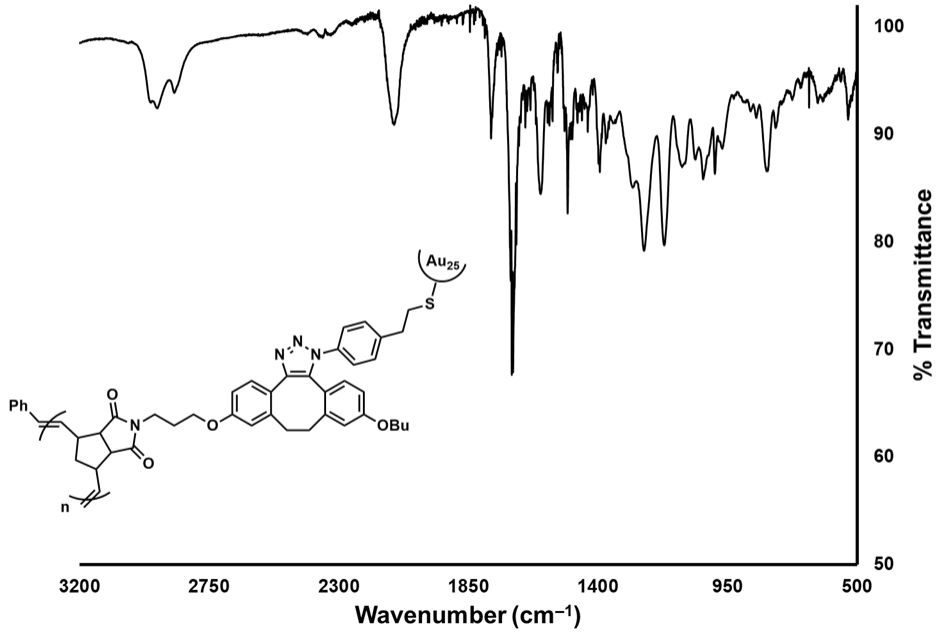

Figure C1. FT-IR spectrum of polymer (**16**).

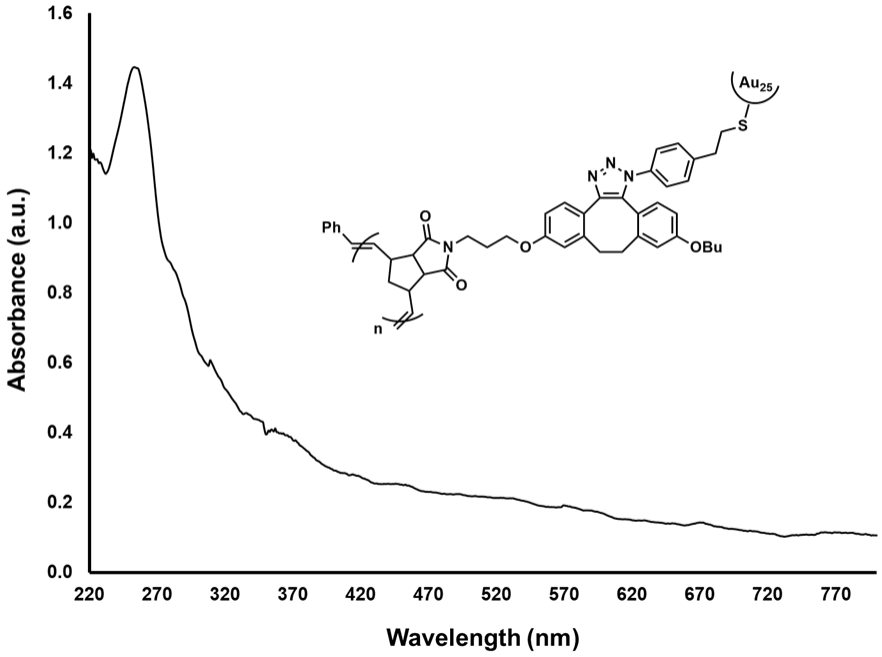

Figure C2. UV-Vis spectrum of polymer (**16**) in DCM.

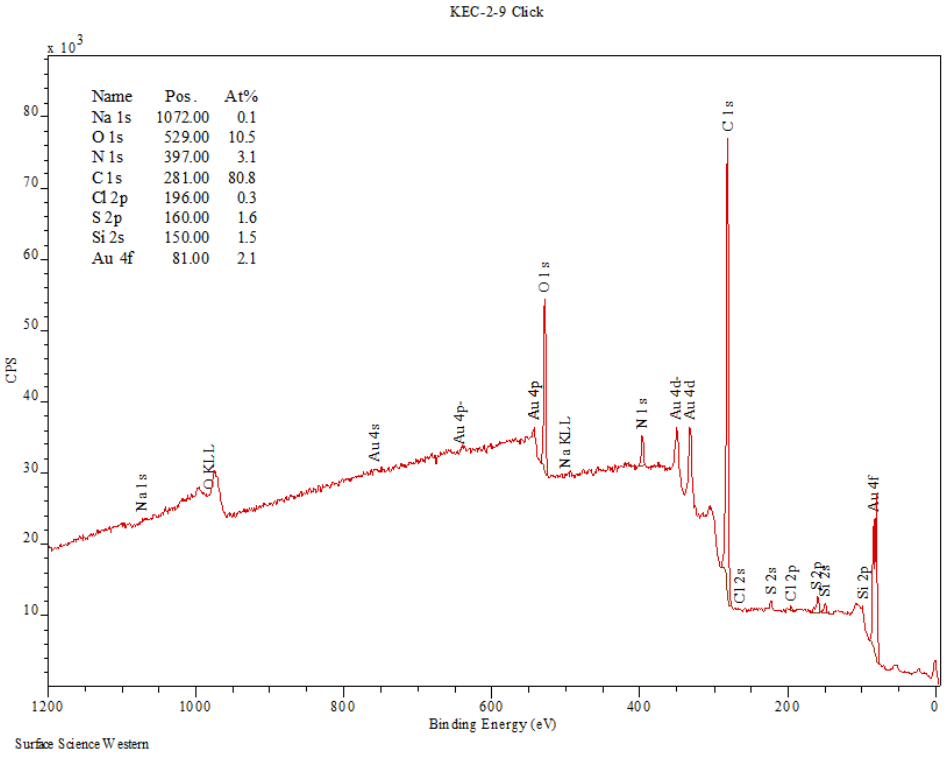

Figure C3. XPS survey scan of polymer (**16**).

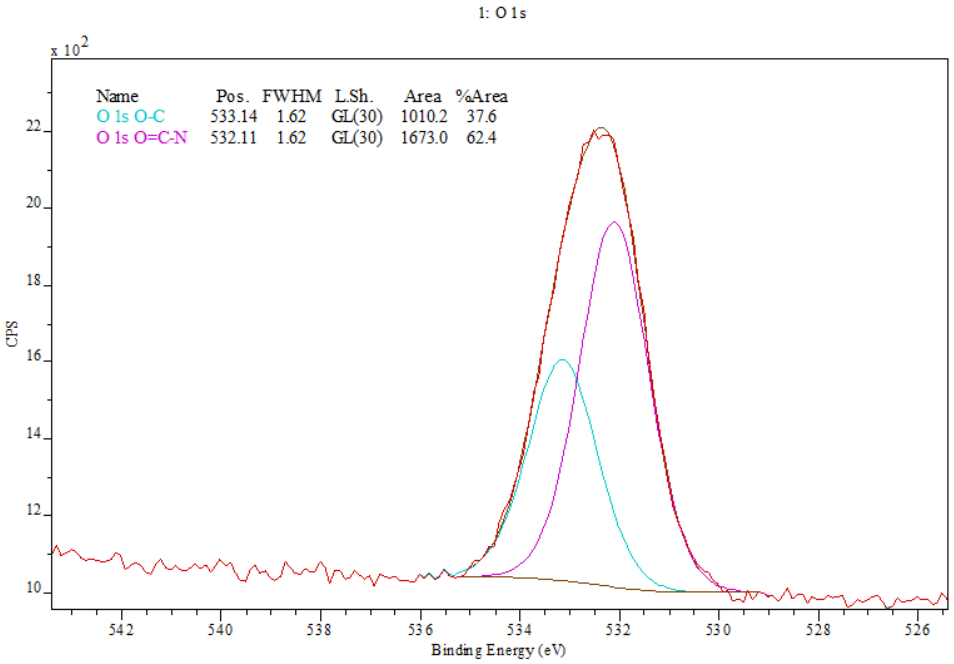

Figure C4. XPS O_{1s} high-resolution scan of (**16**).

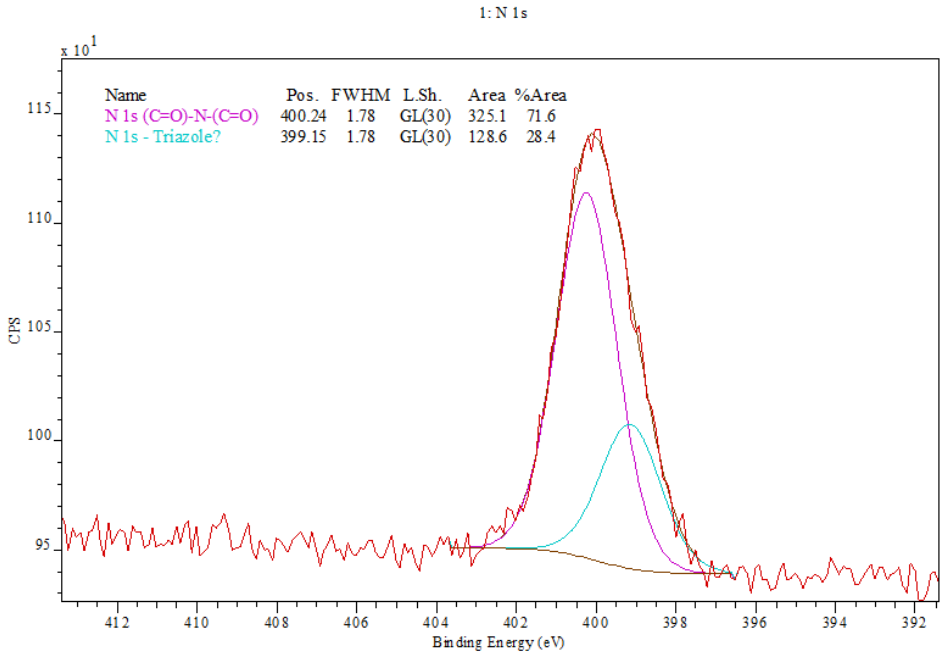

Figure C5. XPS N_{1s} high-resolution scan of (**16**).

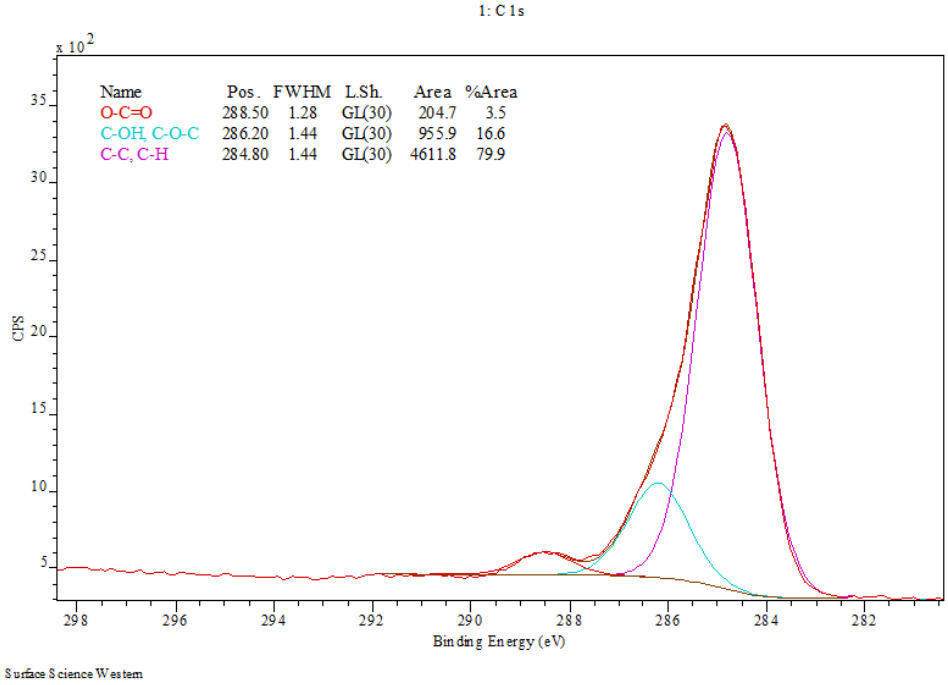

Figure C6. XPS C_{1s} high-resolution scan of (**16**).

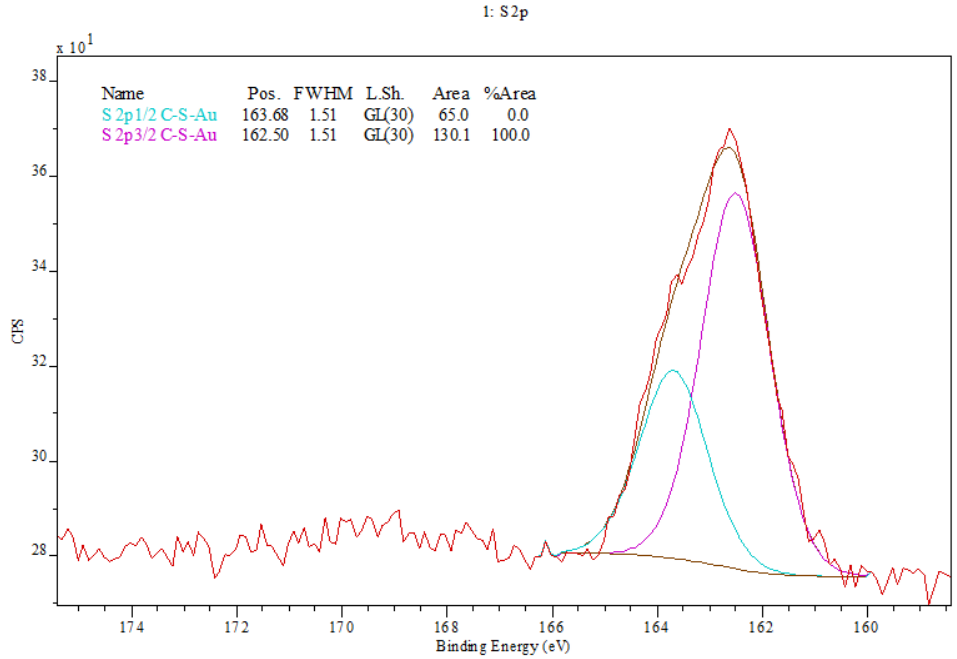

Figure C7. XPS S_{2p} high-resolution scan of (**16**).

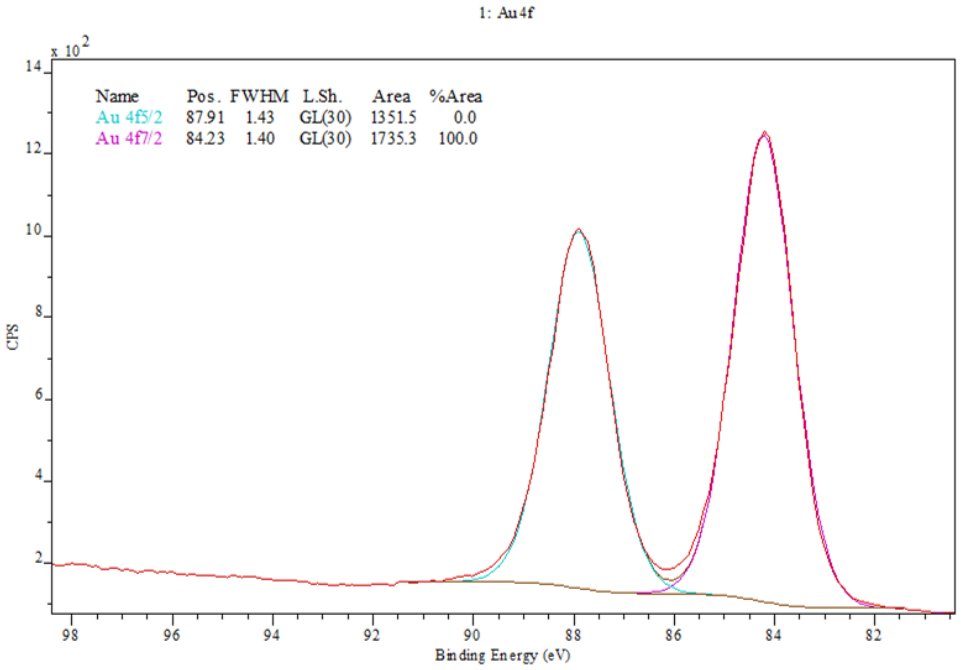

Figure C8. XPS Au_{4f} high-resolution scan of (**16**).

Curriculum Vitae

Name: Kyle Classen

Post-secondary Education and Degrees:

The University of Western Ontario
London, Ontario, Canada
2014–2018 B.Sc.

The University of Western Ontario
London, Ontario, Canada
2018–Present (2020) M.Sc.
Supervisor: Dr. Mark Workentin

Honours and Awards:

Lipson-Baines Award – M.Sc. stream
2020

Related Work Experience

Teaching Assistant (Chem. 2213, Chem. 2283)
The University of Western Ontario
2018–2020

Undergraduate Research Thesis Course
The University of Western Ontario
2018
Supervisor: Dr. Beth Gillies

Research Technologist
Imperial Oil Canada
05/2016–08/2016

Publications:

Rabiee Kenaree, A; Sirianni, Q.E.A.; Classen, K.; Gillies, E.R. Thermo-Responsive Self-Immolative Polyglyoxylamides. *Biomacromolecules*, **2020**, *xx*, xxx-xxx. (Just Accepted Manuscript Aug 17, 2020)

Presentations:

Conference Poster Presentation (National): Kyle Classen and Mark S. Workentin. A Bioorthognal Approach to Functional Nanomaterials: Towards the Fabrication of a Biocompatible, Clickable Nanomaterial, 102nd Canadian Chemistry Conference and Exhibition, Quebec City, QC, Canada, June 3 – June 7, 2019.

Course Work

Chem 9503R – NMR I
Chem 9563Q – Total Synthesis
Chem 9603T – NMR II
Chem 9651S – Organomet. Bond Activ.
Chem 9657 – Pass (Top presentation in M.Sc. stream)